



AALBORG UNIVERSITY
DENMARK

Aalborg Universitet

Efficient Multicast in Next Generation Mobile Networks

Wang, Haibo

Publication date:
2008

Document Version
Publisher's PDF, also known as Version of record

[Link to publication from Aalborg University](#)

Citation for published version (APA):
Wang, H. (2008). *Efficient Multicast in Next Generation Mobile Networks*. Aalborg Universitet.

General rights

Copyright and moral rights for the publications made accessible in the public portal are retained by the authors and/or other copyright owners and it is a condition of accessing publications that users recognise and abide by the legal requirements associated with these rights.

- ? Users may download and print one copy of any publication from the public portal for the purpose of private study or research.
- ? You may not further distribute the material or use it for any profit-making activity or commercial gain
- ? You may freely distribute the URL identifying the publication in the public portal ?

Take down policy

If you believe that this document breaches copyright please contact us at vbn@aub.aau.dk providing details, and we will remove access to the work immediately and investigate your claim.



Department of Electronic Systems

Efficient Multicast in Next Generation Mobile Networks

by

Haibo Wang, MSc

Dissertation

Presented to the International Doctoral School of Technology and Science,

Aalborg Universitet,

in Partial Fulfillment of the Requirements for the Degree of

Doctor of Philosophy

Aalborg Universitet

22 October 2008

Supervisors:

Hans-Peter Schwefel, Associate Professor, PhD, Aalborg University

Thomas Skjodeberg Toftegaard, PhD, TietoEnator, Aarhus

Assessment Committee:

Professor Tan Zhenhui, Beijing Jiaotong University, China

Professor Christoph Mecklenbräuer, Vienna University of Technology, Austria

Troels B. Sørensen, Associate Professor (chairman), Aalborg University

Moderator:

Tatiana Kozlova Madsen, Associate Professor, PhD, Aalborg University

Copyright © October 2008 by

Haibo Wang

Aalborg University

Niels Jernes Vej 12

Aalborg Øst

Denmark

e-mail: hw@es.aau.dk

All rights reserved by the author.

Printed in Aalborg, Denmark

Dedicated to...
my family for their unconditional support

Abstract

The next generation mobile cellular networks are expected to transmit rich multimedia services, which often require large transmission bandwidth, low delay and the same content to be delivered to several users. Due to the broadcast nature of radio transmission, the most efficient way to provide such services is to employ *wireless multicast*. By sending one copy of the service content to several multicast group members with a shared downlink channel, the bandwidth consumption can be significantly reduced and the efficiency of using scarce radio resource can be improved. On the other hand, the diversity of the channel conditions among multiple receivers raise challenges to the radio resource management (RRM) algorithm design for such a multicast channel. In this PhD project, a comprehensive RRM study with both analytical and simulative approaches is fulfilled to explore the tradeoff between spectral efficiency and reliability in this wireless multicast channel.

First, a performance metric has been built to balance the multicast system spectral efficiency and the user perceived Quality of Service (QoS). A simple modulation rate adaptation scheme is proposed to maximize such metric in an OFDMA-based multicast channel. Then the metric is simplified to reduce its sen-

sitivity to its weight factors, and a more sophisticated modulation rate adaptation algorithm is proposed to optimistically relax the instantaneous Bit Error Ratio (BER) constraints based on the BER history of each multicast user. The proposed algorithm has been evaluated in connection to other link adaptation schemes by simulations, which shows significant spectral efficiency advantage under the given QoS constraint.

To reveal the performance upper-boundary of multicast link adaptations in general, an analytical model is built. The optimization problem is reformulated to a constraint optimization problem with joint power and modulation rate adaptation under flat- and block-fading Rayleigh channels. The optimal and suboptimal adaptation approaches along different dimensions (power and modulation rate) are derived from this analytical model, as well as the corresponding achievable spectral efficiency values. The criteria of switching from unicast channel mode to multicast channel mode is also revealed from the analytical results.

All these studies reveals that the worst channel state degrades the overall multicast system performance, and this penalty increases as the multicast group size grows. Automatic Repeat request (ARQ) can help to improve the overall spectral efficiency under poor channel conditions, but facing scalability problems in multicast. This dissertation proposes a cross-layer framework to jointly optimize Adaptive Modulation and Coding (AMC) and ARQ scheme, and adopts packet-combining to solve the scalability problem under practical group size assumptions.

In summary, this dissertation presents how RRM approaches can be employed to improve multicast spectral efficiency with reliability constraints. It re-

veals that violating the reliability constraint temporarily for the worst link can improve the average spectral efficiency per user significantly, without sacrificing the average reliability in long term. It is also proved that even though rate adaptation alone can achieve similar performance as joint power and rate adaptation can do if the data rate can be changed continuously, the latter still outperforms in more realistic cases where only discrete data rates are available. Last but not the least, cross-layer design with innovative multicast ARQ scheme can further exploit the spectral efficiency and reliability trade-off if a certain delay is tolerable.

Dansk Resumé

Næste generations mobile netværk giver mulighed for transmission af avancerede multimedie-services. Disse services kræver ofte en høj transmissions-båndbredde, lav forsinkelse af trafik samt at de transmitterede data skal nå frem til flere modtagere. Eftersom radiotransmissioner kan høres af flere modtagere samtidigt er den mest effektive metode for udbydelse af sådanne services at benytte trådløs multicast. En enkelt strøm af data kan sendes samtidigt til adskillige medlemmer af en multicast-gruppe gennem en delt downlink kanal. På denne måde kan brugen af båndbredde reduceres betydeligt samtidig med at de begrænsede radioressourcer kan udnyttes mere effektivt. På den anden side oplever de enkelte modtagere forskellige kanalforhold hvilket stiller udfordringer til designet af radio resource management (RRM) algoritmer for multicast-kanaler. I dette PhD projekt er gennemført et omfattende RRM studie hvor analytiske og simuleringsbaserede fremgangsmåder danner grundlag for at studere afvejningen mellem spektral effektivitet og pålidelighed i trådløse multicast-kanaler.

Initierende er en ydelsesparameter blevet defineret til at beskrive forholdet mellem spektral effektivitet og Quality of Service (QoS) som brugeren oplever den. For at maksimere denne parameter i en OFDM-baseret multicast kanal intro-

duceres en simpel modulationsrate adapteringsteknik. En simplificering af ydelsesparameteren er blevet indført for at mindske dens følsomhed overfor egne interne parametre. Efterfølgende er en mere sofistikeret modulationsrate adapteringsteknik blevet introduceret der lempet kravene til den øjeblikkelige Bit Error Ratio (BER) givet at den gennemsnitlige BER er inden for kravene. Ved brug af simulering er den foreslåede algoritme blevet evalueret i forhold til andre link-adapteringsteknikker. Målt på spektral effektivitet viser den foreslåede algoritme en signifikant fordel under de benyttede QoS krav.

En analytisk model er blevet opstillet for at fastlægge en øvre grænse for den mulige ydelse af multicast link-adaptering. Optimeringsproblemet er blevet omformuleret som et afgrænset optimeringsproblem der håndterer kombineret adaptering af sendestyrke og modulationsrate under antagelse af en flat- og block-fading Rayleigh kanal i et single-carriersystem. Baseret på den analytiske model er udledt optimale og suboptimale adapteringsmetoder i forskellige dimensioner (sendestyrke og moduleringsrate) samt tilhørende værdier for den opnåelige spektrale effektivitet. Fra de analytiske resultater er også blevet udledt kriterier for at foretage et skifte fra en unicast kanal til en multicast kanal.

De udførte studier viser at den, af en modtager, værst oplevede kanaltilstand forringer den overordnede ydelse af multicast systemet. Denne forringelse forøges når størrelsen af multicast-gruppen stiger. Automatisk Repeat reQuest (ARQ) kan benyttes til at forbedre den overordnede spektrale effektivitet under dårlige kanalforhold, men med multicast kan dette give anledning til skaleringsproblemer. I denne afhandling introduceres en cross-layer metode der muliggør kombineret optimering af Adaptive Modulation og Coding (AMC) og ARQ hvor Coding-teknik

benyttes på pakkeniveau for at løse skaleringsproblemerne under realistiske antagelser om gruppestørrelser.

Denne afhandling præsenterer hvordan RRM-teknikker kan anvendes til at forbedre den spektrale effektivitet under multicast med pålidelighedskrav/QoS krav. Det er vist hvordan en signifikant forbedring i spektral effektivitet kan opnås ved at tillade midlertidige brud på pålidelighedskravene uden at det har betydning for den gennemsnitlige pålidelighed på lang sigt. Under antagelse af en trinløs indstilling af transmissionsraten kan rateadaptering alene, opnå lignende ydelse som under kombineret transmissionsstyrke- og rateadaptering. Det er dog bevist hvordan sidstnævnte fremgangsmåde er bedre i realistiske tilfælde hvor kun diskrete data rater er tilgængelige. Slutteligt skal fremhæves hvordan cross-layer designet med den innovative multicast ARQ-teknik giver mulighed for at udnytte afvejninger af spektral effektivitet og pålidelighed hvis en givet forsinkelse kan tolereres.

Acknowledgments

First of all, I would like to express my heartiest gratitude to my PhD Supervisors, Associate Prof. Hans-Peter Schwefel at Aalborg University and Thomas Skjodeberg Toftegaard at TietoEnator. Since I met Hans as a master student in 2004, he has always been encouraging me to follow my curiosity, to challenge my limit, and to achieve the new height I had never imagine before. Whenever I have difficulties, he has always been there for me. As my supervisor in TietoEnator, Thomas has guided me to develop my competence in both the academia and in the industry. He has inspired me with a broad version, combining both technology enthusiasm and market sense. What I have learned from Hans and Thomas will always be a great treasure in my future career.

Thanks to Assistant Prof. Persefoni Kyritsi. Whenever I have trouble on the channel and antenna issues, she has always helped me out with her clear picture of knowledge and great patience. Also thanks to Associate Prof. Jon E. Johnsen for verifying my mathematics model.

Thanks to Megumi Kaneko, Chenguang Lu, Guillaume Monghal, and many other

fellow PhD students in our Electronic System Department for their support and discussions, which have enriched my knowledge and inspired me during my entire PhD project. Especially thanks to Jesper Grønbæk, my officemate and fellow PhD student, who has made great efforts to translate the abstract of this dissertation into the Dansk Resumé.

Thanks to Prof. Ye (Geoffrey) Li for hosting me in his lab as a visiting student in Georgia Institute of Technology. This was a great experience and the cross-layer design in my thesis was inspired during this visiting.

Thanks to all my friends I have met in Denmark and USA, and to all my friends back in China.

No expressions can express my gratitude to my parents and my grandmother. Their love and caring has always been supporting me and make me strong, though they are far away from Denmark.

HAIBO WANG

Aalborg Universitet

October 2008

Contents

Abstract	vi
Dansk Resumé	ix
Acknowledgments	xii
List of Figures	xix
List of Tables	xxii
Chapter 1 Introduction	1
1.1 Motivation	1
1.2 Problem Delimitation	4
1.2.1 Optimization Scenario	4
1.2.2 Problem Statement	8
1.2.3 Objectives and Scope of the Work	9
1.3 Summary of the Contributions	11
1.4 Organization of Thesis	14

Bibliography	16
Chapter 2 Background	19
2.1 Wireless Channel Features	19
2.1.1 Path-loss and Shadowing	20
2.1.2 Multipath Fading	21
2.1.3 Channel Fading versus Modulation	22
2.2 Orthogonal Frequency Division Multiplexing (OFDM)	24
2.2.1 OFDMA	28
2.2.2 OFDMA-Based Standards Groups	30
2.3 Radio Resource Management (RRM)	33
2.3.1 AMC and Power Adaptation	34
2.3.2 Water-Filling Principle	35
2.3.3 ARQ	37
2.4 State-of-the-art	40
2.4.1 OFDM link adaptation and multi-user diversity	40
2.4.2 Related work with multiple unicast users	41
2.4.3 Related work with one multicast group	42
2.5 Summary	42
Bibliography	44
Chapter 3 Rate Adaptation for Mobile Multicast	51
3.1 Motivation	52
3.2 System Model and Assumptions	53
3.2.1 OFDMA	54

3.2.2	Channel Model	54
3.2.3	BER Approximations	55
3.3	Simulator Description	56
3.3.1	Simulation Scenario	56
3.3.2	System Level Simulator	57
3.4	Reward Function-Based Adaptation	58
3.4.1	Performance Evaluation Approach	58
3.4.2	Different Adaption Strategies	60
3.4.3	Numerical Result and Analysis	63
3.4.4	Sub-Conclusion	69
3.5	History-Based BER Threshold Adaptation	70
3.5.1	Performance Evaluation Metric	70
3.5.2	Different Adaptation Strategies	71
3.5.3	Simulation Results and Analysis	75
3.5.4	Sub-Conclusion	79
3.6	Conclusion	79
Bibliography		82
Chapter 4 Multi-Dimensional Optimization with Analytical Model		85
4.1	Motivation	85
4.2	Single-Carrier System Model	87
4.3	Problem Formulation	89
4.4	Solutions with Continuous Rate Adaptation	92
4.4.1	Adaptation Schemes	92

4.4.2	Numerical Result of Case Studies	96
4.5	Solutions with Discrete Rate Adaptation	103
4.5.1	Discrete Rate and Optimal Power (DRSopt)	103
4.5.2	Discrete Rate and Constant Power (DRSc)	107
4.5.3	Numerical Results of Case Studies	108
4.6	Conclusion and Future Work	110
Bibliography		112
Chapter 5 Cross Layer Design for Multicast		114
5.1	Motivation	114
5.2	Related Work	116
5.3	Cross-Layer System Model	119
5.4	Multicast ARQ with Packet-Combining	123
5.4.1	Two Users Group	124
5.4.2	N Users Group	125
5.5	AMC Strategies	127
5.6	Evaluation Methods	129
5.7	Case Study I: $N = 2$	130
5.7.1	Performance Analysis in Close-Form Expression	130
5.7.2	Numerical Results	135
5.8	Case Study II: $N \geq 2$	137
5.8.1	Numerical Results	138
5.9	Conclusion and Future Work	142
Bibliography		146

Chapter 6	Conclusion	148
6.1	Summary	148
6.2	Outlook	151
Appendix A	Additional Results of the Cross-Layer Strategies	153
Appendix B	List of Abbreviations	157
Appendix C	List of Math Notations and Symbols	161

List of Figures

1.1	General Scenario	5
1.2	Multicast Transmitter and Receivers	6
2.1	Wireless Channel Propagation Phenomena	20
2.2	OFDM with 8 Sub-Carriers	25
2.3	An OFDM Transceiver Diagram	26
2.4	OFDMA with Static FDMA Scheme	28
2.5	OFDMA with Fully Dynamic Frequency-Time Block Allocation .	29
2.6	OFDMA Sub-Channel Modes	30
2.7	Illustration of "Water-Filling" Solution	36
3.1	An OFDMA Adjacent Sub-Channel for Multicast	53
3.2	BER Approximations for BPSK and MQAM	56
3.3	Simulator Diagram	58
3.4	Reward under $E(SNR) = 28dB$	64
3.5	Throughput and satisfaction ratio ($E(SNR) = 28dB$)	65
3.6	Cumulative Distribution Function (CDF) of SNR, Mean=28dB,STD=11dB	66
3.7	SNR CDF, Mean=35dB,STD=11dB	68

3.8	Reward under $E(\text{SNR})=35\text{dB}$	68
3.9	Satisfaction Ratio under $E(\text{SNR}) = 35\text{dB}$	69
3.10	Best Reward AM with Heuristic BER Constraint	73
3.11	Reward Comparison, $E(\text{SNR})=20\text{dB}$	75
3.12	Average BER Comparison, $E(\text{SNR})=20\text{dB}$	76
3.13	Impacts of δ Settings on Adaptive BER Algorithm, $E(\text{SNR})=20\text{dB}$	77
3.14	Impacts of θ_1 Settings on Adaptive BER Algorithm, $E(\text{SNR})=20\text{dB}$	78
3.15	Spectrum Efficiency of AM Strategies, $E(\text{SNR})=20\text{dB}$	79
4.1	S/\bar{S} versus $\min\{\bar{\gamma}\}$	97
4.2	k versus $\min\{\bar{\gamma}\}$	98
4.3	Spectrum Efficiency per User in Rayleigh Channel	99
4.4	Impact of Cut-Off SNR (Rayleigh PDF, Mean=10dB)	101
4.5	Linear Power Adaptation, Impact of Slope β on Spectrum Efficiency	102
4.6	Integration Region of 2 UE, D-Rate	106
4.7	Optimal Power Schemes with Discrete Modulation Rate	107
4.8	Per User Spectral Efficiency of All Adaptation Schemes	108
5.1	Multicast System Model with Cross-Layer Design	120
5.2	Multicast Packet Loss Pattern for 2 UEs	124
5.3	Integration Region of 2 UEs, D-Rate	132
5.4	Rate Regions of Max-SINR Strategy	134
5.5	Performances of Different Adaptation Strategies, $N = 2$	136
5.6	Performances of AMC-ARQ Strategies VS Group Size, $\overline{\text{SINR}} =$ 10dB	139

5.7	Spectral Efficiencies of S1 with Different ARQs, $\overline{SINR} = 10\text{dB}$	141
A.1	Performances of AMC-ARQ Strategies VS Group Size, $\overline{SINR} = 5\text{dB}$	155
A.2	Performances of AMC-ARQ Strategies VS Group Size, $\overline{SINR} = 15\text{dB}$	156

List of Tables

2.1	OFDM Parameters in Mobile WiMAX [11]	32
3.1	Selected OFDMA Parameters	54
3.2	Important System Assumptions	57
3.3	The Best Local Reward Algorithm	62
3.4	SNR Thresholds for $BER < 10^{-3}$	63
3.5	BER Estimations	67
3.6	The Best Local Reward Algorithm with Fixed BER Threshold	72
3.7	Adaptive BER Threshold Algorithm	74
5.1	Transmission AMC Modes with Convolutional-Coded Modulation	121

Chapter 1

Introduction

1.1 Motivation

At present, wireless multimedia applications like multi-party video conferences, Video on Demand, or on-line mobile gaming are demanding high bandwidth while at the same time posing real-time requirements on the communication infrastructure. On the other hand, a large part of the content in these applications are common information required by a group of users. Hence to allow multiple users to share the same network resource (wired network resource or radio resource) via Multicast/Broadcast is highly attractive in providing current and future wireless multimedia services.

Broadcast and multicast are the two modes of point-to-multipoint (PTM) communications. In Broadcast, the same content is delivered to all receivers within the transmission range from the sender. Known examples are radio and TV services, which are broadcasted over the air (either terrestrial or via satellite) and over cable networks. In Multicast, on the other hand, each content are solely delivered to users who have joined a particular multicast group. Normally, a multicast group is a group of users interested in a certain kind of content, for example, sports,

news, cartoons. A multicast-enabled network ensures that the content is solely distributed over those links that are serving receivers which belong to the corresponding multicast group. In large scale networks like the Internet, the available content to be delivered are so diversified and the content senders and intended receivers are distributed so far apart that broadcast is nearly impossible. Hence multicast is the main concern of this dissertation.

Basically, wireless multicast can be done in either infrastructure-based mobile networks or Ad-Hoc mobile networks. In infrastructure-based networks like Global System for Mobile Communications (GSM) and Universal Mobile Telecommunications Systems (UMTS), Mobile Terminals (MTs) communicate with a base station (BS) connecting to a backbone networks, which can help one MT to communicate with any other MT, fixed phone or Internet server anywhere. An *ad-hoc* network is a self-organized network made up of a group of wireless mobile hosts [1], where each host has to forward data for others due to the limited transmission range of each mobile host. Such type of networks are usually designed for specific purpose, e.g, the battlefield networks, sensor networks. Whereas the wireless multimedia content requiring multicast are usually provided by servers located in infrastructure-based networks. That is, this dissertation only covers wireless multicast in infrastructure-based networks.

Wireless multicast has been drawing a lot of attention from both industry and academia, i.e, UMTS Multimedia Broadcast and Multicast Service (MBMS) is a framework designed by the Third Generation Partnership Project (3GPP) to extend IP multicast to current 3G mobile networks [2, 3]. However, there are still many open issues to solve in both the fixed backbone part and the radio cell part in order

to fully adopt multicast in mobile networks. In the backbone side, the problems posed by mobility include: (a) the movement of the multicast source, if the content sender is also a MT; (b) the movement of the multicast group members, thus the multicast routing topology (namely the multicast tree) needs to be reconfigured quickly; (c) data transmission reliability during hand-over, to avoid packet drop or enable lost data recovery; (d) signalling overhead due to frequently changed multicast tree topology and membership. In the radio cell side, challenges are mainly upon the radio resource management.

Radio Resource Management (RRM) is the system level control of radio transmission characteristics in wireless communication systems [4]. RRM includes strategies and algorithms controlling transmit power, channel allocation, handover criteria, modulation schemes, error-control-coding schemes [7]. The objective is to utilize the limited radio spectrum resources and radio network infrastructure as efficiently as possible. RRM considers multi-user system capacity issues, rather than just point-to-point link capacity.

Though the problems of multicast on the wired network part have been investigated extensively [7, 8, 9, 10, 11, 12, 13], the challenges on the air interface part have not been discussed thoroughly. Multicast problems on the air interface are as interesting as those in the wired network part, and the reason is two-fold:

- Multicasting in air interface is very challenging since the wireless transmission is highly error-prone due to different fading phenomena and user mobility. The radio resources from a transmitter serving its receivers have to be limited to control the interferences to receivers served by other transmitters. Even though the radio resource management approaches have been fully de-

veloped for Unicast mobile receivers, they may not be the right solutions for multicast mobile users.

- The wireless transmission is broadcasting in its nature, therefore the multicasting on the air interface can utilize such nature to save the scarce radio resource. In the infrastructure-based networks today such as UMTS, the downlink radio resource (from base station to mobile terminals) is “scarce” due to the limitation enforced by the interference problem. By multicasting the same content in a common channel to multiple receivers rather than unicasting via multiple channels, not only radio resources are saved but also the interferences among multiple channels are reduced.

Therefore, this dissertation focus on the wireless multicast performance optimization on the air interface with RRM approaches.

1.2 Problem Delimitation

1.2.1 Optimization Scenario

This dissertation assumes a single cell mobile system as depicted in Fig. 1.1, where a BS located in the center and N users randomly distributed in this hexagonal cell. The N users are all members of a multicast group, and there is a common downlink channel dedicated to the multicast service demand by these users. The multicast signal is sent to different User Equipments (UEs) within the same transmission burst but experiencing different channel conditions due to, e.g., their different distance to the BS and different surroundings. The users are moving only within the cell hence no handover is considered. The channel conditions of every users are

assumed as block-fading channels, which will not change during a transmission burst.

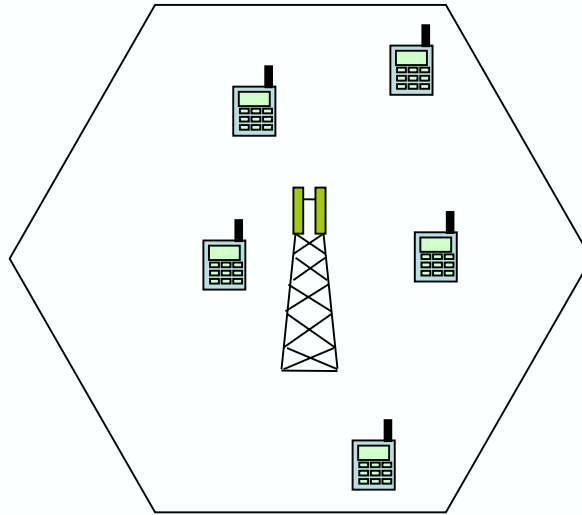


Figure 1.1: General Scenario

The assumed multicast transmitter and receivers are illustrated in Fig. 1.2. The transmitter at the BS is equipped with AMC, power control and ARQ functionalities. The instantaneous channel state of each UE can be reported to the BS with delay-free and error-free feedback channels, such report is usually called Channel State Information (CSI) in wireless systems. This ideal assumption about CSI is made to exclude the possible impacts of CSI error or delay in order to simplify the performance analysis for downlink RRM algorithms. Besides, the ARQ feedback from the receivers are also assumed error-free but with delay, as shown in Fig. 1.2.

We investigate a single cell to exclude the handover problem, as well as the impact of inter-cell interferences from neighbor cells to multicast receivers. However, to control the inter-cell interferences from the investigated multicast channel to neighbor cells, the BS transmission power has to be limited. This limitation

will be reflected in either average power constraint or the resulted average Signal-to-Noise-Ratio (SNR) or Signal-to-Interference-and-Noise-Ratio (SINR) settings, depending on the investigation methods applied in each chapter of optimization proposals. The common scenario and system assumptions in Fig. 1.1 and Fig. 1.2

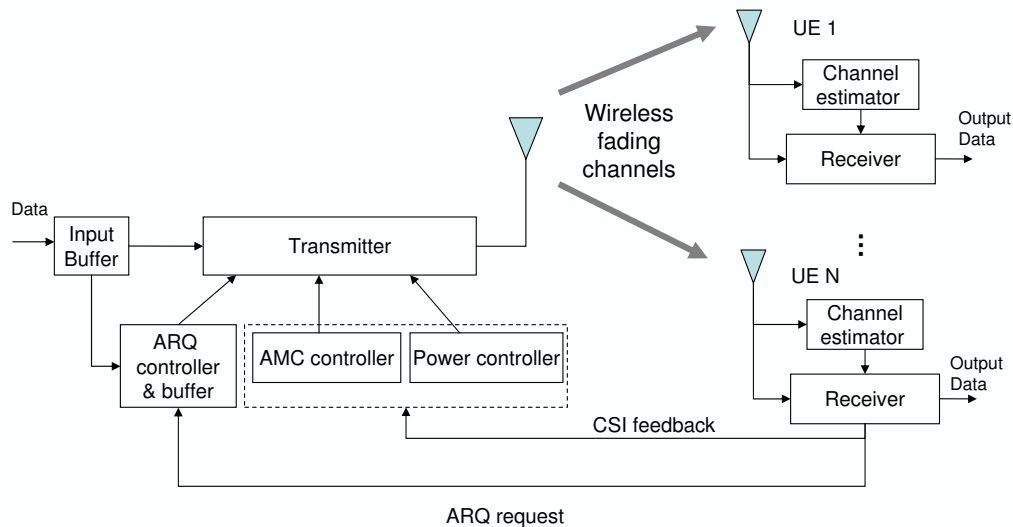


Figure 1.2: Multicast Transmitter and Receivers

will be narrowed down to address more specific issues in the following chapters.

Resource resource management (RRM) includes a wide range of radio resource allocation and adaptation approaches, namely access control, bandwidth allocation and scheduling, link adaptation (LA) (including rate and power adaptation), ARQ, hand-over, etc. In the general scenario and assumptions of this dissertation, the single cell and single group assumption means that access control and handover are out of our scope. The rest RRM approaches will be reviewed in the context of OFDM based next generation mobile systems in Chapter 2.

The ultimate target of network performance optimization is to achieve user satisfaction by conveying applications successfully. QoS is a collective of service

performances reflecting the degree of satisfaction of a user on a service [6], which can be quantitatively evaluated with parameters like transmission data rate, delay, jitter, error ratio (in bit error ratio or packet error ratio). Contemporary research in multicast link adaptations mainly focuses on maximizing the system spectral efficiency alone, but often neglect discussing the impact of their approaches upon the user perceived QoS in different service categories. Our work, on the other hand, optimizes the system performance from QoS perspective, specifically for realtime multimedia services.

Considering the most-used QoS metrics for a multicast video-streaming service in a mobile network, data rate and error ratio are largely effected by the air interface, while the delay and jitter are impacted by many factors from physical layer, network layer up to application layer. For data rate and error ratio, comparing to the scarce of radio resource and error-prone feature of radio network, the wired backbone networks, often based on optical transmission facilities, are bandwidth-sufficient and can provide nearly errorless transmission. Delay and jitter, however, could happen anywhere in the wired networks due to the bursty nature of data traffics, and need to be controlled with end-to-end approaches. Therefore, our optimization mainly concerns average data rate and error ratio per user in the radio cell. One may argue that link level ARQ on the air interface also introduces delay for retransmissions, but if the error ratio in the wireless transmission is effectively controlled, the probability that retransmission is required will be too small to be the main cause of user perceived delay and jitter.

1.2.2 Problem Statement

The problems of multicast optimization in a single cell system are mainly caused by two factors, the diversity of channel conditions among all group members, and the time-varying nature of the worst link.

1.2.2.1 Channel Diversity of Users

In a cell, different MTs experience different channel conditions. When each of them can be assigned a dedicated channel as in unicast case, the BS can allocate/schedule radio resources like time-slots, carrier frequencies or antennas for the user who has the best channel condition at the moment, and the radio resource can be adapted to be optimal for this user's channel condition. This is called multi-user diversity. Whereas in multicast, the same content to different users with different channel conditions has to be transmitted in the common channel simultaneously, hence such benefit of diversity-based scheduling is lost. In this situation, it is impossible to achieve the optimal radio resource allocation or adaptation for each group member at the same time, thus the optimization effort has to be compromised for the benefit of the whole group. Without scheduling and handover options, multicast RRM reduces to mainly Link Adaptation (LA) approaches, e.g. Adaptive Modulation and Coding (AMC), power control, Automatic Repeat request (ARQ), etc.

In a system with AMC, the modulation and coding formats are changed to match the current received signal quality, i.e., the users with high SNR or SINR are typically assigned higher-order modulations and high coding rates (e.g., 64-Quadrature Amplitude Modulation (64-QAM) with rate-3/4 convolutional cod-

ing), whereas the users with low SNR or SINR are assigned low modulation-order and/or low code rate (e.g., Quadrature Phase-Shift Keying (QPSK) and 1/2 convolutional coding). With power control, the power of the transmitted signal is adjusted to meet a target signal quality at the receiver [14]. ARQ is an error control method for data transmission, where the transmitter will know whether a packet has been received correctly by getting acknowledgment messages from the receiver, or timeouts. If a packet or frame is known to be lost, the transmitter with ARQ function usually re-transmits the frame/packet. More details about link adaptation methods will be described in chapter 2.

1.2.2.2 Time-varying of the Worst Link

If the same QoS standard (i.e, BER or PER) had to be achieved for all group members, the worst link condition among users will limit the spectral efficiency of the whole group. Intuitively multicast LA can be adapted to the worst link in the group during a transmission burst. However, the wireless link conditions are highly time-varying due to user mobility and channel fading phenomena, and each receiver could be in poor channel conditions at some time. The larger the group, the higher will be the probability that one or several users are in very bad link conditions. Hence the LA strategy for the worst link may keep the data rate low for large multicast group size [9].

1.2.3 Objectives and Scope of the Work

To this end, the focus of this PhD project is to optimize radio resources management approaches in providing B3G/4G multicast services on the air interface. The

challenges within this optimization work include

- **Efficient use of radio resources for multi-cast traffic:**

New power and AMC schemes need to be proposed as existing Uncash-oriented link adaptation schemes cannot be suitable for multicast services. As analyzed in the problem statement, existing uncash power control and AMC schemes cannot match the different channel conditions of group members simultaneously. Hence multicast group-based performance metric need to be defined and power and AMC need to be designed to optimize such metric.

- **QoS Provisioning/Reliable multi-cast schemes**

It is a challenge how to provide QoS for multiple users in the same group under different channel conditions. For the concerned QoS metric, to improve average data rate per user matches the RRM goal to maximize the system performance in terms of average spectral efficiency, bits/s/Hz; while the BER/PER are posing reliability requirements to the wireless system. In wireless systems there exists a tradeoff between spectral efficiency and reliability. I.e., under a given signal quality, transmission with higher modulation-order and coding rate will result in higher data rate but with more errors than the transmission with low modulation-order and coding rate. Hence the former achieves better spectral efficiency but less reliability, while the latter achieves better reliability with less spectral efficiency, roughly speaking. In multicast, since the reliability will be limited by the worst channel condition, the tradeoff between reliability and spectral efficiency will be even more significant.

- **Switch between Point-to-Point (PTP) and Point-to-Multipoint (PTM)**

The switch between PTP and PTM communication modes in order to opti-

mize spectral efficiency may depend on the number of multicast group members and their distance to BS. I.e, when the group size is small and the channel conditions of the users are highly diversified, it is arguable whether to adopt multicast with a common channel or uncash with multiple dedicated channels.

- **Diversity approaches to enhance Multicast efficiency or reliability**

Transmit or receive diversity techniques can enhance the spectral efficiency and/or the reliability in wireless fading channels, such as time domain diversity like Automatic Retransmission request (ARQ), spatial domain diversity like Multiple Input Multiple Output (MIMO). It is an open issue how to utilize these diversities for multicast. E.g, ARQ schemes is usually considered non-scalable if the number of receivers is large [2]. If ARQ is going to be employed in multicast, the scalability problem has to be solved in the first place.

As the scenario description and problem formulation have stated, scheduling and handover are out of the scope of this dissertation. New optimization schemes are proposed and evaluated with both simulation and analytical approaches.

1.3 Summary of the Contributions

The contributions in multicast RRM in mobile cellular systems are:

Utility-based adaptive modulation strategies A utility metric named Rewarding function is build to balance the system multicast performance and the user perceived Quality of Service (QoS). A simple multicast modulation rate

adaptation scheme is proposed to maximize such metric in an OFDMA single cell setting. Then the metric is simplified to reduce its sensitivity to the metric parameters, and a more sophisticated modulation rate adaptation algorithm with history-based adaptive BER threshold is proposed and evaluated. By using this algorithm the multicast performance of the user group is significantly improved compared to other link adaptation strategies.

Optimal and sub-optimal joint power and rate adaptation solutions To reveal the performance upper-boundary of link adaptation approaches in general, an analytical model is built. The focus of this analytical model is the joint power and rate adaptations, hence the optimization problem was simplified to a constraint optimization problem. The advantages and disadvantages of adaptation approaches along different dimensions (power and modulation rate) are discussed based on this analytical model. The criteria of switching from unicast channel mode to multicast channel mode is also discussed according to the analytical results.

Cross-layer design model An innovative solution where AMC and ARQ schemes are jointly designed within a cross-layer framework. Packet-combining schemes are proposed using packet level 'XOR' operations to reduce the retransmission times, so that the scalability problem of multicast ARQs can be solved. An average-PER-based (average over instantaneous group PERs) rate adaptation algorithm is developed to exploit more spectral efficiency gain given ARQ exists. The numerical results shows that the joint design of the average-PER-based rate adaptation and the optimal packet-combining ARQ achieve the best spectral efficiency in the selected evaluation scenario, and success-

fully keep the residual PER constraint at the same time. The results also reveal that the gain of cross-layer design over non-cross-layer design with the same rate adaptation strategy is stable under different ARQ schemes.

These contributions have been presented in the following publications.

- H. Wang, D. Prasad, X. Zhou, J. M. Llorente, F. Delawarde, G. Coget, P. Eggers and H. P. Schwefel, “Improved Channel Allocation and RLC block scheduling for Downlink traffic in GPRS,” in *Proc. IEEE 61st Semiannual Vehicular Technology Conference (VTC’05 Spring)*, Stockholm, Sweden, May 2005.
- H. Wang, D. Prasad, O. Teyeb and H. P. Schwefel, “Performance Enhancements of UMTS networks using end-to-end QoS provisioning,” in *Proc. International Wireless Summit(IWS’05)*, Aalborg, Denmark, Sept. 2005.
- H. Wang, H. P. Schwefel and T. T. Nielsen, “Adaptive Modulation for a Downlink Multicast Channel in OFDMA systems,” in *Proc. IEEE Wireless and Networking Conference (WCNC’07)*, HongKong, China, Mar. 2007.
- H. Wang, H. P. Schwefel and T. S. Toftegaard, “History-based Adaptive Modulation for a Downlink Multicast Channel in OFDMA systems,” in *Proc. IEEE Wireless and Networking Conference (WCNC’08)*, Las Vegas, USA, Mar. 2008.
- H. Wang, H. P. Schwefel and T. S. Toftegaard, “The Optimal Joint Power and Rate Adaptation for Mobile Multicast: A Theoretical Approach,” in *Proc. IEEE Sarnoff Symposium*, Princeton, USA, Mar. 2008.

- H. Wang, H. P. Schwefel and T. S. Toftegaard, “Mobile Multicast: the Optimal Power and Rate Adaptations in a Unified View,” in preparation.
- H. Wang, H. P. Schwefel and T. S. Toftegaard, “A Cross-layer Design for Mobile Multicast with Packet-Combining ARQ,” in preparation.

1.4 Organization of Thesis

The thesis is organized as follows:

Chapter 2 introduces the background knowledge related to our multicast RRM problems, from wireless channel features to available RRM options in the chosen multicast scenario.

Chapter 3 investigates the data rate adaptation problem in an OFDMA system. The studied OFDMA system model and simulator are first described, and then the proposed optimization metric as well as rate adaptation strategies are explained, finally the simulation results are presented and discussed.

Chapter 4 analyzes the theoretical optimal performance and corresponding power and rate adaptation solutions. It starts with formulating the problem into a constrained optimization problem to maximize the per user spectral efficiency under average power and instantaneous BER constraints. Then the problem is solved with Lagrange methods and the results are analyzed with different parameter settings. It is revealed that the constant power and continuous rate adaptation can perform nearly as good as the optimal joint power and rate adaptation scheme, but much more simple than the latter; whereas when the available data rates are discrete, the performance of the optimal power

scheme outperforms the constant power scheme significantly. Another result in this chapter is that it is always more efficient to switch to multicast mode whenever there are more than one user requiring the same service, under *independent and identical-distributed* (i.i.d) channels.

Chapter 5 presents a framework to apply cross-layer design method in multicast RRM. Both the AMC scheme and ARQ are optimized to maximize the overall spectral efficiency. The performance is derived with an analytical model in combination with Monte-Carlo method. The scalability problem of multicast ARQ is solved with packet combining for different group sizes.

Chapter 6 concludes the dissertation and proposes guidelines for future work.

Bibliography

- [1] T. Imielinski and H. F. Korth, *Mobile Computing*, Kluwer Academic Publishers, 1996.
- [2] 3GPP TS 23.246, “Multimedia Broadcast/Multicast Service; Architecture and Functional Description Networks (PDN)”.
- [3] 3GPP TR 23.846 6.1.0, “Multimedia Broadcast/Multicast Service (MBMS); Architecture and functional description”, release 6, Dec. 2002.
- [4] J. Zander, S-L Kim, M. Almgren and O. Queseth, *Radio Resource Management for Wireless Networks*, Artech House Publishers, 2001.
- [5] G. L. Stüber, *Principles of Mobile Communication*, 2nd ed., Kluwer Academic Publishers, 2001.
- [6] ITU-D SG 2 and ITC, *Teletraffic Engineering Handbook*,
<http://www.tele.dtu.dk/teletraffic/handbook/telehook.pdf>
- [7] T. G. Harrison, C. L. Williamson, W. L. Mackrell and R. B. Bunt, “Mobile multicast(MoM) protocol: multicast support for mobile hosts,” in *Proc.*

- ACM/IEEE International Conference on Mobile Computing and Networking*, pp. 151-160, Budapest, Hungary, Sept. 1997.
- [8] C. R. Lin and C. J. Chung, "Mobile reliable multicast support in IP networks," in *Proc. IEEE ICC 2000*, vol. 3, pp. 1421-1425, New Orleans, USA, Jun. 2000.
- [9] W. Jia, W. Zhou and J. Kaiser, "Efficient algorithm for mobile multicast using anycast group," in *IEE Proc. Commum.*, vol. 148, no. 1, pp. 14-18, Feb. 2001.
- [10] M. Hauge and Ø. Kure, "Multicast in 3G Networks: Employment of Existing IP Multicast Protocols in UMTS," *IEEE WoWMoM'02*, Atlanta, USA, Sept. 2002.
- [11] G. Leoleis, L. Dimopoulou, V. Nikas and I. S. Venieris, "Mobility Management for Multicast Sessions in a UMTS-IP Converged Environment," *IEEE ISCC'04*, Alexandria, Egypt, Jun. 2004.
- [12] R. Rümmler, Y. W. Chung and A. H. Aghvami, "Modeling and Analysis of an Efficient Multicast Mechanism for UMTS," *IEEE Trans. Vehicular Tech.*, vol. 54, no. 1, pp. 350-365, Jan. 2005.
- [13] A. Garyfalos, K. C. Almeroth and K. Sanzgiri, "Deployment Complexity Versus Performance Efficiency in Mobile Multicast," *International Workshop on Broadband Wireless Multimedia (BroadWiM)*, San Jose, USA, Oct. 2004.
- [14] K. L. Baum, T. A. Kostas, P. J. Sartori and B. K. Classon, "Performance Characteristics of Cellular Systems With Different Link Adaptation Strategies," *IEEE Trans. Vehicular Tech.*, vol. 52, no. 6, pp. 1497-1507, Nov. 2003.

- [15] N. Jindal, Z.Q.Luo, "Capacity Limits of Multiple Antenna Multicast," *International Symposium on Information Theory (ISIT)*, Seattle, USA, July 2006.
- [16] S. Sesia, G. Caire, and G. Vivier, "On the Scalability of H-ARQ Systems in Wireless Multicast," in *Proc. IEEE ISIT'04*, pp. 321-321, 2004.

Chapter 2

Background

In this section we will briefly introduce the features of wireless channels and Orthogonal Frequency Division Multiplexing (OFDM) techniques, and then analyze their impacts to wireless multicast transmission scenarios. Afterward, the available RRM approaches in such scenarios will be discussed. All the optimizations in the following chapters will be developed based on these scenario assumptions and RRM approaches.

2.1 Wireless Channel Features

While the radio signal propagates from the transmitter antenna to the receiver antenna, it will experience energy loss, delay, phase and frequency shift due to many effects, e.g., free-space loss, absorption, obstruction, diffraction, reflection, etc. In general, all these wireless channel propagation effects can be categorized as path-loss, shadowing and multi-path fading [7], as depicted in Fig. 2.1.

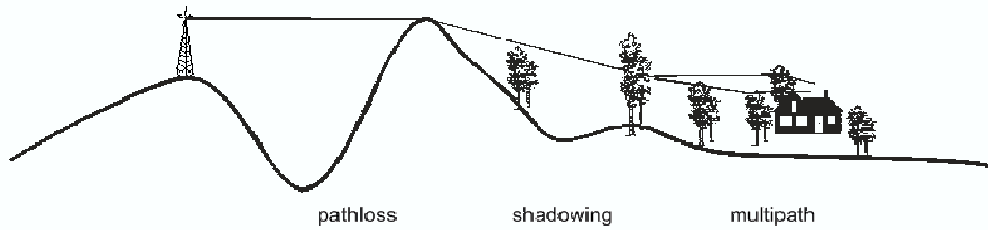


Figure 2.1: Wireless Channel Propagation Phenomena

2.1.1 Path-loss and Shadowing

Path-loss is the direct energy loss while the radio signal propagates from the transmitter to the receiver. It is mainly caused by: *free-space loss*, as the radio wave front expands in the shape of an ever-increasing sphere; *absorption*, since the signal usually propagates through non-transparent media rather than free space; and *diffraction*, since part of the radiowave front may be obstructed by opaque obstacles. Path-loss is usually expressed in the following form,

$$L = 10 \cdot n \cdot \log_{10}(d) + C \quad (2.1)$$

where L is the path-loss in decibels (dB), n is the path-loss exponent, normally in the range of 2 to 4 (2 is for free space propagation, 4 is for relatively serious loss environments), d is the distance between the transmitter and the receiver, and C is a constant which depends on the carrier frequency, environment type (e.g., rural, urban, suburban, indoor), and other system loss factors. In wireless channel modelling, this path-loss expression is in a deterministic form once the environment type is specified.

Shadowing is a large scale fading phenomenon caused by obstacles like hills,

buildings, trees, in the main signal path which results in attenuation of the signal. The signal attenuation level of shadowing is decided by the carrier frequency, the size and shape of obstacles. Unlike path-loss, shadowing is usually modelled with a random variable following Log-normal distribution (in linear unit, or a Normal distribution in log scale) [7].

2.1.2 Multipath Fading

Multipath fading is introduced by the signal reflection by the objects between the transmitter and the receiver, which can be anything on the signal propagation path, from buildings, trees, vehicles, hills to human beings. Thus, multiple reflections from the same transmission source will arrive at the receiver with different signal strength and phases. The received signal is the constructive or destructive combination of these random reflected signals. If a direct transmission path exists between the transmitter and the receiver, called Line-Of-Sight (LOS) path, the channel can be modelled with a Rice distribution; if there is no LOS path, the channel can be modelled with a Rayleigh distribution [7], [3].

Delay spread is an important effect of multipath. If we use impulse response to represent the multipath channel model, delay spread is defined as the time difference between the first and the last received impulses. Thus,

$$T_d := \max_{i,j} |\tau_i(t) - \tau_j(t)| \quad (2.2)$$

The delay spread together with the transmitted *signal bandwidth*, B_s , decide whether the channel is a frequency flat fading channel or a frequency-selective fading channel.

The channel transfer function is the Fourier transform of the impulse response, in which the amplitude or power spectrum changes as frequency varies [3], as depicted in Fig. 2.2(b) and 2.2(a). How quickly the channel changes in frequency can be measured with frequency coherence, namely *coherence bandwidth*, B_c . This parameter is defined as the smallest value of frequency difference Δf for which the frequency correlation function equals some suitable correlation coefficient, e.g. 0.5 or 0.9.

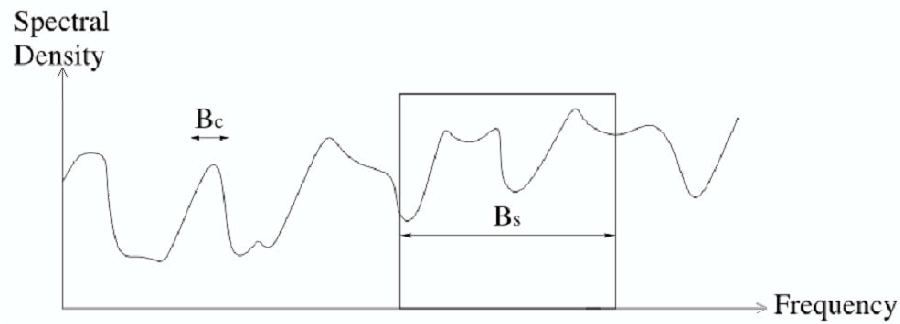
$$B_c \propto \frac{1}{T_d} \quad (2.3)$$

Coherence bandwidth is inversely proportional to delay spread, and the exact mapping between them depends on the correlation coefficient. Therefore, if $B_s \gg B_c$ as illustrated in Fig. 2.2(a), this channel is a frequency selective channel, whereas if $B_s \ll B_c$ as illustrated in Fig. 2.2(b), this channel is a frequency flat fading channel.

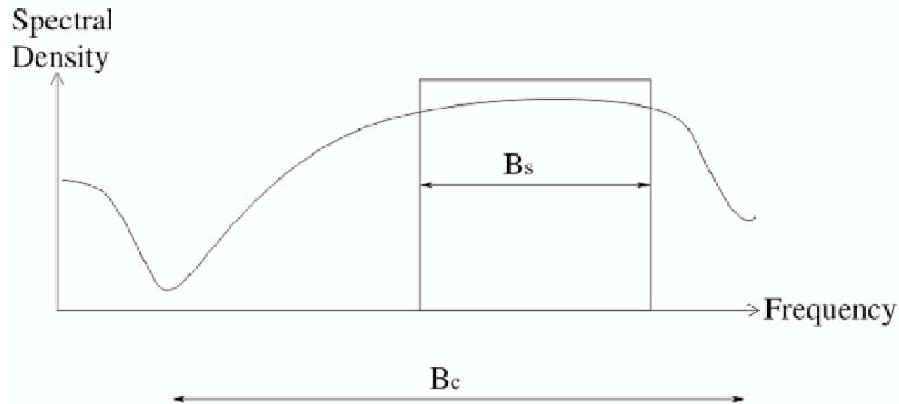
2.1.3 Channel Fading versus Modulation

Pathloss and shadowing are semi-static phenomena, and the signal attenuation due to them can be compensated with careful cellular network planning and power control. But the effect of Multipath fading is much more difficult to cope with.

For wide-band wireless communication systems, multipath fading causes frequency-selective fading, because the coherence bandwidth of the channel is always smaller than the whole transmission bandwidth. For Single Carrier Modulation (SCM) transmission, each baseband data symbol is modulated over the whole transmission bandwidth, and the symbol duration is very short since the data rate is high. Complex Equalizers at the receiver are needed to compensate the



(a) Spectral Density of A Frequency-Selective Fading Channel



(b) Spectral Density of A Flat-Fading Channel

frequency-selective channel transfer function in wide-band SCM systems. If the frequency-selective fading cannot be compensated, this effect results in the time domain distortion of each symbol on baseband, and leads to Inter-Symbol interference (ISI). Symbol errors caused by ISI are also hard to be corrected by error control coding, since these errors are correlated. It is difficult to combat frequency-selective fading with Equalizers because the multipath fading characteristics are random, varying fast and unpredictable.

In Multiple Carrier Modulation (MCM) transmission, the whole bandwidth is divided into multiple sub-carriers and multiple baseband symbols are modulated on these sub-carriers on parallel. If the spacing between neighbor sub-carriers is larger than the coherence bandwidth, the fading level on each subcarrier is usually

flat and the ISI is eliminated. However, the fading level difference still exists among different sub-carriers, but it can be exploited by link adaptation schemes, namely, frequency diversity. If the signal quality on one subcarrier is too poor and the symbol on this subcarrier cannot be correctly received, it will not effect other symbols. Besides, such symbol errors are independent and are relatively easy to be corrected by error control coding schemes such as convolutional codes.

In summary, to combat multipath fading in wide-band wireless communications, this is one important reason to introduce MCM transmission technique such as OFDM.

2.2 Orthogonal Frequency Division Multiplexing (OFDM)

OFDM is a multi-carrier modulation (MCM) technique as well as a multiplexing technique, in which a data stream is split into several lower data-rate sub-streams and they are used to modulate several sub-carriers in parallel. OFDM was created in theory back in 1960s, though only did it become commercially practical when the semi-conductor industry made Fast Fourier Transform (FFT) chips cheap enough. Before OFDM became the main-stream technique for the next generation wireless communications (e.g., in 3GPP Long Term Evolution (LTE) and IEEE 802.16 standards group), it has already been used in Asymmetric Digital Subscriber Line (ADSL), Digital Audio Broadcasting (DAB), Digital Video Broadcasting - Terrestrial (DVB-T) and the 5 GHz-Band Wireless Local Area Networks (WLAN) standard, namely IEEE 802.11a.

One of the main advantage of OFDM is its robustness to frequency selective fading and narrow-band interference. Such kind of fading or interference may

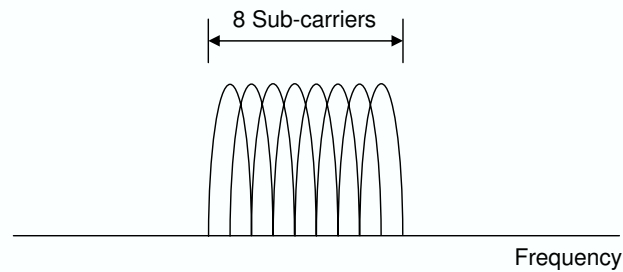


Figure 2.2: OFDM with 8 Sub-Carriers

corrupt an entire SCM link, but it can only affect a small portion of sub-carriers of a MCM link [1]. Due to this reason, a complex and expensive equalizer is needed in SCM receivers to compensate the channel transfer function, while in a MCM system like OFDM, no or only a very simple equalizer is needed.

OFDM is different comparing to FDM in its frequency sub-bands are overlapping to achieve the maximum spectrum efficiency, as shown in Fig. 2.2. By carefully selecting symbol rate and via DFT/IDFT implementation, the inter-subcarrier interference can be perfectly removed though the sub-carriers are actually overlapping, which is the so-called *orthogonality*. The main features of OFDM can be concluded as follow:

- Robustness again frequency selective fading and narrow-band interference.
- Maximum spectral efficiency due to no guard bands and the sub-carrier overlapping.
- Orthogonality among sub-carriers.
- Eliminate the inter-symbol interference by inserting a cyclic prefix into each symbol period.

- Easy and cheap implementation with FFT/IFFT and no or only simple channel equalizer needed.
- Sensitive to time-frequency synchronization to keep the orthogonality, such as sub-carrier synchronization.
- Sensitive to non-linear amplification.

The strict mathematical deduction and more detailed explanation of these listed OFDM features can be found in [1], [7] and [3].

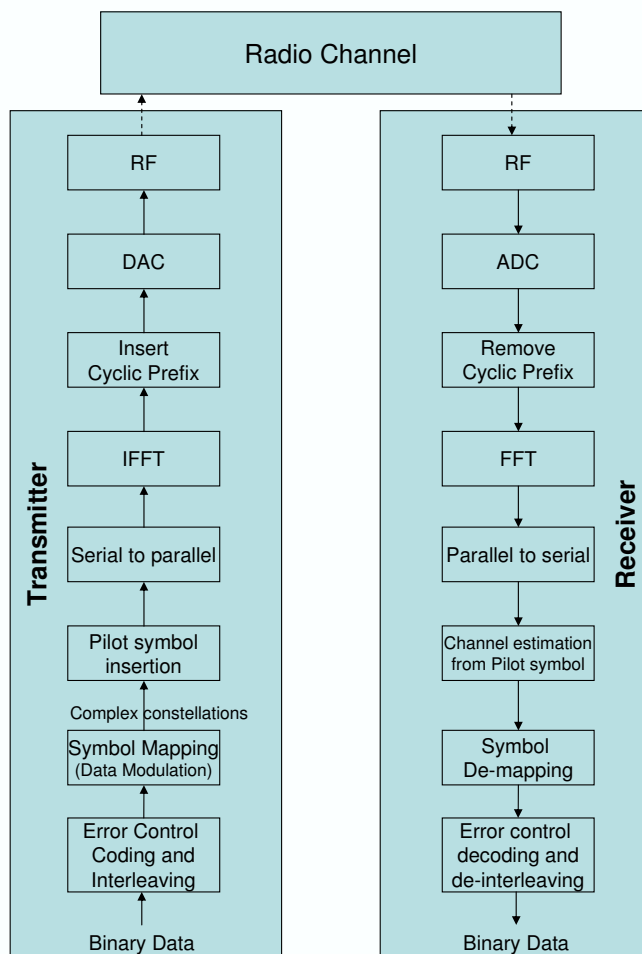


Figure 2.3: An OFDM Transceiver Diagram

A complete OFDM transceiver system diagram is depicted in Fig. 2.3. On

the transmitter side, binary data is input and Forward Error Correction (FEC) coding and interleaving are added to protect the data. Interleaving can re-distribute burst errors introduced by wireless transmission as random errors among original data, which are easier for FEC decoder to correct than burst errors. Afterwards, a block of coded bits are assigned to different OFDM sub-carriers (1 bit maps to 1 symbol for Binary Phase Shift Keying (BPSK), 2 bits per symbol for QPSK, 4 for 16 16QAM, etc.) and modulated to different constellation points respectively. At this stage, the data is mapped into a serial stream of complex numbers. Then pilot symbols are inserted. The serial symbols are converted to parallel form and the Inverse Fast Fourier Transform (IFFT) operation is applied. A Cyclic prefix [1] is inserted in every data symbol according to the system specification, and the data is now in serial form (time domain) again. So far the baseband OFDM modulation has been completed, and a Digital to Analogue Converter (DAC) is applied to transform the digital symbols to analog signal. Finally Radio Frequency (RF) modulation is performed to up-convert the signals onto the carrier frequency.

After the transmitted OFDM signal has gone through the wireless channel, the signal is captured by the receiver antenna and downconverted to baseband, and further converted to digital domain with Analog-to-Digital Converter (ADC). FFT is then performed to demodulate the OFDM signal, and the parallel symbols are mapped back to serial. At this point, channel estimation can be fulfilled with the demodulated pilots. The estimations helps detecting the data from the signal constellation points. At the end, FEC decoding and de-interleaving are performed to recover the originally bit stream.

2.2.1 OFDMA

A fraction of OFDM sub-carriers can be grouped to make up a sub-channel, and different sub-channels can be allocated to different users to construct the multiple access technique, namely OFDMA. At the beginning it was proposed for Cable Television (CATV) systems [5], and later for wireless communications [6].

The simplest OFDMA channel resource allocation scheme is to assign sub-channels to users in a static way as depicted in Fig. 2.4. In this scheme, the sub-channel assignment stays the same for the user during a whole connection, or at least for a considerable time period, i.e., during a service session. However,

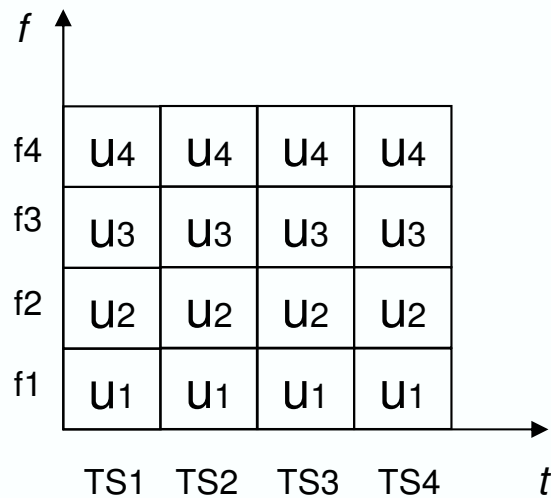


Figure 2.4: OFDMA with Static FDMA Scheme

such a static Frequency Division Multiple Access (FDMA) scheme is not efficient when a specific user is in deep fading channel. Actually sub-channels and Time-Slots (TS) can both be dynamically allocated to users according to their channel conditions and data rate requirements as shown in Fig. 2.5. Theoretically it has been proved that if the instantaneous channel condition on each subcarrier of each user is available, optimal allocation for subcarrier, time-slot and power in each

subcarrier will be possible to fully utilize user-diversity and to achieve the best system performance (i.e., maximum cell throughput, low BER) [8].

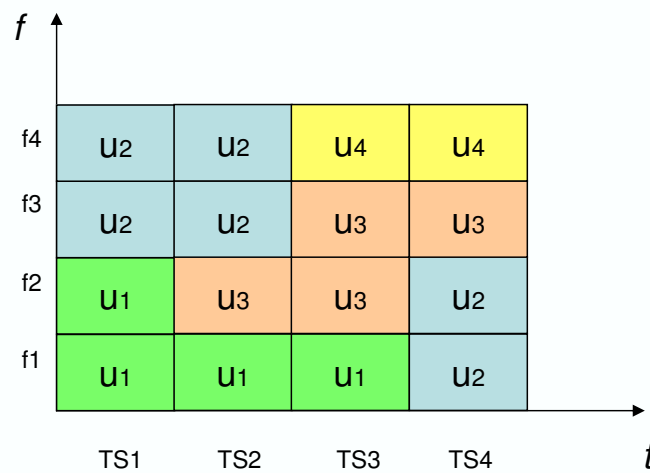


Figure 2.5: OFDMA with Fully Dynamic Frequency-Time Block Allocation

There are also two methods to construct sub-channels, the adjacent mode and the distributed mode [7], depending on whether the sub-carriers in a sub-channel are adjacent to each other or distributed among the whole transmission bandwidth with a certain frequency interval [9]. As illustrated in Fig. 2.6, the sub-carriers of a sub-channel in adjacent mode are contiguous, and the channel conditions of them may be similar. In this case one pilot sub-carrier can be used to detect the channel condition of the whole sub-channel, which may reduce the channel information feedback needed by AMC in the transmitter side. Also one modulation and coding combination can be applied to one sub-channel. Both of these advantages reduce the implementation complexity of sub-channel allocation and AMC. However, channel fading will also degrade the throughput of an adjacent sub-channel seriously, since one fading ditch in the channel transfer function curve (see Fig. 2.2(a)) can effect on several sub-carriers. In the distributed mode,

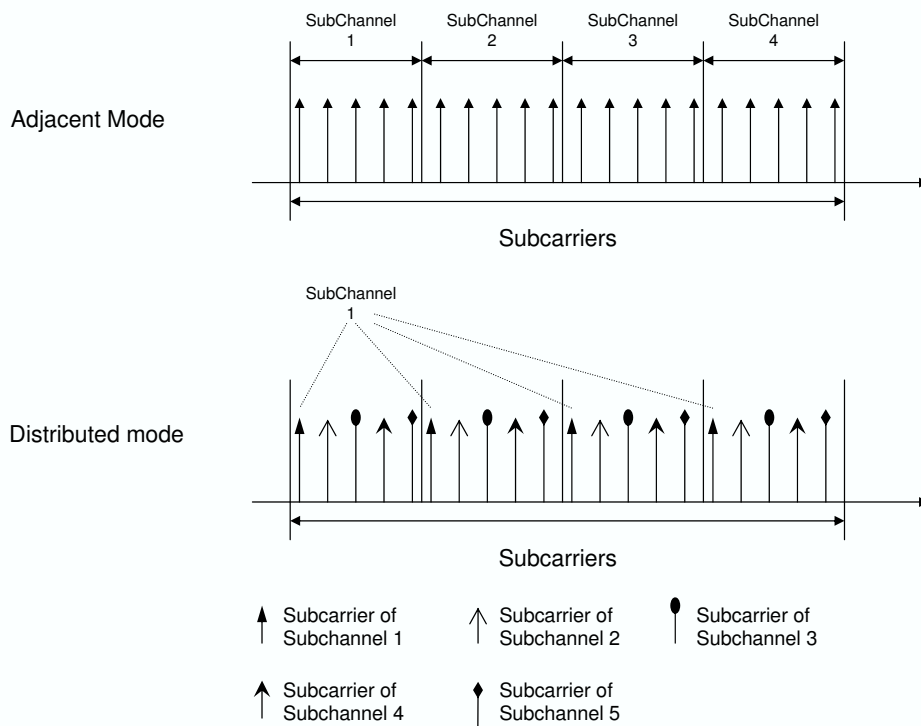


Figure 2.6: OFDMA Sub-Channel Modes

the sub-carriers are much further apart to each other, so they are more independent and more robust against frequency-selective fading, especially under harsh channel environment (i.e., when users are with high mobility). This is called channel diversity gain. On the other hand, it would be complex to make channel allocation and hard to implement AMC in distributed mode.

2.2.2 OFDMA-Based Standards Groups

There are two main next generation mobile OFDMA standards groups, the IEEE 802.16e (or the so-called WiMAX) and the 3GPP UMTS-LTE. They basically selected very similar specifications on the physical (PHY) layer, e.g., both of them support scalable channel bandwidth, AMC, MIMO techniques. Their difference

is that WiMAX is a group trying to include different stands covering from fixed wireless Internet access network to cellular-like mobile networks, while 3GPP LTE is a evolution from the pure mobile cellular system, UMTS.

2.2.2.1 IEEE 802.16 Standards Group

The IEEE 802.16 standards group is also called Worldwide Inter-operability for Microwave Access (WiMAX). This standardization group is proposed to provide wireless data in a variety of ways, from fixed point-to-point links to full mobile cellular type access. In this group, the amendment 802.16e-2005 (often referred to in shortened form as 802.16e) is called *Mobile WiMAX* since it covers full mobility support and promises to provide high data rate service anytime, anywhere [10].

Mobile WiMAX allows for scalable channel bandwidth from 1.25 MHz to 20 MHz in both licensed and unlicensed frequency bands, namely scalable OFDMA [11]. The scalable channel bandwidth is implemented through variable sub-channelization structure and FFT size to enables optimum performance in different scenarios limited by radio band allocation policy, available bandwidth, target user mobility, etc. Scalable OFDMA supports FFT size varying from 128 to 2048 points, and operates on $2 \sim 6GHz$ with fixed sub-carrier spacing around 11kHz. The main OFDM parameters in 802.16 standards group are listed in table 2.1.

Parameter	Mobile WiMAX Scalable OFDMA-PHY			
	FFT size	128	512	1024
Number of used data subcarriers	72	360	720	1440
Number of pilot subcarriers	12	60	120	240
Number of null subcarriers	44	92	184	368
Cyclic prefix (T _g /T _b)	1/32, 1/16, 1/8, 1/4			
Channel bandwidth (MHz)	1.25	5	10	20
Subcarrier frequency spacing (kHz)	10.94			
Useful symbol time (μ s)	91.4			
Guard time assuming 12.5 % (μ s)	11.4			
OFDM symbol duration (μ s)	102.9			
Number of OFDM symbol in 20ms frame (μ s)	198.0			

Table 2.1: OFDM Parameters in Mobile WiMAX [11]

2.2.2.2 UMTS-LTE

The 3GPP working groups have developed their radio access network standards in Universal Terrestrial Radio Access Network (UTRAN) from Wideband Code Division Multiple Access (WCDMA) to High-Speed Downlink Packet Access (HSDPA) and High-Speed Uplink Packet Access (HSUPA), all based on single carrier CDMA technique. OFDMA has been proposed for the long term evolution of UTRAN (called Evolved UTRAN (EUTRAN)) as downlink multiple access technique, while Single-Carrier FDMA (SC-FDMA) will be adopted for uplink [12, 13]. LTE feasibility study has been finalized on September 2006, after which actual specification development would be fulfilled.

The DL OFDMA in LTE also supports scalable bandwidth from 1.25 to 20MHz, with fixed sub-carrier spacing 15kHz. LTE fully exploits advanced techniques like Layer 1 Hybrid Automatic Repeat request (L1 HARQ), frequency domain scheduling, MIMO antenna technologies and AMC [12, 13]. Comparing to

UTRAN, EUTRAN has more functionalities on Node B and shortens the Transmission Time Interval (TTI) even to 0.5 ms (TTI is 2 ms in HSDPA). With the help of such short TTI and fast L1 ARQ, the round-trip delay can be reduced to 5 ms. More detailed LTE specifications can be found in the 3GPP website.

2.3 Radio Resource Management (RRM)

As introduced in the first chapter, RRM approaches are investigated for wireless multicast in this PhD project. This section discusses the available degrees of freedom in multicast scenarios as well as some OFDM specific issues.

The dominant cost for deploying a wireless network is normally the base stations (real estate costs, planning, maintenance, distribution network, energy, etc), and sometimes frequency license fees is also highly expensive. Therefore the typical objective of RRM is to maximize the system spectral efficiency in bit/s/Hz (or Erlang/MHz) per base station, with a certain level of QoS constraints. The constraints involve BER, packet loss rate or outage rate (as well as other metrics like delay, jitter, etc) due to noise, attenuation caused by long distances, fading caused by shadowing and multipath fading, co-channel interference and other forms of distortion. The QoS is also affected by blocking due to admission control, scheduling starvation or unable to the guarantee quality of service class that is requested by the users.

In general, RRM optimization problem can be formulated as either minimizing a cost metric (e.g. transmit power) or maximizing a reward metric (e.g. throughput) under system hardware constraints, service specific QoS requirements and the overall system state (e.g. the channel fading states of all the receivers

within a cell). In this thesis, our target is to maximize performance metric under QoS constraints.

Though RRM covers a wide range of approaches, in the scenario delimited in chapter 1 we are mainly interested in the link adaptation methods, namely AMC, power control and ARQ for our multicast problems. Admission control, handover and scheduling among different users/services are out of the scope of our work.

2.3.1 AMC and Power Adaptation

The term *power control* was frequently used to refer to the process of varying transmitting power level in order to keep a stable SINR target for voice service (with fixed transmission data rates) like in GSM and WCDMA, or in order to suppress interferences. However in the context of performance optimization for multimedia services, power is adjusted according to the channel condition rather to provide high data rate. Hence the term 'power adaptation' is employed instead of 'power control' from now on. Varying modulation rate and coding rate, no matter separately or jointly, change the transmitted data rate. So AMC (or just Adaptive Modulation or Adaptive Coding alone) can also be called data rate adaptation.

AMC and power adaptation pro-actively adjusts the transmitting data rate and power to adapt to the estimated channel conditions. If the estimated channel conditions are accurate, theoretically they can exploit the channel capacity in every transmission burst. The price is that the overhead in feedback channels to report channel conditions could be large. It has been proved in [15] that the Shannon capacity of a flat-fading channel can either be achieved by varying both transmission rate and power, or be achieved by varying the transmit power alone [16]. More-

over, it has also been revealed in [15] that varying both power and rate leads to a negligible capacity gain over varying the rate alone. Similar conclusions were drawn for achievable data rates in [17, 18].

2.3.2 Water-Filling Principle

In this subsection we discuss the possible dynamic schemes specific in OFDM for multicast radio channel. The available radio resources that can be manipulated include transmit power, modulation and coding allocation schemes, subcarrier or subchannel allocation. The dynamic utilizing of resources can exploit the frequency-selective nature of wireless channels due to Multipath fading. Usually the sub-carrier spacing of OFDM systems is larger than the channel coherence bandwidth, hence the attenuation within each sub-carrier is flat and the fading level of different sub-carrier is independent to each other.

For a time interval smaller than the channel coherence time of a wide-band wireless channel, the fading level on each sub-carrier stay constant, while the level among different sub-carriers are identical independent distributed (i.i.d) due to the frequency-selective nature of the channel. The optimal power allocation scheme on OFDM sub-carriers to maximize the channel capacity is given by the "water-filling" theorem [19] based on information theory, as illustrated in Fig. 2.7. This theorem states, when the total transmit power is fixed, more power should be assigned to the frequency areas with less attenuation (better channel condition), until the sum of assigned power and the reciprocal of channel gain per frequency is a

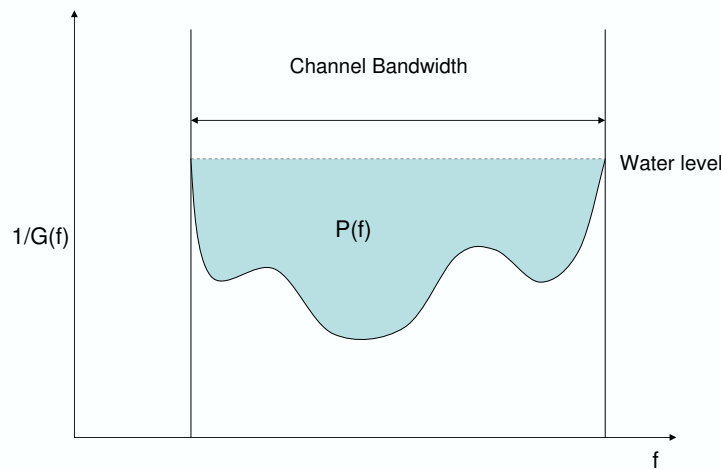


Figure 2.7: Illustration of "Water-Filling" Solution

constant over the whole bandwidth. Such as:

$$S(f) + \frac{1}{G(f)} = \text{constant} \quad (2.4)$$

where $S(f)$ is the power function along frequency, $G(f)$ is the channel gain function along frequency.

The water-filling solution is not directly implementable for two reasons. First the OFDM sub-carriers are discrete rather than continuous as in the water-filling solution; secondly, there is not a directly continuous mapping between power and bits per second in practice. The feasible data rate are a discrete set of numbers achieved by different combinations of modulation and error control coding schemes. Besides, any practical modulation has a certain "gap" between its achievable bits per second and the Shannon capacity. These issues will be discussed further in the following chapters.

The water-filling principle can be implemented in some discrete version of it, in terms of bit- or power-loading algorithms. In the optimal form the number of

bits transmitted per sub-carrier and the power assigned on each sub-carrier should be jointly allocated. But either bit- or power-loading can be implemented alone to achieve a certain sub-optimal performance for simplicity. Therefore, all these bit- and/or power-loading algorithms are referred to as adaptive loading algorithms in further discussion.

The joint power and rate allocation in water-filling form may apply not only along frequency dimension, but also along the channel gain distribution and more dimensions. How this form could be adopted in multicast channel is to be studied in the rest of this thesis.

2.3.3 ARQ

ARQ schemes can be divided into the following categories :

- Plain ARQ

Well-know plain ARQ schemes include Stop-And-Wait (SAW), Go-Back-N (GBN), and Selective Retransmission (SR), and more details can be found in International Engineering Task Force (IETF) Request for Comments (RFC) 3366 and [23].

- SAW ARQ

In SAW ARQ, a sender sends one data packet, and then waits. The receiver sends an Acknowledgement (ACK) once receiving a correct packet. The sender will only send the next packet once it receives the ACK for the first packet within a certain time. If the ACK has not come in time, known as a timeout, the sender sends the first packet again. In SAW, the fact that the sender needs to wait for every ACK wastes its transmission

capacity during the waiting time.

– GBN ARQ

GBN is more efficient than SAW in that it allows the sender continue sending a number of packets limited by a sliding window without receiving an ACK. The GBN ARQ receiver keeps tracking the received packet sequence numbers, and if one packet is incorrect, it will reject the following packets even if they are correct. The sender, after sending all packets in its window, will have to go back to the last ACK and restart sending from the first lost packet. In this protocol, some packets could have been correctly accepted by the receiver but may be rejected only because they follow an incorrect packet, and are to be resend, which also wastes transmission capacity.

– SR ARQ

Unlike GBN, SR ARQ allows the receiver to accept packets until the sender has emptied its window, and the sender needs only to resend the lost packets identified by ACKs/NACKs. Hence SR ARQ is more efficient than GBN.

• Hybrid-ARQ (HARQ)

Hybrid-ARQ combines ARQ and Forward-Error-Correction coding (FEC). There exist three types of HARQ: Type I, Type II and Type III, where Type III HARQ can be seen as a variation of Type II HARQ.

– Type I HARQ

In Type I HARQ, the original information and Error Detection (ED) parity bits are further encoded by a FEC encoder (such as a Turbo coder)

[35, 45] and sent to the receiver; if the receiver fails to decode this data block correctly, the same data block will be send again as in a pure ARQ. The receiver can either discard the first block or store it to combine with the retransmitted block, which is called Chase Combining (CC) in UMTS HSDPA [45]. Here FEC and ARQ are operated separately, or so-called Layered FEC-ARQ [26].

– Type II HARQ and Type III HARQ

In Type II HARQ, multiple parity code blocks are created for the original information, with Incremental Redundancy (IR)/reliability as the number of parity blocks increase. Only the original information and the least parity blocks are sent in the first transmission, and more parity blocks will only be sent as the receivers request [35, 45]. If each retransmission packet can be decoded independently, such HARQ is called Type III HARQ.

The performance of each of these ARQ protocols in uncash channels has been studied systematically. Plain ARQ (SAW and SR), Type I and Type II HARQ in uncash mobile link was analyzed in [35]. It revealed that pure ARQ achieves the best throughput efficiency under good channel condition, but degrades the most as channel condition get worse; Type I HARQ performs better in poor channel condition while lost efficiency in good channel; Type II HARQ with SR performs the best in both cases. It is proved in [45] that IR (Type II HARQ) is slightly more efficient in throughput than CC (Type I HARQ) in a very detailed HSDPA simulation environment, but the difference is very small or even diminishes as the link adaptation error decreases.

Also there are many existing works on the ARQ performance study for multicast links. The performance of plain ARQ schemes have been investigated in [31, 32, 33, 34], which confirmed that SAW is the most inefficient in terms of throughput [33], and SR is more efficient than GBN [33, 34]. Multicast HARQ schemes based on Reed-Solomon codes (namely Maximum Distance Separable (MDS) code) are analyzed for satellite links in [36]. The authors of [37] further utilized Generalized Minimum Distance (GMD) decoding for MDS, which improved the throughput a bit but increased the decoding complexity and delay. Three HARQ schemes based on packet level Reed-Solomon codes were designed in [5] for UMTS downlink multicast channel, and the authors pointed out which design is better would rather depend on the multicast channel error process in reality (e.g, independent error model or burst error model). The authors of [6] further proposed two more HARQ schemes as the extensions of scheme A2 and A3 in [5] and achieved a certain improvement in throughput and mean Service Data Unit delay, especially when the Multicast group size is large. However, the scalability of multicast ARQ protocols remains a problem [2].

2.4 State-of-the-art

In this section we discuss how the link adaptation approaches introduced in Sec. 2.3 can be adopted in multi-user systems, as well as the related works.

2.4.1 OFDM link adaptation and multi-user diversity

LA assigns modulation, coding, transmit power, and/or other signal transmission parameters according to the instantaneous channel condition, in order to increase

the spectrum efficiency and reliability of wireless systems. The water-filling principle introduced in Sec. 2.3.2 reveals, for an OFDM system with power constraint, the system spectral efficiency is maximized by transmitting with higher data rate (higher modulation constellation and less coding protection) and more power when the channel condition is good, while transmitting with lower data rate and less power when the channel condition is bad.

Different users in a wireless system experience different and independent channel attenuations and noise/interferences, which can be exploited as multi-user diversity. It is quite unlikely that a user is in deep fading on all the subcarriers, or all users are in deep fading on the same subcarrier. Hence the time-subcarrier can be dynamically assigned to different users according to their instantaneous channel conditions on different subcarriers to improve the spectral efficiency, as illustrated in Fig. 2.5, such dynamic approach is also called scheduling.

2.4.2 Related work with multiple unicast users

Based on water-filling principle and multi-user diversity, joint allocate/adapt subcarrier and data rate to multiple users was first proposed by Wong [8], target at minimizing total transmitting power with data rate and BER constraints. Similar dynamic allocation and adaptation work was done in [47], but the optimization target is to maximize data rate with power and BER constraints. However, the computational complexity of Wong's algorithm [8] is very high, and several more practical algorithms are proposed in [48].

Scheduling can maximize the system spectral efficiency, but it may also have the users in bad channel conditions experiencing high delay and low data rate.

Proportional Fair Scheduling (PFS) is designed to allowing all users a minimal level of QoS by assigning each data flow a scheduling priority which is inversely proportional to its anticipated resource consumption [50]. PFS can be tailored to integrate different QoS classes and achieve a high average user satisfaction [50]. On the other hand, joint time-subcarrier scheduling with PFS in OFDM system is a prohibitively complex problem. The authors of [51] derived the upper bounds for optimal PFS with convex optimization, and proposed sub-optimal solutions with much lower complexity comparing to the optimal one.

2.4.3 Related work with one multicast group

With one group of multicast users sharing a common downlink channel, scheduling is not an option any longer and link adaptation and ARQ remains the main dynamic adaptation approaches. An iterative optimization algorithm using link adaptation was proposed to minimize the total error ratio of all users under power and data constraints in OFDM [52]. In [53], based on a dominant SNR-based LA scheme, the authors appropriately discarded some inefficient transmission modes to convert the goodput-maximization problem to a concave optimization problem, and derive the optimal adaptation power and AMC modes correspondingly. However, in this approach, only the goodput is considered but there is no error constraints included.

2.5 Summary

This chapter presents the channel features and OFDM transmission technique related to our wireless cellular scenario, as well as available link adaptation tech-

niques for the multicast channel. For the concerned wide-band wireless system, multipath fading is the most difficult fading issue to cope with, and OFDM can help to split the whole frequency-selective fading channel into a set of frequency-flat fading channels over each subcarrier, where different LA (e.g., AMC, power adaptation, ARQ) can be adopted to improve wireless multicast performance.

Bibliography

- [1] Shinsuke Hara and Ramjee Prasad, *Multicarrier Techniques for 4G Mobile communications*, pp. 27-39, Artech House, 2003.
- [2] G. L. Stüber, *Principles of Mobile Communication*, 2nd ed., Kluwer Academic Publishers, 2001.
- [3] D. Tse and P. Viswanath, *Fundamentals of Wireless Communications*, Cambridge University Press, 2005.
- [4] M. I. Rahman, *Channelization, Link Adaptation and Multi-antenna Techniques for OFDM(A) Based Wireless Systems*, PhD thesis, Sept. 2007.
- [5] H. Sari, Y. Levy and G. Karam, “Orthogonal Frequency-Division Multiple Access for the Return Channel on CATV Networks,” in *Proc. IEEE ICT’96*, Istanbul, April 1996.
- [6] H. Sari, Y. Levy and G. Karam, “An Analysis of Orthogonal Frequency-Division Multiple Access,” in *Proc. IEEE GLOBECOM’97*, vol. 3, pp. 1635-1639, Nov. 1997.

- [7] H. Yaghoobi, "Scalable OFDMA Physical Layer in IEEE 802.16 Wireless MAN," in *Intel Technical Journal*, vol. 8, no. 3, pp. 201-212, 2004.
- [8] C. Y. Wong, R. S. Cheng, K. Letaief, and R. Murch, "Multiuser OFDM with adaptive subcarrier, bit and power allocation," in *IEEE J. Select. Areas Commun.*, vol. 17, no. 10, pp. 1747-1758, Oct. 1999.
- [9] D. Galda and H. Rohling, "A Low Complexity Transmitter Structure for OFDM-FDMA Uplink Systems," in *IEEE VTC'02 Spring*, Birmingham, USA, May 2002.
- [10] The IEEE 802.16 Working Group on Broadband Wireless Access Standards, "Part 16: Air Interface for Fixed and Mobile BraodbandWireless Access Systems," in *Tech. Rep., IEEE P802.16e Standard Document*, Dec. 2005.
- [11] Z. Abichar, Y. Peng and J. M. Chang, "WiMAX: The Emergence of Wireless Broadband," in *IEEE IT Magazine*, vol. 8, no. 4, pp. 44 – 48, Jul. 2006.
- [12] 3GPP Technical Report, "Physical layer aspects for evolved Universal Terrestrial Radio Access (UTRA), release 7," TR 25.814, v7.0.0, Jun. 2006.
- [13] A. Toskala, H. Holma, K. Pajukoski and E. Tiirola, "UTRAN Long Term Evolution in 3GPP," in *proc. IEEE PIMRC'06*, Helsinki, Finland, Sept. 2006.
- [14] J. Zander, "Radio Resource Management in Future Wireless Net works : Requirements and Limitations," in *IEEE Commun. Magazine*, pp. 30-36, Aug. 1997.
- [15] A. J. Goldsmith and P. Varaiya, "Capacity of fading channels with channel

- side information,” in *IEEE Trans. Inform. Theory*, vol. 43, pp 86-92, Nov. 1997.
- [16] G. Caire and S. Shamai, “On the capacity of some channels with channel state information,” in *IEEE Trans. Inform. Theory*, vol. 45, pp 2007-2019, Sept. 1999.
- [17] A. J. Goldsmith and S. Chua, “Variable-rate variable-power MQAM for fading channels,” in *IEEE Trans. Commun.*, vol. 45, pp. 1218 – 1230, Oct. 1997.
- [18] Seong Taek Chung, Andrea J. Goldsmith, “Degrees of Freedom in Adaptive Modulation: A Unified View,” in *IEEE Trans. Commun*, vol. 49, no. 9, pp 1561-1571, Sept. 2001.
- [19] C. E. Shannon, “Communication in the presence of noise,” in *Proc. IRE*, vol. 37, pp. 10-21, Jan. 1949.
- [20] M. Ergen, S. Coleri, and P. Varaiya, “QoS aware adaptive resource allocation techniques. for fair scheduling in OFDMA based broadband wireless systems,” in *IEEE Trans. Broadcasting*, vol. 49, no. 4, December 2003.
- [21] H. Yin and H. Liu, “An efficient multiuser loading algorithm for OFDM based broadband wireless systems,” *IEEE Globecom*, 2000.
- [22] C. Zhou, G. Wunder, and T. Michel, “Utility Maximization for OFDMA systems over discrete sets,” in *Proc. IEEE Int. Conf. on Communications (ICC)*, Glasgow, June 2007.
- [23] A. S. Tanenbaum, *Computer Networks*, 4th ed., pp. 200-223, Person Education International, 2003.

- [24] P. Larsson and N. Johansson, "Multi-User ARQ," *Proc. of IEEE VTC'06-Spring*, Melbourne, Australia, May 2006.
- [25] J. W. Atwood, "A classification of reliable multicast protocols," *IEEE Nextwork*, vol. 18, no. 3, pp. 24-34, May-June 2004.
- [26] J. Nonnenmacher; E. W. Biersack, and D. Towsley, "Parity-based loss recovery for reliable multicast transmission," *Networking, IEEE/ACM Transactions on*, vol. 6, no. 4, pp. 349-361, Aug. 1998.
- [27] L. H. Lehman, S. J. Garland, D. L. Tennenhouse, "Active reliable multicast," *Proc. IEEE INFOCOM'98*, vol 2, pp. 581-589, 29 March-2 April, 1998.
- [28] P. Radoslavov, C. Papadopoulos, R. Govindan, D. Estrin, "A comparison of application-level and router-assisted hierarchical schemes for reliable multicast," *Networking, IEEE/ACM Trans.*, vol 12, no 3, pp. 469-482, June 2004.
- [29] E. R. Berkekamp, *Algebraic Coding Theory*, McGrawHill, 1968.
- [30] F. J. MacWilliams and N. J. A. Sloane, *The Theory of Error Correcting Codes*, North-Holland, 1977.
- [31] S. B. Calo and M. C. Easton, "A broadcast protocol for file transfer to multiple sites," *IEEE Trans. Commun.*, vol. 29, no. 11, pp. 1701-1707, Nov. 1981.
- [32] K. Mase, T. Takenaka, H. Yamamoto, and M. Shinohara, "Go-back-N ARQ schemes for point-to-multipoint satellite communications," *IEEE Trans. Commun.*, vol. 31, no. 4, pp. 583-589, Apr. 1983.
- [33] I. S. Gopal and J. M. Jaffe, "Point-to-multipoint communication over broadcast links," *IEEE Trans. Commun.*, vol. 32, no. 9, pp. 1034-1044, Sept. 1984.

- [34] K. Sabnani and M. Schwartz, "Multidestination protocols for satellite broadcast channels," *IEEE Trans. Commun.*, vol. 33, no. 3, pp. 232-240, Mar. 1985.
- [35] R. Comroe, D. Costello, "ARQ Schemes for Data Transmission in Mobile Radio Systems", *IEEE Selected Areas in Commun.*, vol. 2, no. 4, pp. 472-481, July 1984.
- [36] J. J. Metzner, "An improved broadcast retransmission protocol," *IEEE Trans. Commun.*, vol. 32, no. 6, pp. 679-683, Jun. 1984.
- [37] K. Sakakibara, M. Kasahara, "A multicast hybrid ARQ scheme using MDS codes and GMD decoding," *IEEE Trans. Commun.*, vol. 43, no. 12, pp. 2933-2940, Dec. 1995.
- [38] L. Andrey, V. Vladimir, and Y. Mikhail, "Multicast QoS Support in IEEE 802.11 WLANs," *IEEE MASS'07*, Oct. 2007.
- [39] J. Y. Lim, T. M. Chung, "Enhanced token delivery scheme for reliable multicasting in wireless networks," In *Proc. IEEE PRIS'01*, pp. 214-217, Dec. 2001.
- [40] F. Fitzek, M. Rossi, and M. Zorzi, "Error Control Techniques for Efficient Multicast Streaming in UMTS Networks," in *Proc. SCI 2003*, 2003.
- [41] G. D. Papadopoulos, G. Koltsidas, and F. N. Pavlidou, "Two Hybrid ARQ Algorithms for Reliable Multicast Communications in UMTS Networks," *IEEE Commun. Letters*, vol. 10, no. 4, pp. 260-262, Apr. 2006.

- [42] Y. Yamauchi, "On the packet radio multicast scheme for the personal communications era," in *Proc. IEEE ICCS'94*, vol. 2, pp. 576-580, Singapore, Nov. 1994.
- [43] M. Chipeta, M. Karaliopoulos, B. G. Evans and R. Tafazolli, "On the use of packet-level FEC and data carousels for the delivery of broadcast/multicast services to mobile terminals," *IEEE VTC '05-Spring*, Stockholm, Sweden, May 2005.
- [44] Q. Zhang; F. Fitzek; V. B. Iversen, "Design and Performance Evaluation of Cooperative Retransmission Scheme for Reliable Multicast Services in Cellular Controlled P2P Networks," *IEEE PIMRC 2007*, Athens, Greece, Sept. 2007.
- [45] F. Frederiksen and T. E. Kolding, "Performance and Modeling of WCDMA/HSDPA Transmission/H-ARQ Schemes," In *Proc. IEEE VTC'02-Fall*, Vancouver, Canada, Sept. 2002.
- [46] S. Sesia, G. Caire, and G. Vivier, "On the Scalability of H-ARQ Systems in Wireless Multicast," in *Proc. IEEE ISIT'04*, pp. 321-321, 2004.
- [47] Y. J. Zhang and K. B. Letaief, "Multiuser Adaptive Subcarrier- and-Bit Allocation with Adaptive Cell Selection for OFDM Systems," *IEEE Trans. Wireless Commun.*, vol. 3, no. 5, pp. 1566, Sept. 2004.
- [48] G. Song and Y. Li, "Cross-Layer Optimization for OFDM Wireless Networks Part II: Algorithm Development," *IEEE Trans. Wireless Commun.*, vol. 4, no. 2, pp. 625 ~ 634, Mar. 2005.

- [49] H. J. Kushner and P.A. Whiting, "Convergence of proportional-fair sharing algorithms under general conditions," *IEEE Trans. Wireless Commun.*, vol. 3, no. 4, pp. 1250 ~ 1259, July 2004.
- [50] P. Svedman, S. K. Wilson and B. Ottersten, "A QoS-aware proportional fair scheduler for opportunistic ," *IEEE Vehicular Technology Conference, 2004. VTC2004-Fall.*, 26-29 Sept. 2004.
- [51] M. Kaneko, P. Popovski and J. Dahl, "Proportional Fairness in Multi-Carrier System with Multi-Slot Frames: Upper Bound and User Multiplexing Algorithms," *IEEE Trans. Wireless Commun.*, vol. 7, no. 1, pp. 22-26, Jan. 2008.
- [52] A. Demarez and D. Boulinguez, "Adaptive Bit And Power-Loading For Multicast OFDM Transmissions In Rayleigh Fading Channels," *International Symposium on Wireless Communication System*, 6-8 Sept. 2006.
- [53] Q. Du and X. Zhang, "Joint Power and Constellation Size Adaptation for Mobile Multicast Employing MQAM Over Wireless Fading Channels," *IEEE International Conference on Communications (ICC '07)*, 24-28 June 2007.
- [54] J. Y. Lee, J. Choi, K. Park, and S. Bahk, "Realistic Cell-oriented Adaptive Admission Control for QoS Support in Wireless Multimedia Networks," in *IEEE Trans. on Vehicular Tech.*, 52(3), May 2003.
- [55] Q. Liu, S. Zhou, and G. B. Giannakis, "Cross-Layer combining of adaptive Modulation and coding with truncated ARQ over wireless links," *IEEE Trans. Wireless Commun.*, vol. 3, no. 5, pp. 1746-1755, Sept. 2004.

Chapter 3

Rate Adaptation for Mobile Multicast

In this chapter we investigate the Adaptive Modulation (AM) strategies for Multicast service in OFDMA systems. To maximize the average throughput for a group of Multicast users, and keep as many as possible group members having acceptable QoS during a service session, a Reward function is firstly defined to evaluate this two-tuple optimization problem. Then a Local Reward strategy is designed and evaluated together with other AM schemes with a self-developed simulation tool. Based on the evaluation results, the evaluation metric is improved, and a history-based BER threshold adaptation is proposed to exploit the throughput-BER tradeoff further.

The chapter is organized as follows. Sec.3.1 explains the motivation. Sec. 3.2 presents the system model and assumptions. Sec. 3.3 describes our simulation tool. Sec. 3.4 proposes the first Reward function, corresponding AM schemes and numerical results, and Sec. 3.5 presents the second Reward function, corresponding AM algorithms and results. Sec. 3.6 summarizes the whole chapter.

3.1 Motivation

OFDM-based link adaptation techniques (e.g., power allocation, subcarrier allocation, adaptive modulation and coding) for uncash scenarios have been extensively studied in [6], [7], [8]. AM has been proved as an effective approach to improve the system performance if CSIs are provided. For uncash services, OFDM subcarriers can be allocated adaptively to different mobile users in downlink based on their channel quality. This diversity option helps the subchannel of each user avoid deep fading caused by multipath frequency-selective fading. By using Adaptive Modulation, high spectral efficiency can be achieved by selecting the highest modulation rate with a given acceptable BER constraint [8]. However, in the multicast case if all group members have to share the same downlink subchannel, deep fading subcarriers cannot be skipped by frequency scheduling. In this case whether and how the per subcarrier AM can improve efficiency (such as throughput) while keeping the BER acceptable is a problem.

A straight-forward strategy is to adapt modulation schemes always to the worst instantaneous channel among receivers, which can guarantee the multicast transmission reliability. However, due to the highly space-time varying nature of mobile receivers, each receiver could be in poor channel conditions at some time. Hence the adaptation strategy for worst case may keep the data rate low especially when the multicast group size is large [9].

3.2 System Model and Assumptions

In this section we describe our OFDMA system scenario, channel model and BER approximation approach. Based on the general system model presented in chapter 1, the common downlink multicast channel is assumed as a OFDMA subchannel occupying a portion of all the OFDM subcarriers, as shown in Fig. 3.1. The BS has perfect knowledge of the instantaneous channel quality in terms of SNRs of each subcarrier for each multicast group member within this multicast sub-channel, noted as $SNR(i, j)$, where $i = 1 \dots N$ is the index of multicast receivers, and j is

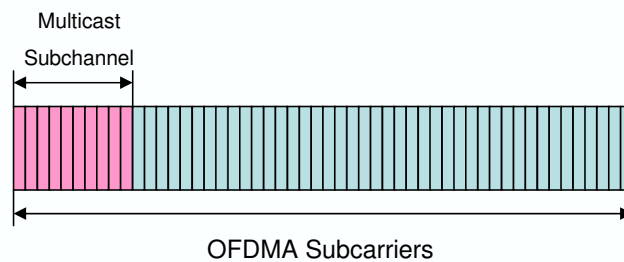


Figure 3.1: An OFDMA Adjacent Sub-Channel for Multicast

the index of OFDM subcarriers within a multicast subchannel. The base station has to allocate the appropriate modulation scheme to each OFDM subcarrier in the multicast subchannel for each transmission burst. The modulation scheme can be selected among BPSK, 4QAM, 16QAM, 64QAM, 256QAM, and "turn off", meaning no bit will be loaded to this subcarrier. We denote these options with K_M , where M is the modulation mode, and $K_M \in (0, 1, 2, 4, 6, 8)$ represents the number of bits per symbol on a subcarrier corresponding to this modulation mode.

3.2.1 OFDMA

The investigated system refers to the 802.16e scalable OFDMA PHY layer but not limited to it. The selected parameters for the OFDMA system in this work are listed in Tab. 3.1. Adjacent channel mode is selected here (also as illustrated in Fig. 3.1), because AMC is usually implemented in this mode as explained in chapter 2. The chosen frame size and duration is the largest in scalable OFDMA standard since we assume the users are pedestrians, where the channel coherence time is greater than 20ms.

Parameters	Values
Carrier Frequency	2GHz
Subcarrier spacing	11 kHz
FFT size (N-FFT)	128
Subcarrier Number in multicast subchannel	32
Subchannel mode	Adjacent mode
OFDMA Frame Size	198 symbols
OFDMA Frame duration	20ms

Table 3.1: Selected OFDMA Parameters

3.2.2 Channel Model

In this single cell scenario, inter-cell interference is not considered, and the Cyclic Prefix is assumed big enough to delimitate Inter Carrier Interference and Inter Symbol Interference. Hence the frequency selective fading presents the main effect of multipath distortion. The model from [12] is implemented to create one multipath fading level for each OFDM subcarrier during the channel coherence time. This model is chosen because it can easily scale to different OFDM system

settings. The normalized exponential delay profile is presented as

$$v_d = \frac{1}{V} e^{-\frac{d}{2D_{rms}}} \cdot w_d, \text{ for } d = 0, 1, \dots, D_{max} \quad (3.1)$$

where

v_d : the sampled complex delay profile;

D_{rms} : the rms delay in sample unit;

D_{max} : the maximum delay spread;

w_d : a complex Gaussian process with $mean = 0$ and $var = 1$;

V : the normalization factor.

Therefore the N-point complex channel gain is the N-FFT of v_d .

3.2.3 BER Approximations

To select the optimal modulation corresponding to received SNR level during each transmission, we need the close-form BER expression for each modulation scheme. For BPSK, it is

$$BER_{BPSK}(SNR) = \frac{1}{2} \text{erfc} \left(\sqrt{SNR} \right) \quad (3.2)$$

However, it is hard to find such close-form expression for non-binary modulation such as MQAM ($M = 4, 16, 64, 256, \dots$). Hence some BER approximation of MQAM has been proposed as [11]

$$BER_{MQAM}(M, SNR) \approx 0.2 \exp\left(\frac{-1.6 \cdot SNR}{2^{K_M} - 1}\right) \quad (3.3)$$

With the help of expression (3.2) and (4.12), the implemented adaptive strategies can choose modulation schemes based on continuous SNR-BER mapping. The complete BER approximation curves are depicted in Fig. 3.2, in which $BER \leq 10^{-3}$ is the target of all AM strategies.

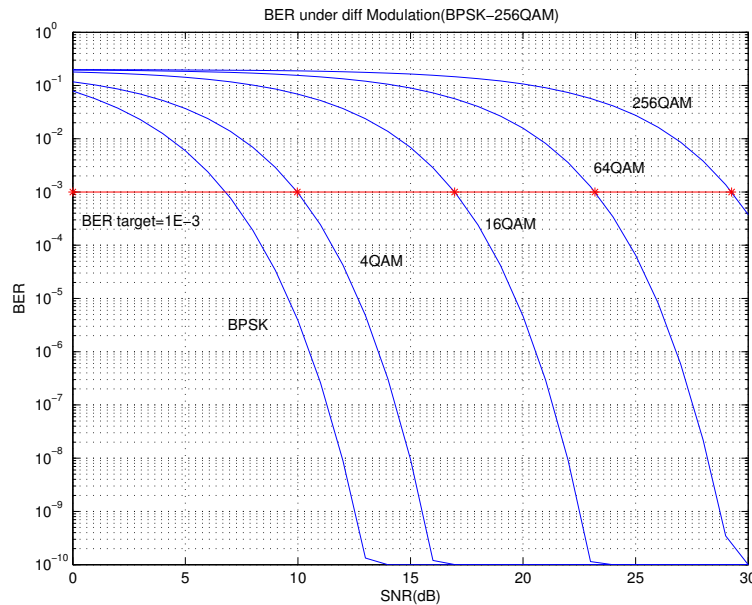


Figure 3.2: BER Approximations for BPSK and MQAM

3.3 Simulator Description

3.3.1 Simulation Scenario

The simulated scenario is a hexagon cell with three 120 degree antennas in the center. The mobile users are moving randomly within the cell. Hand-over is not considered so that the user who is going to cross the cell boundary will be bounced back. The important assumptions and parameter settings are described in Tab. 3.2.

Parameters	Values
Mobility model	TU3
Cell radius	1000m
User distance to BS	10 ~ 1000m
Antenna type	3 × 120 degree antennas
Antenna Gain	9dB
Distance attenuation coefficient	3.76
Lognormal STD	8dB
Correlation distance of slow fading	50m
UE noise figure	9dB
thermal noise density	-174dBm
Channel CSI report	Ideal
Modulation update interval	Every 4 Frames

Table 3.2: Important System Assumptions

3.3.2 System Level Simulator

The simulations were fulfilled in a self-designed system level simulator, as depicted in Fig. 3.3. The Geometry trace files are generated separately using some functions enhanced from Rudimentary Network Emulator (RUNE) [13], which include the changing positions of all the mobiles during one simulation run and the pathloss and the shadowing effects at each position. The mobile multicast users have uniformly distributed initial positions inside the cell and move randomly during the whole simulation. To explore all the possible geometry distribution of a multicast group, 20 different trace files have been generated and taken as input to test each modulation strategy. Among the system elements in Fig. 3.3, transmission power and noise are fixed during the whole simulation; Geometry is updated according to the user mobility speed on second level. Instantaneous channel gain is updated every transmission burst, which is 80ms long and equal to 4 OFDMA frames. Once the SNRs for all subcarriers in one transmission burst is generated, it is reported to the AM function. Finally the chosen modulation schemes and SNRs are put into the mapping functions to calculate the throughput and error bits of this

transmission (the error bits number is assumed to equal to its expectation, which is the expected BER times frame size).

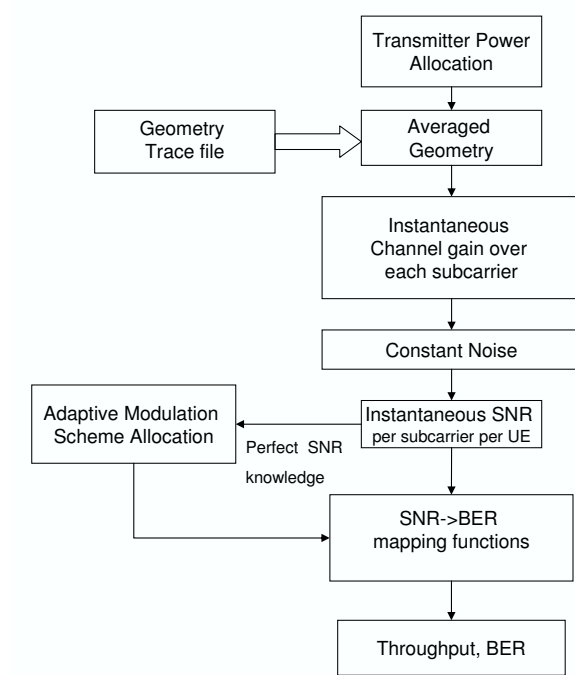


Figure 3.3: Simulator Diagram

3.4 Reward Function-Based Adaptation

3.4.1 Performance Evaluation Approach

The basic problem of adaptive modulation in OFDMA is to allocate modulation schemes, coding schemes, power among all the subcarrier/subchannels or any combination of these parameters. Assume the SNR reports from the UEs to the BS are perfect, we focus on the optimal modulation schemes assignment for a dedicated multicast subchannel. The power level of the subchannel is constant and evenly allocated among all subcarriers. Here the optimization target at not only the maximum throughput per user but also the user perceived QoS such as average

BER. The argument is that if the user perceived QoS is not at an acceptable level, high data rate alone will not make the user satisfied. Hence we defined the Reward function to include both:

$$R(T, S) = W1 \times T + W2 \times S \quad (3.4)$$

where

S represents the user satisfaction rate defined as

$$S = \frac{\sum_{i=1}^N J(\overline{BER}_i \leq \theta)}{N} \quad (3.5)$$

where J is defined as

$$J = \begin{cases} 1, & \text{if condition satisfied} \\ 0, & \text{otherwise} \end{cases} \quad (3.6)$$

N is the number of mobiles in the investigated multicast group.

T represents the Normalized Average user Goodput per session, defined as:

$$T = \left(\frac{1}{N} \sum_{i=1}^N Goodput_i \right) / Throughput_{256QAM}$$

$Goodput_i$ counts only the correctly received bits by receiver i during one service session, while

$Throughput_{256QAM}$ is the maximum possible throughput (always with the highest modulation rate and error-free) for the same duration. Hence T is normalized to be between $[0, 1]$.

\overline{BER}_i refers to the average BER of receiver i during the whole multicast service session.

θ is the average BER constraint, $\theta = 10^{-3}$.

W_1, W_2 are the relative weights of T and S in Reward function, $W_1 = W_2 = 1$, because we consider efficiency (throughput) and QoS (BER) equally important.

Although R can reflect the joint performance of throughput and BER, it cannot help to exclude the case that one strategy can result in a high Reward by using extremely high modulation rate such as 256QAM and a very low satisfaction rate where only a small portion of mobiles with high channel quality might be satisfied, which is not the purpose of a multicast service. So we add an additional evaluation constraint that only the strategy with $S \geq 50\%$ would be considered as a proper candidate for further performance analysis. This constraint can be easily included in Equation. 3.4, but to better reflect the behavior of all possible strategies we keep it separately.

3.4.2 Different Adaption Strategies

The main dilemma for a shared multicast channel is that different mobiles are experiencing different SNRs but they have to listen to the same signal, which makes it impossible to make the modulation optimal to each single mobile. The sub-optimal modulation scheme will be to provide the highest throughput within the BER boundary for most of the mobiles. Intuitively either the minimum, mean or the maximum SNRs of all mobiles on each subcarrier can be chosen as the Channel Quality Indicator to make the modulation rate selection. The drawback is that a single SNR value cannot reflect the instantaneous SNRs distribution of all the mobiles, hence the modulation scheme based on these strategies might not achieve the optimal Reward. To achieve the maximal Reward value for a multicast session, we defined a Best Local Reward strategy for adaptive modulation

and compared the performance among Mean SNR based AM strategy, Best Local Reward strategy and fixed modulation (BPSK/4QAM) strategy.

3.4.2.1 Best Local Reward Strategy

This strategy interpret the performance metric (3.4) into a Reward during each transmission burst, and chooses the modulation mode which can maximize this 'local' Reward, denoted as R' . To distinguish this R' (counted per transmission) from the performance metric, we call it Local Reward, and this AM strategy is named Best Local Reward strategy. That is, this strategy will use instantaneous SNR per UE per subcarrier to estimate the possible Local Reward of each modulation mode (BPSK,4/16/64/256QAM), and select the mode which maximizes Local R' for the current transmission burst, as illustrated in Tab.3.3:

<p>Input: $SNR(i, j), i \in (1, \dots, N)$.</p> <p>For subcarrier $j = 1:32$</p> <p>For modulation mode $M = \text{BPSK, 4/16/64/256QAM}$,</p> $S'(M, j) = \frac{1}{N} \sum_{i=1}^N J(\text{BER}(M, SNR_{i,j}) \leq \theta);$ $T'(M, j) = \frac{1}{N} \sum_{i=1}^N K_j(M)(1 - \text{BER}(M, SNR_{i,j}))/K_{256QAM};$ $R'(M, j) = W1 \times T' + W2 \times S';$ <p>End;</p> $M_{opt}(j) = \arg \max R'(M, j);$ <p>Assign M_{opt} to subcarrier j;</p> <p>End.</p>
<p>$BER(M, SNR_{i,j})$: the BER of receiver i on subcarrier j, estimated from the modulation mode and SNR value.</p> <p>K: the number of bits per symbol of each modulation mode.</p> <p>$S'(M, j)$: the local satisfaction rate of mode M on subcarrier j</p> <p>$T'(M, j)$: the local goodput of mode M on subcarrier j</p> <p>$R'(M, j)$: the local Reward of mode M on subcarrier j</p> <p>$M_{opt}(j)$: the optimal modulation mode on subcarrier j</p>

Table 3.3: The Best Local Reward Algorithm

3.4.2.2 Mean SNR Strategy

This strategy takes the average SNR among all the multicast group members over each subcarrier, and then choose the highest modulation rate which allow the $BER(M, SNR) < \theta$ for this subcarrier. This algorithm can be simplified as

$$\text{Mode } M \text{ is chosen for subcarrier } j \text{ if } \frac{1}{N} \sum_{i=1}^N SNR_{i,j} \in [\Gamma_m, \Gamma_{m+1})$$

where the SNR thresholds of each modulation mode, Γ_M , can be derived from Eq.3.2 and 4.12 as:

$$\Gamma_M = \begin{cases} (\operatorname{erfc}^{-1}(2\theta))^2, & K = 1 \quad (\text{BPSK}) \\ -\frac{\ln 5\theta}{1.6} (2^K - 1), & K = 2, 4, 6, 8 \quad (4, \dots, 256\text{QAM}) \end{cases} \quad (3.7)$$

and the resulted SNR boundaries of each mode for $\theta = 10^{-3}$ are listed in Tab. 3.4.

Modulation Scheme	SNR Thresholds (Γ_M, Γ_{M+1}] (dB)
BPSK	$(-\infty, 10]$
4QAM	$(10, 17]$
16QAM	$(17, 23]$
64QAM	$(23, 29]$
256QAM	$(29, +\infty)$

Table 3.4: SNR Thresholds for $BER < 10^{-3}$

3.4.2.3 Fixed BPSK/MQAM Strategy

As the simplest case, to always use one modulation scheme on all the subcarriers during the whole simulation.

3.4.3 Numerical Result and Analysis

In this section we first compare the performance of different AM strategies in the case $mean(SNR) = 28dB$. Then the impact of the SNR distribution on BER is analyzed. After that, the performance from the scenario $mean(SNR) = 35dB$ is presented.

3.4.3.1 Performance Comparison

The following figures are the final Reward curves from different AM strategies. While the global R in the evaluation metric keeps the same weights $W_1 = W_2 = 1$,

different weights combinations have been tried in R' to reveal best weights setting to maximize the Reward.

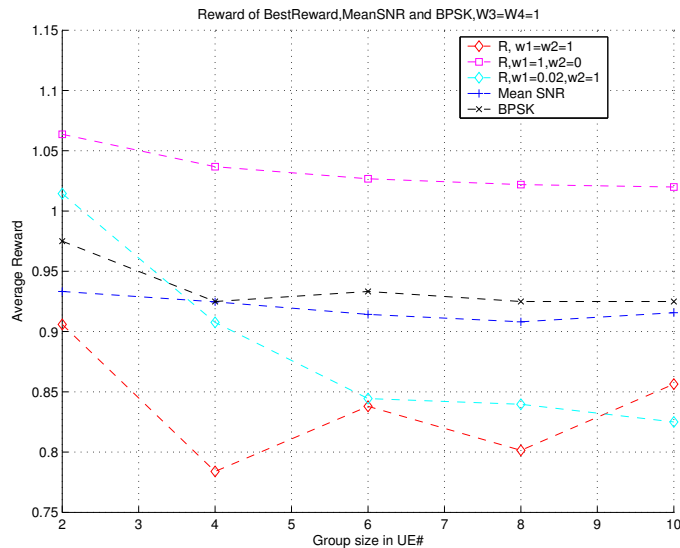
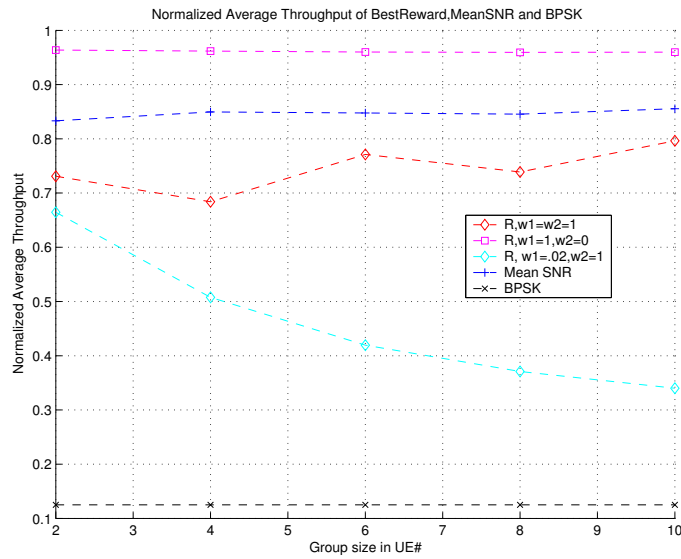


Figure 3.4: Reward under $E(SNR) = 28dB$

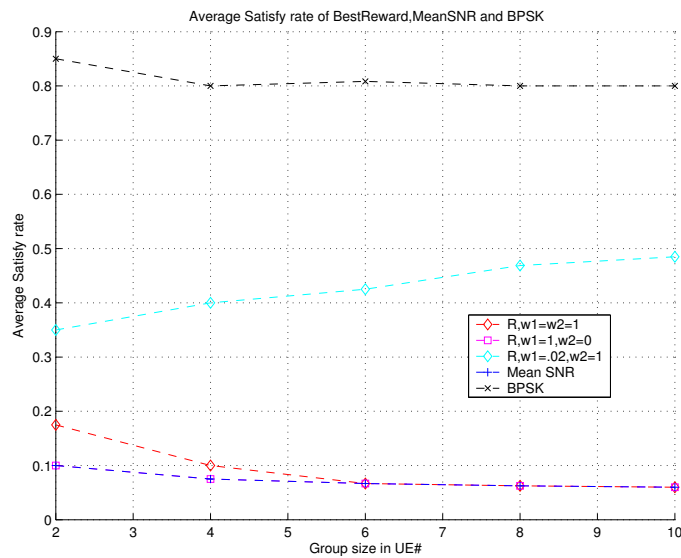
Surprisingly, in Fig. 3.4 it is not the $R'(w'_1 = w'_2 = 1)$ but the $R'(w'_1 = 1, w'_2 = 0)$ shows the best Reward performance. The former one which keeps the same weight setting shows a performance even worse than Mean SNR and BPSK strategy.

To reveal the reason, the normalized throughput and satisfaction rate are also plotted separately as in Fig. 3.5(a) and Fig. 3.5(b).

The throughput curves are as we expected: the $R'(w'_1 = 1, w'_2 = 0)$ which only takes throughput into account achieved the highest output; the $R'(w'_1 = w'_2 = 1)$ and Mean SNR make the median ones; and the BPSK only gives the lowest output. On the other hand, in Fig. 3.5(b) only the BPSK can achieve an average BER satisfying more than half of the mobiles, according to the second requirement of performance comparison. Other strategies all lead to the selection of a higher mod-



(a) Throughput under $E(SNR) = 28dB$



(b) Satisfaction Ratio under $E(SNR) = 28dB$

Figure 3.5: Throughput and satisfaction ratio ($E(SNR) = 28dB$)

ulation rate and sacrifice the BER. In this scenario (Mean(SNR)=28dB), adaptive strategies such as Mean-SNR based AM can achieve at most similar Reward as BPSK. Considering the extra computational complexity and CSI feedback load introduced by adaptive algorithms in the BS, adaptive strategies did not supply any gain in this case.

3.4.3.2 Impact of SNR on Average BER

An average SNR of 28dB is already a very high value in the real cellular system. To reveal why most of the strategies implemented failed to stay inside the BER requirement under such a high mean SNR, the impact of SNR on average BER in multicast scenario need to be analyzed. The SNR distribution of all subcarriers from all mobiles at each transmission is depicted in Fig. 3.6. If fixed modulation

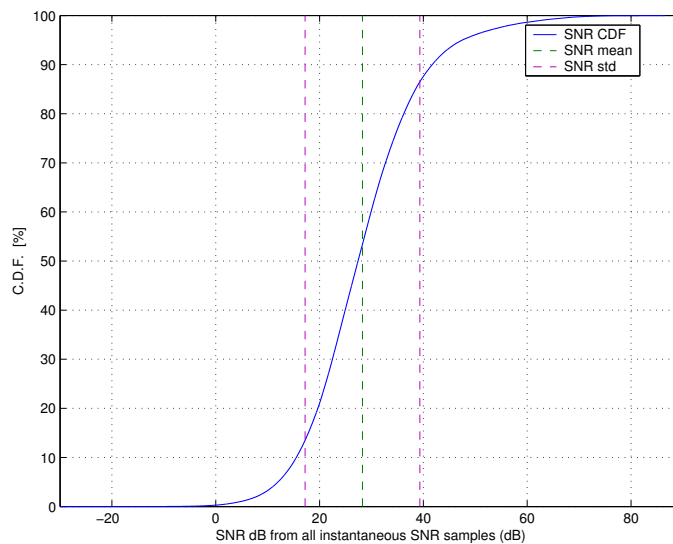


Figure 3.6: Cumulative Distribution Function (CDF) of SNR, Mean=28dB,STD=11dB

schemes are used for the simulation, the average BER for each modulation from instantaneous BERs of all SNR samples will be as shown in Tab. 3.5. This estimation implies that if most of the group members are expected to have an average

Modulation	E(BER)
BPSK	6.0×10^{-4}
4QAM	1.0×10^{-3}
16QAM	4.7×10^{-3}
64QAM	1.6×10^{-2}
256QAM	4.0×10^{-2}

Table 3.5: BER Estimations

BER within 10^{-3} , the modulation rate should not be higher than 4QAM. However, the normalized throughput in Fig. 3.5(a) shows on average the $R'(w'_1 = w'_2 = 1)$ led to 16QAM, whose data-rate is 75% of 256QAM, which results in a satisfaction rate lower than 20%.

This effect shows that even under an average SNR as high as 28dB, the average BER will be seriously downgraded due to those instantaneous deep fading, though they only occupy a very small portion in all the SNR samples. I.e, the SNR boundary for BPSK to achieve a $\text{BER} < 10^{-3}$ is about 7dB. There are 1.33% of all the SNR samples that fall into the region lower than this boundary.

3.4.3.3 Performance with a Higher SNR

To further investigate the performance of different modulation strategies, the transmitter power was increased until the average SNR reaches 35dB, as shown in Fig. 3.7. The Reward depicted in Fig. 3.8 shows that Mean SNR and $R'(w'_1 = w'_2 = 1)$ still resulted in poor performances. Rewards of BPSK and 4QAM keep stable as expected. $R'(w'_1 = 0.05, w'_2 = 1)$ achieved the highest Reward, which is 44% to 20% better than the second highest curve(4QAM) on average, as the group size increase. The vertical bars over $R'(w'_1 = 0.05, w'_2 = 1)$ and 4QAM curves show the 95% confidence intervals of them. The confidence intervals show that even when considering the fluctuation of simulation result, the advantage of

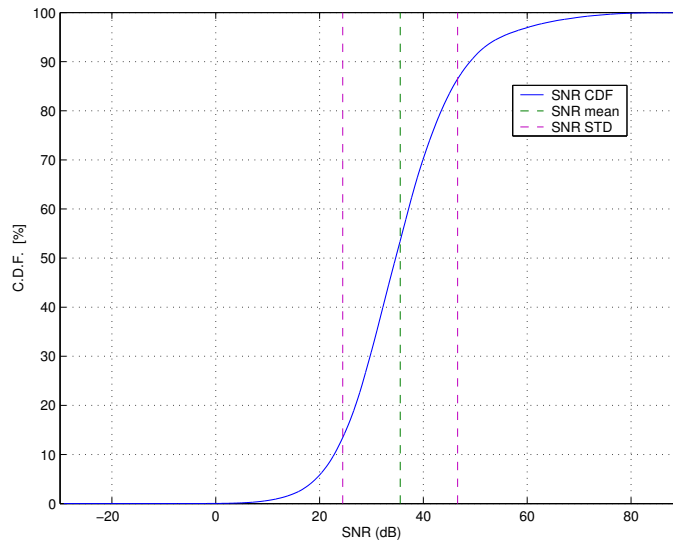


Figure 3.7: SNR CDF, Mean=35dB,STD=11dB

$R'(w'_1 = 0.05, w'_2 = 1)$ is still perceivable. Besides Reward, its satisfaction rate

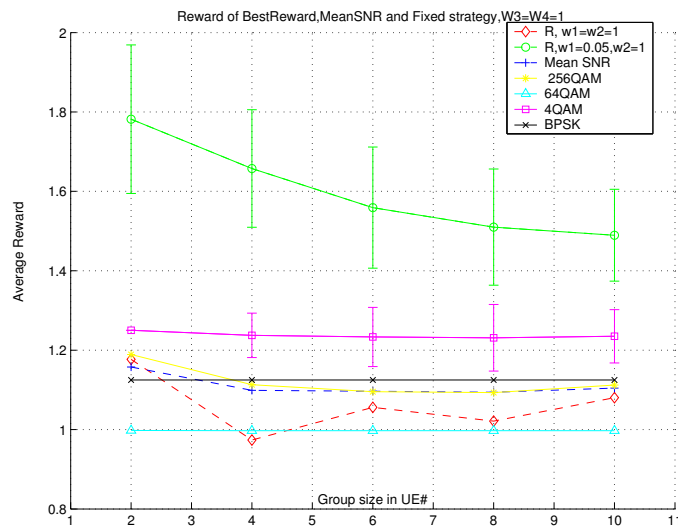


Figure 3.8: Reward under $E(\text{SNR})=35\text{dB}$

also achieved over 90% as in Fig. 3.9.

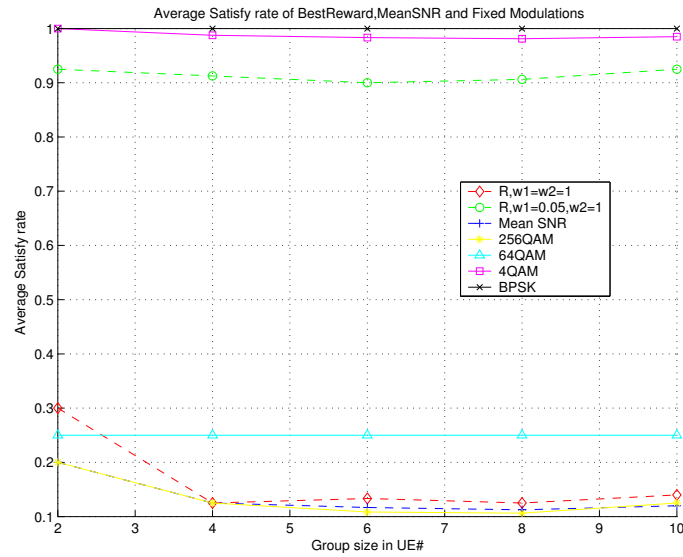


Figure 3.9: Satisfaction Ratio under $E(SNR) = 35dB$

3.4.4 Sub-Conclusion

In conclusion, whether adaptive modulation strategies can provide Reward gain depends on the SNR distribution scenario. When the average SNR is relatively low (28dB), using Fixed BPSK is the best strategy. When the average SNR is relatively high (35dB), the Local Best Reward strategy with higher weight on Satisfaction rate than on throughput ($w'_1 = 0.05, w'_2 = 1$) can achieve a significant gain comparing to all the other strategies.

Therefore optimizations efforts could be on how to supply the higher average SNR or to reduce the negative effect on BER from the deep fading subcarriers. One possible solution is to turn off some deep fading subcarriers. Another one is to allocate more power to the multicast subchannel or use adaptive power allocation over each subcarrier. If the multicast subchannel is allocated a much higher power than a normal uncash subchannel, the side effect such as interference to neighbor cells need to be considered.

3.5 History-Based BER Threshold Adaptation

The previous section reveals that the system performance is limited by the worst SNRs. If the adaptation strategy allows some instantaneous errors for the multicast receivers in a temporary deep fading, higher data rate can be allocated to the group and higher goodput may be achieved eventually. Since the deep fading stage of a receiver is only temporary, the average BER can still be controlled at an acceptable level in long term. That is, we propose an approach to keep track of cumulative errors of each receiver and optimistically adapt modulation for the multicast transmission, which we called a history-based adaptive modulation.

3.5.1 Performance Evaluation Metric

In the previous section, a Reward function is defined to include both throughput and BER, and the simulation results reflect the tradeoff between them. That is, throughput and BER cannot be maximized together, and the improvement of one always compromise the other. Hence we redefine the optimization target to maximizing the throughput while keeping the average BER constraint for the multicast group, and adopt a modified Reward function (R) as:

For a multicast service session,

$$R = T \cdot S \quad (3.8)$$

and

$$S = J \left(\frac{\sum_{i=1}^N J(\overline{BER}_i \leq \theta)}{N} \geq \mu \right) \quad (3.9)$$

where J has been defined in Eq. 3.6, T has been defined in Eq. 3.4.1.

μ stands for the required percentage of multicast group members within BER constraint. In this section, the target percentage is $\mu = 1$, then

$$R = \begin{cases} T, & \text{if, for all } i, BER_i \leq \theta \\ 0, & \text{otherwise} \end{cases} \quad (3.10)$$

3.5.2 Different Adaptation Strategies

Three AM strategies are compared in this section. Based on the sub-conclusion of Sec. 3.5, sub-carrier turnoff is adopted in each strategy.

(1) Best Local Reward Strategy with Fixed BER Threshold

Similar to the Local Reward strategy in the previous section, this strategy select the modulation mode which maximize the Local Reward R' .

This Best Reward function simply uses a fixed instantaneous BER constraint, θ . Assume receiver i had the lowest SNR on subcarrier j , and M is the highest modulation mode satisfying $BER(M, SNR_{i,j}) \leq \theta$ (which means $BER(M + 1, SNR_{i,j}) > \theta$). Then according to the definition of R' , $R'(M) > 0$ and $R'(M + 1) = 0$, the Best Reward algorithm will choose M . Therefore, on each subcarrier the lowest SNR among all receivers will limit the choice of modulation mode, which is a kind of adapt-to-worst strategy.

Comparing to the definition of R in the previous section, S has much stronger influence in the current R function. In the previous R , lower S may be compensated by higher T ; whereas the current R will switch between T and 0 depending on S . Therefore the new Best Local Reward strategy is even more conservative

<p>Input: $SNR(i, j), i \in (1, \dots, N)$.</p> <p>For subcarrier $j = 1:32$</p> <p> If $\exists SNR_{i,j} < \Gamma_{BPSK}(\theta)$</p> <p> Turn off subcarrier j,</p> <p> Else</p> <p> For modulation mode $M = BPSK, 4/16/64/256QAM$,</p> $T'(M, j) = \frac{K_j(M)}{K_{256QAM}} \times \frac{1}{N} \sum_i [1 - BER(M, SNR_{i,j})]$ $R'(M, j) = \begin{cases} T'(M, j), & \text{if, for all } i, BER_{i,j} \leq \theta \\ 0, & \text{otherwise} \end{cases}$ <p> End;</p> <p> $M_{opt}(j) = \arg \max R'(M, j)$;</p> <p> Assign M_{opt} to subcarrier j;</p> <p> End;</p> <p>End.</p>

Table 3.6: The Best Local Reward Algorithm with Fixed BER Threshold

than the one in previous section, and more optimistic adaptation strategy should be proposed.

(2) Reward strategy with Adaptive BER Threshold

The further proposal is to allow the instantaneous BER boundary to be varied to achieve higher throughput, and still keep the average BER within θ . Therefore, it is necessary to keep track of the cumulated BER, $BER_c(i)$, for each mobile individually, and adapt the $\theta_t(i)$ (instantaneous BER constraint for mobile i at transmission t) according to BER_c . That is, the calculation of the local Reward of each possible modulation becomes

$$R'(M) = \begin{cases} T, & \text{if, for all } i, BER_i \leq \theta_t(i) \\ 0, & \text{otherwise} \end{cases}$$

This idea is implemented in an Adaptive BER Threshold Algorithm, inspired by [14].¹ The coordination procedure between the Best Reward algorithm and the Adaptive BER Threshold Algorithm is illustrated in Fig. 3.10. The Best Local Reward function is mostly the same as in Tab.3.6, except each θ in the former is replaced by $\theta_t(i)$. The Best Reward function will start with the same $\theta_t(i) = \theta$, and the transmission result will be reported to the Adaptive BER Threshold Algorithm to decide $\theta_{t+1}(i)$ to be used by the Best Reward for the next transmission. In this way the BER history knowledge of each user is utilized: when a receiver has the worst SNR on subcarrier j at transmission time t , but it has a good average BER so far, it can have a higher BER limit than θ and the modulation mode allocated for the whole group can be higher.

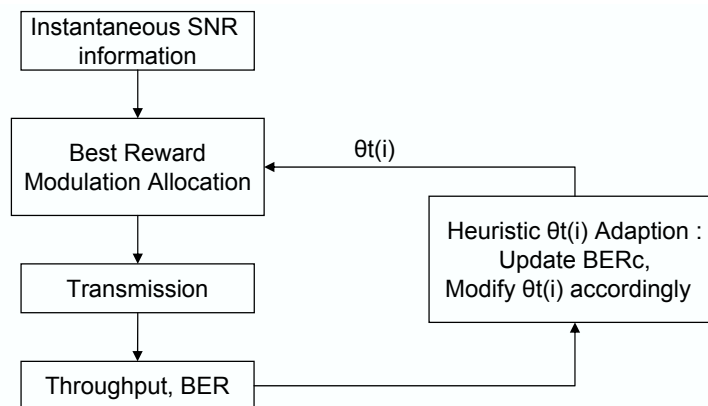


Figure 3.10: Best Reward AM with Heuristic BER Constraint

¹The work in Chapter 3 was inspired by the work in [14] in terms of varying a certain criteria in time domain. But the work in [14] is about access control according to the instantaneous cell load (session arrival, leaving, handover), with Markov chain analysis. The optimization scenario (session level V.S. transmission burst level), target metric, RRM approach (access control V.S. link adaptation) and corresponding parameters are totally different. This history-based BER threshold scheme is novel in the field of link adaptation.

Adaptive BER Threshold Algorithm

The important variables and parameters in this algorithm are:

$BER_c(i)$: $\frac{\text{Number of error bits received}}{\text{Number of bits received}}$ by UE_i from the transmission starts to current time;

θ_1 : The arbitrary lower boundary of the optimal BER interval;

$\theta_t(i)$: Instantaneous BER Threshold for the next transmission for UE_i , initially

$\theta_t(i) = \theta$;

θ_{max} : Maximum allowed value of $\theta_t(i)$;

δ : The multiplicative factor to increase $\theta_t(i)$.

```

For  $i = 1 : N$  % for each multicast group member
  update  $BER_c(i)$  based on the previous transmission output;
  IF  $0 < BER_c(i) < \theta_1$  THEN
    % BER too good, loose threshold
     $\theta_t(i) = \min(\theta_t(i) \times \delta, \theta_{max})$ 
  ELSE IF  $BER_c(i) > \theta$  THEN
    % BER break boundary, tight threshold
    IF  $\theta_t(i) > \theta$ , THEN
       $\theta_t(i) = \theta$ ;
    End
  ELSE IF  $\theta_1 \leq BER_c(i) \leq \theta$ ,
    This is the optimum case, keep  $\theta_t(i)$  unchanged.
  End
End.

```

Table 3.7: Adaptive BER Threshold Algorithm

There are two states in this instantaneous BER threshold varying process: the maximizing utilization state and the compensation state. In the maximizing utilization state, $\theta_t(i)$ will be temporarily increased to gain higher data rate. If $BER_c(i)$ becomes greater than θ afterward, the algorithm will switch to compensation state. In the compensation state the where $\theta_t(i)$ will be decreased, which should result in less instantaneous errors in subsequent bursts until the BER_c fall

back.

There are many ways to increase and decrease $\theta_t(i)$. In the initially design, $\theta_t(i)$ is increased by multiplying with a factor δ , and reduced by setting back to θ .

(3) BPSK with Turn-off Strategy

This strategy is simulated solely for comparison. It either select BPSK, or turn off the subcarrier j when the $\min SNR_{i,j}$ cannot satisfy $BER(BPSK, SNR) \leq \theta$.

3.5.3 Simulation Results and Analysis

The simulation results in terms of Reward are depicted in Fig. 3.11. It shows the Best Reward strategy with adaptive BER threshold achieved the highest Reward. The curve of the Best Reward strategy with fixed instantaneous BER constraints is the second highest and much higher than the fixed BPSK modulation. Fig. 3.12

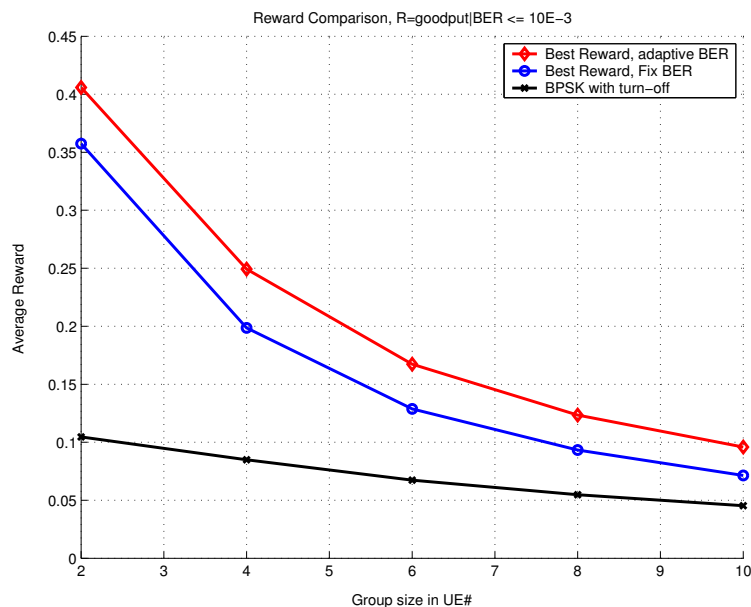


Figure 3.11: Reward Comparison, $E(SNR)=20\text{dB}$

depicts the average BER of these strategies. Fig. 3.11 and Fig. 3.12 together

reflect the trade-off between average BER and Reward. Best Reward with adaptive BER strategy achieved the highest Reward by pushing the average BER level closer to 10^{-3} , while Best Reward with fixed instantaneous BER result in the BER level nearly 10^{-4} and lower Reward. The BPSK scheme, provided the best reliability and the worst Reward as expected. Theoretically it should be possible to push this BER curve even closer to 10^{-3} by algorithm optimization or parameter optimization, to achieve the highest Reward.

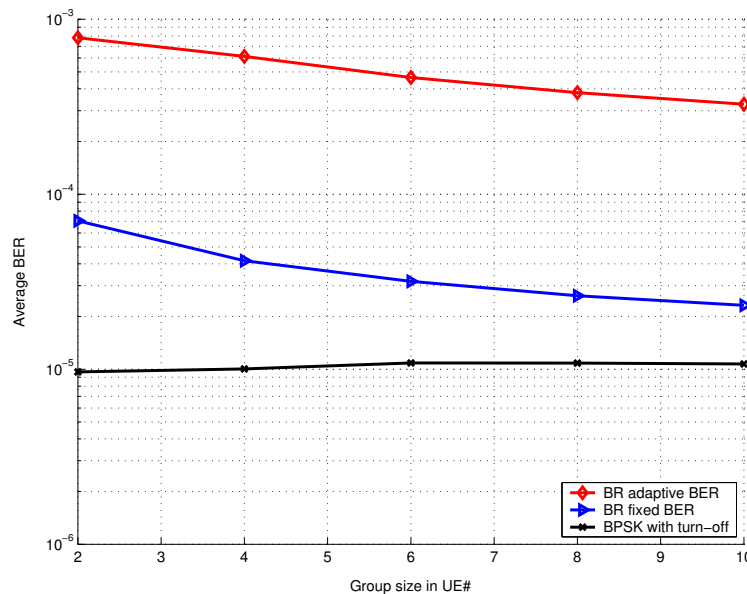


Figure 3.12: Average BER Comparison, $E(SNR)=20dB$

3.5.3.1 Impact of Group Size

In Fig. 3.11 all the Reward curves go down as the group size increase. Because the more users in a group, the higher probability that one of them subjects to deep fading which results in SNRs even lower than the threshold of BPSK. Though there is also higher probability that some members get higher SNR at the same time, they cannot impact on the modulation selection as the lowest SNR can do. The

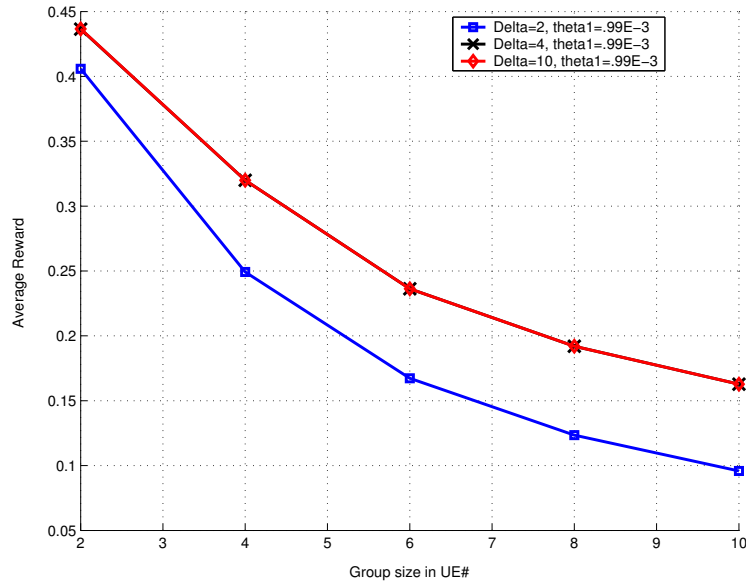


Figure 3.13: Impacts of δ Settings on Adaptive BER Algorithm, $E(\text{SNR})=20\text{dB}$

proposed Best Reward with BER adaption algorithm achieved higher gain as the group size increases, i.e, its Reward values are 13.5%, 25.6%, 30.3%, 32.5%, 34.4% higher than those of Best Reward with Fixed BER Threshold strategy at the group sizes (2, 4, 6, 8, 10), respectively.

3.5.3.2 Impact of Parameters Setting

The parameter δ decides the speed to loosen $\theta_t(i)$. We start with the simplest case that $\delta = 10$, which means $\theta_t(i)$ only needs to switch between θ and θ_{max} . Other initial settings of this algorithm are: $\theta_1 = 0.99 \times 10^{-3}$ and $\theta_{max} = 10^{-2}$. The results in Fig. 3.11 and Fig. 3.12 came from these initial settings. Later some selective input parameter sets are also tested to reveal their impact on the performance of Best Reward with Adaptive BER algorithm, as shown in Fig. 3.13 and 3.14. Fig. 3.13 shows that stepwise adaptation of $\theta_t(i)$ (e.g., $\delta = 2, 4$) did not further improve Reward gain comparing to the simplest case $\delta = 10$. On the other

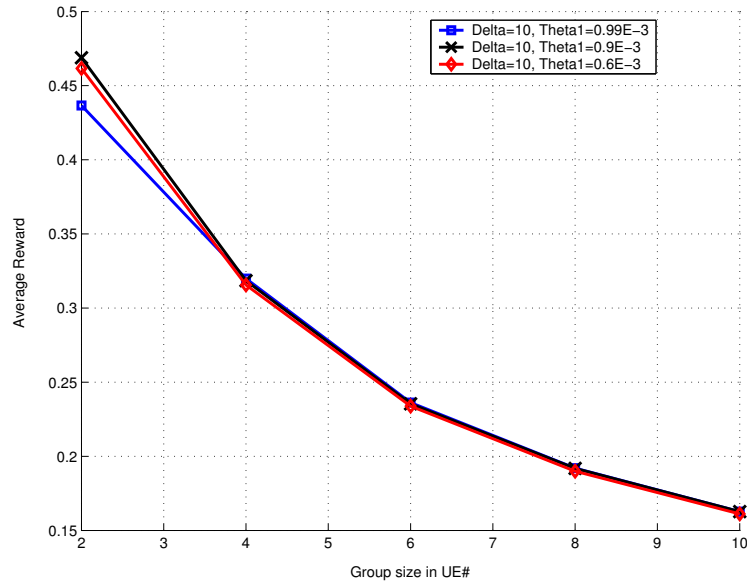


Figure 3.14: Impacts of θ_1 Settings on Adaptive BER Algorithm, $E(\text{SNR})=20\text{dB}$

hand, different θ_1 settings only have minor impact on R as presented in Fig. 3.14, mainly on the small group size case (2 users only). Therefore it is better to simply switch $\theta_t(i)$ between θ and θ_{max} .

3.5.3.3 Spectrum Efficiency Gain

When we interpret the result back to spectral efficiency, it is counted from a cell perspective how much information has been effectively served to multicast users per unit bandwidth, calculated as

$$\frac{\sum_{i=1}^N \text{Successfully received bits/sec of } UE_i}{\text{Bandwidth of the multicast channel}}$$

The result in Fig. 3.15 verified that the spectral efficiency of the proposed AM algorithm outperforms the others, and it can gain as high as 6.58 bps/Hz comparing to the Best Reward with Fixed Threshold algorithm at large group size. In this figure the curve of the Best Reward with Fixed Threshold strategy is not in-

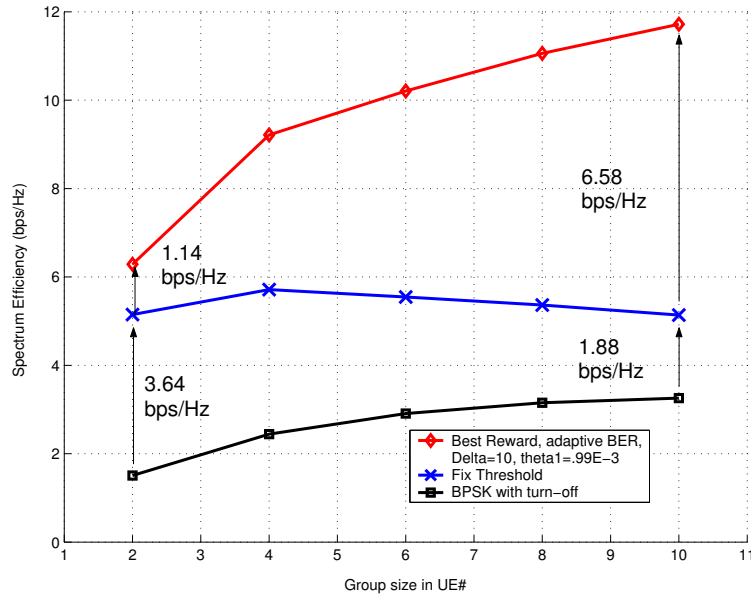


Figure 3.15: Spectrum Efficiency of AM Strategies, $E(\text{SNR})=20\text{dB}$

creasing monotonically, meaning the loss in average throughput may not always be compensated by the increment of group members.

3.5.4 Sub-Conclusion

In this section, the Best Reward with Adaptive BER threshold algorithm optimistically relaxes the instantaneous BER constraints based on the BER history of each multicast user, and achieves large performance gain. The proposed algorithm shows even bigger advantage comparing to other strategies when the group size is large.

3.6 Conclusion

In this chapter the OFDM-based AM approaches are studied with Reward functions as performance metrics. The Reward functions are designed in order to include both the throughput and the average BER per multicast receiver (in terms

of satisfaction rate S). It is more convenient to include BER in the Reward function of Sec. 3.5 than in the Reward of Sec. 3.4, since it is not easy to decide what weight settings for throughput and satisfaction rate would be the best.

A few AM schemes are proposed and their performances are compared via simulations. For the first Reward function, the simulation results show that it is necessary to turn off the subcarriers where some receivers are in deep fading, since these cases degrade the satisfaction rate seriously. Without subcarrier turnoff, the Best Local Reward strategy only outperform other AM schemes when the average SNR is very high. For the second Reward function, all the AM schemes adopt subcarrier turnoff option, and a history-based BER threshold adaptation is proposed to cooperate with the Best Local Reward strategy. Simulation results prove that this new proposal gain extra performance in both Reward and spectral efficiency by comprising the average BER, but still keep the BER constraint inviolated.

Based on the work of this chapter, further optimization efforts can be made in the following directions:

Defining more objective performance metric The design of a precise Reward function for mobile multicast services should better be supported the data from mobile network operators or service providers. As it is difficult to get such data, researchers often propose different Reward functions for the same problem and the outputs are difficult to compare. So it is better to use more objective performance metrics, which also reflect both throughput and BER, for further optimization.

Investigation method The investigation in this chapter is based on simulations, which include many detailed parameter settings, and the results and conclu-

sions are rather specific to such a simulation scenario. Even though the simulation can be repeated for different parameters settings, when the number of parameters is large or when the simulation is time-consuming, it is impossible to tryout many different parameters combinations. In this case, it is hard to predict the possible behaviors of the investigated algorithms in different scenarios, or to explain why some behaviors happen. Hence further work can be done to build analytical models.

More degrees of freedom Beside rate adaptation, power adaptation should also be investigated together for multicast link adaptations.

Note: The works presented in this chapter have been published in [15] and [16].

Bibliography

- [1] M. Hauge and Ø. Kure, “Multicast in 3G Networks: Employment of Existing IP Multicast Protocols in UMTS,” in *The Fifth International Workshop on Wireless Mobile Multimedia (WoWMoM 2002)*, Atlanta, USA, Sept. 2002,.
- [2] Y. Silva and A. Klein, “Adaptive Beam-forming and Spatial Multiplexing of Unicast and Multicast Services,” in *The 17th Annual IEEE International Symposium on Personal, Indoor and Mobile Radio Communications (PIMRC 2006)*, Helsinki, Finland, Sept. 2006.
- [3] J. L. Brito, A. Correia and A. Adetti, “Wireless techniques for capacity enhancement of broadcast and multicast for UMTS networks,” in *IEEE Vehicular Technology Conference 2004 (VTC’04-Fall)*, Los Angeles, USA, Sept. 2004.
- [4] Y. Sun and K. J. R. Liu, “Transmit diversity techniques for multicasting over wireless networks,” in *Wireless Communications and Networking Conference 2004 (WCNC’04)*, Atlanta, USA, March 2004.
- [5] K. Mori, K. Naito, H. Kobayashi and H. Aghvami, “Dynamic Subband and Code Channel Assignment for Multicast Band Division MC-CDMA Systems,”

- in *The 17th Annual IEEE International Symposium on Personal, Indoor and Mobile Raido Communications (PIMRC 2006)*, Helsinki, Finland, Sept. 2006.
- [6] C. Y. Wong, R. S. Cheng, K. B. Letaief and R. D. Murch, "Multiuser OFDM with Adaptive Subcarrier, Bit, and Power Allocation," in *IEEE Journal on Selected Areas in Communications*, vol. 17, no. 10, pp. 1747-1758, Oct. 1999.
- [7] S. Pietrzyk, G. J. M. Janssen, "Multiuser Subcarrier Allocation for QoS Provision in the OFDMA Systems," in *IEEE Vehicular Technology Conference 2002 (VTC'02-Fall)*, Vancouver, Canada, Sept. 2002.
- [8] E. Lawrey, "MULTIUSER OFDM," in *International Symposium on Signal Processing and its Applications 1999 (ISSPA'99)*, Brisbane, Australia, Aug. 1999.
- [9] N. Jindal, Z.Q.Luo, "Capacity Limits of Multiple Antenna Multicast," in *IEEE International Symposium on Information Theory 2006 (ISIT'06)*, Seattle, USA, July 2006.
- [10] J. Nonenmacher, E. Biersack, and D. Towsley, "Parity-based Loss Recovery for Reliable Multicast Transmission," in *ACM Trans. Networking*, vol. 6, no. 4, pp. 349-361, Aug. 1998.
- [11] S. T. Chung, A. J. Goldsmith, "Degrees of Freedom in Adaptive Modulation: A Unified View," in *IEEE Trans. Commun.*, vol. 49, no. 9, pp. 1561-1571, Sept. 2001.
- [12] S. Yoon, C. Suh, Y. Cho and D. S. Park, "Orthogonal Frequency Division Multiple Access with an Aggregated Sub-channel Structure and Statistical

Channel Quality Measurement,” in *IEEE Vehicular Technology Conference 2004 (VTC'04-Fall)*, Los Angeles, USA, Sept. 2004.

- [13] Zander.J and S.L.Kim, *Radio Resource Management for Wireess Networks*, Artech House, 2001, ISBN 1-58053-146-6
- [14] J. Y. Lee, J. Choi, K. Park, and S. Bahk, “Realistic Cell-oriented Adaptive Admission Control for QoS Support in Wireless Multimedia Networks,” in *IEEE Trans. on Vehicular Tech.*, 52(3), May 2003.
- [15] H. Wang, H. P. Schwefel and T. T. Nielsen, “Adaptive Modulation for a Downlink Multicast Channel in OFDMA systems,” in *Proc. IEEE Wireless and Networking Conference (WCNC'07)*, HongKong, China, Mar. 2007.
- [16] H. Wang, H. P. Schwefel and T. S. Toftegaard, “History-based Adaptive Modulation for a Downlink Multicast Channel in OFDMA systems,” in *Proc. IEEE Wireless and Networking Conference (WCNC'08)*, Las Vegas, USA, Mar. 2008.

Chapter 4

Multi-Dimensional Optimization with Analytical Model

The optimization approaches in the previous chapter are analyzed with simulations tools. When comparing different multicast link adaptation schemes, it is interesting to know the optimum performance limits of them, and to analytically reveal why some adaptation approaches are better than others. In this chapter, we assume a single carrier system and build an analytical framework to find out the achievable spectrum efficiency upper boundary of such a scenario. The optimal and sub-optimal adaptation schemes are derived under this framework and detailed parameter analysis are fulfilled. The problem of switching-threshold between unicast and multicast is also investigated in this chapter.

4.1 Motivation

The basic constraint in physical layer multicast adaptation is that, given a certain Bit-Error-Ratio (BER) constraint, the instantaneous transmission mode has to adapt to the worst instantaneous channel state among all the receivers, namely

worst-channel-limit. The investigations in [2], [4] and [3] propose approaches with MIMO and Beam-forming techniques to improve the worst channel condition of a multicast group, whereas the work in [3] develops rate adaptation schemes for multicast in OFDM systems. These approaches can certainly improve the multicast performance, but do not reveal what is the best possible adaptation scheme in their scenarios. Some other works propose theoretical approaches for optimal rate and/or power adaptation based on the Shannon capacity ([9], [1], [2]). However, the Shannon capacity requires some ideal assumptions which could be far from the constraints in reality[4]. For example, according to Shannon capacity

$$\frac{\mathcal{C}}{\mathcal{B}} = \log_2(1 + SNR) \quad (4.1)$$

where \mathcal{C} is the ideal channel capacity in bit/s and \mathcal{B} is the transmission bandwidth in Hz, and \mathcal{C}/\mathcal{B} is the ideal spectral efficiency in bit/s/Hz. The achievable spectral efficiency of practical modulation schemes can be estimated as

$$\frac{\mathcal{R}}{\mathcal{B}} = \log_2\left(1 + \frac{SNR}{\Upsilon}\right). \quad (4.2)$$

where \mathcal{R} is the data rate of practical modulations (e.g., QAM), Υ represent a 'gap' between Shannon capacity and the achievable capacity of real modulations and it is not constant. Hence the optimal multicast performance and the corresponding adaptation strategy from information theory perspective may not be achievable.

Another issue related to the worst-channel-limit is, since multicast adaptation cannot be as efficient as unicast adaptation for each receiver itself, whether it is always worth switching from multiple unicast to multicast mode even when the group size is small (e.g., only two-receivers-group).

To address these efficient multicast issues, we investigate the average multicast spectral efficiency per receiver with different combinations of the transmit power and rate adaptations. We assumed the investigated adaptation strategies are subject to an average power and instantaneous BER constraints. The data rate is adaptable due to varied modulation constellations, but the effect of adaptive channel coding is not considered. We first investigate the power and rate adaptation given the modulation constellations can be varied continuously, and then analyze the more realistic scenario where only a discrete set of constellations as well as data rate are available.

4.2 Single-Carrier System Model

Based on the general assumptions described in Chapter 1, the transceiver system is now assumed as a single carrier system. The channel models of N multicast receivers are assumed as discrete-time flat-fading channels, with stationary and ergodic time-varying gain and Additive White Gaussian Noise (AWGN). Since the channel gains are stationary, the distributions of them are independent of time and the time reference is omitted in our expressions. The received symbols at the i -th multicast receiver, denoted as y_i , can be characterized as

$$y_i = g_i x + n_i, i = 1, \dots, N \quad (4.3)$$

where x is the transmitted Multicast symbols, g_i is the channel gain of receiver i and n_i is the additive white Gaussian noise with variance σ_i^2 . Hence the SNR of each receiver at each time-slot can be written as

$$SNR_i = \frac{S|g_i|^2}{\sigma_i^2} \quad (4.4)$$

in which S is the transmission power. Assume the average transmission power is \bar{S} , and the received instantaneous SNRs under this power level are

$$\gamma_i = \frac{\bar{S} \cdot |g_i|^2}{\sigma_i^2}, \quad (4.5)$$

which can be measured by the receivers (i.e, with the help of the pilot channel). In this work, γ_i is called Normalized SNR and taken as the main channel quality indicator. We further assume that the receivers can detect their γ_i under this constant power level, i.e, by measuring the signal in the downlink pilot signal, and report them in a non-delay and error-free feedback channel. The base station fulfills downlink power control according to $\gamma_i (i = 1..N)$ and transmits the Multicast content with instantaneous power S . Therefore the actually received SNRs of each time-slot can be rewritten as

$$SNR_i = \frac{S}{\bar{S}} \cdot \frac{\bar{S} \cdot |g_i|^2}{\sigma_i^2} = \frac{S}{\bar{S}} \cdot \gamma_i \quad (4.6)$$

The Probability Density Functions (PDFs) of γ_i follow Independent Identical Distributions (i.i.d), noted as $p(\gamma_i)$. The random vector $\vec{\gamma} := (\gamma_1, \gamma_2, \dots, \gamma_N)$ represents a fading state of the Multicast group, with probability density function $p^*(\vec{\gamma}) = \prod_{i=1}^N p(\gamma_i)$.

As introduced in the first section, we are looking for the optimal power S (watt) and rate k (bits/ symbol) adaptation schemes to maximize the spectral efficiency. S is assumed to be continuous non-negative function of the instantaneous

channel fading state $\vec{\gamma}$, noted as $S(\vec{\gamma})$. The average level of S is limited to be no more than \bar{S} to control the interference of the multicast channel toward other cells. k is a non-negative function of $\vec{\gamma}$, noted as $k(\vec{\gamma})$, which can be either continuous or discrete. Besides, the multicast channel can also be turn-off in some fading states, where $S = 0$ and $k = 0$.

The BER constraint could be either average or instantaneous, depend on the characters of the service investigated. Given the instantaneous BER limit, the transceiver system has to guarantee that the probability of bit error in each channel state is no more than a constant value; whereas under the average BER constraint, only the BER level averaged along time or channel fading states need to be maintained, and the BER limit for different channel states could be different. In providing real-time multimedia services via multicast, it is crucial to keep a low instantaneous frame error ratio (FER) for good user-perceived quality of services. Instantaneous FER can be derived from instantaneous BER, therefore a instantaneous BER constraint is chosen in our investigation.

4.3 Problem Formulation

The optimization target is the average spectral efficiency per multicast receiver, which equals the average data rate per unit bandwidth. When the signal is sent at modulation mode M with k bits/symbol, the instantaneous data rate $\mathcal{R} = k/T_s$ bps, where T_s is the symbol time. Under Nyquist sample rate $\mathcal{B} = 1/T_s$, hence $\mathcal{R} = k \cdot \mathcal{B}$, and the instantaneous spectral efficiency becomes

$$\frac{\mathcal{R}}{\mathcal{B}} = k.$$

The mathematical expectation of the spectral efficiency on the transmitter side is the instantaneous spectral efficiency averaged over all possible fading states, noted as $(\mathcal{R}/\mathcal{B})_T$,

$$\left(\frac{\mathcal{R}}{\mathcal{B}}\right)_T = \int_{(\mathbb{R}_0^+)^N} k(\vec{\gamma})p^*(\vec{\gamma})d\vec{\gamma} \quad (4.7)$$

$(\vec{\gamma})$ in Eq.4.7 and all the following integrations is in linear unit, hence it is always integrated in $(\mathbb{R}_0^+)^N$, a N-dimensional space of positive real numbers. Considering the errors introduced by the wireless channel, the spectrum efficiency at receiver i is

$$\left(\frac{\mathcal{R}}{\mathcal{B}}\right)_i = \int_{(\mathbb{R}_0^+)^N} k(\vec{\gamma})p^*(\vec{\gamma}) [1 - BER_i(k(\vec{\gamma}), S(\vec{\gamma}), \vec{\gamma})] d\vec{\gamma} \quad (4.8)$$

and the average spectral efficiency of the multicast receivers should be

$$\overline{\left(\frac{\mathcal{R}}{\mathcal{B}}\right)} = \frac{1}{N} \sum_{i=1}^N \int_{(\mathbb{R}_0^+)^N} k(\vec{\gamma})p^*(\vec{\gamma}) [1 - BER_i(k(\vec{\gamma}), S(\vec{\gamma}), \vec{\gamma})] d\vec{\gamma} \quad (4.9)$$

Likewise the average power constraint over all fading states is

$$\mathbb{E}\{S(\vec{\gamma})\} := \int_{(\mathbb{R}_0^+)^N} S(\vec{\gamma})p^*(\vec{\gamma})d\vec{\gamma} \leq \overline{S}. \quad (4.10)$$

For a multicast group, there exist N instantaneous BER constraints:

$$BER_i(k(\vec{\gamma}), S(\vec{\gamma}), \vec{\gamma}) \leq \theta, \quad (4.11)$$

where θ represent the required BER constraint value (e.g., 10^{-3} or 10^{-6}).

An instantaneous BER estimation for un-coded MQAM [4] is employed for the continuous k :

$$BER_i \approx 0.2 \exp\left(\frac{-1.6\gamma_i \frac{S(\vec{\gamma})}{S}}{2^{k(\vec{\gamma})} - 1}\right) \quad (4.12)$$

It needs to be mentioned that this estimation is tight only when $\gamma_i \cdot \frac{S(\vec{\gamma})}{S} \geq 1$.

The instantaneous BER constraint is a rather strong limitation, since the error probability scale exponentially to $\frac{S}{S}\gamma_i$ as shown in Eq. (4.12). It would be wise to turn off the transmission rather than assign huge power and very low rate to meet θ when the fading state is too bad. That is, we can assume a region $\Omega \subset (\mathbb{R}_0^+)^N$ such that k and S are positive functions if and only if $\vec{\gamma} \in \Omega$, and zero otherwise. More detailed discussion on this region will be presented in the following sections.

Problem Simplification

To reduce the complexity of maximizing Eq.(4.9), some simplifications are made. Typically θ is a very small value, and if this constraint holds during the transmission, the difference between the spectrum efficiency at transmitter side and receiver side is negligible. Therefore, the maximization target can be approximated as

$$\overline{\left(\frac{\mathcal{R}}{\mathcal{B}}\right)} \approx \int_{(\mathbb{R}_0^+)^N} k(\vec{\gamma}) p^*(\vec{\gamma}) d\vec{\gamma}. \quad (4.13)$$

We take Eq.4.13 as the estimation of the *average spectrum efficiency* of the multi-cast group to be maximized, for simplicity $\overline{\left(\frac{\mathcal{R}}{\mathcal{B}}\right)}$ is just written as $\frac{\mathcal{R}}{\mathcal{B}}$ in the following sections.

To ensure instantaneous $BER_i \leq \theta$, it must be guaranteed that

$$\max\{BER_i(k(\vec{\gamma}), S(\vec{\gamma}), \vec{\gamma})\} = \theta,$$

which equals to $BER(\min\{\vec{\gamma}\}) = \theta$. This is exactly the adapt-to-worst case. With this simplification we can derive from Eq.(4.12):

$$k(\vec{\gamma}) = \log_2 \left[1 - \frac{1.6 \min\{\vec{\gamma}\} \frac{S(\vec{\gamma})}{\bar{S}}}{\ln(5\theta)} \right], S > 0. \quad (4.14)$$

4.4 Solutions with Continuous Rate Adaptation

In this section we apply Lagrange method to derive the optimal spectral efficiency and corresponding rate and power solutions, given the transmission data rate k can be continuously adapted to the channel conditions. A sub-optimal solution with constant power and other alternative solution are also developed and analyzed for comparison.

4.4.1 Adaptation Schemes

4.4.1.1 Optimal Power and Continuous Rate Adaptation (CRSopt)

Using the expansion of $k(\vec{\gamma})$ in Eq.(4.14), the N instantaneous BER constraints can be dropped and it remains to look for S such that the integral in Eq.(4.7) is maximized under the power constraint Eq.(4.10). Eq.(4.7) can be re-written in the form

$$\begin{aligned} & \int_{(\mathbb{R}_0^+)^N} k(\vec{\gamma}) p^*(\vec{\gamma}) d\vec{\gamma} \\ &= \int_{(\mathbb{R}_0^+)^N} \log_2 \left[1 - \frac{1.6 \min\{\vec{\gamma}\} \frac{S(\vec{\gamma})}{\bar{S}}}{\ln(5\theta)} \right] p^*(\vec{\gamma}) d\vec{\gamma} \\ &=: \int_{(\mathbb{R}_0^+)^N} g(S(\vec{\gamma}), \vec{\gamma}) d\vec{\gamma} \end{aligned} \quad (4.15)$$

We construct the Lagrange function of this problem as

$$\begin{aligned} \mathcal{J}(S(\vec{\gamma}), \vec{\gamma}) &:= \int_{(\mathbb{R}_0^+)^N} g(S(\vec{\gamma}), \vec{\gamma}) d\vec{\gamma} \\ &+ \lambda_0 \left[\int_{(\mathbb{R}_0^+)^N} S(\vec{\gamma}) p^*(\vec{\gamma}) d\vec{\gamma} - \bar{S} \right] \end{aligned} \quad (4.16)$$

The problem reduces to find the optimal function $S(\vec{\gamma})$ with the average power \bar{S} limit.

Define

$$\mathcal{I}(\varepsilon) := \mathcal{J}(S + \varepsilon\sigma)$$

where σ is an arbitrary function and ε is a small enough number. Given the optimal $S(\vec{\gamma})$ exists, there should be

$$\forall \varepsilon, \mathcal{I}(\varepsilon) \leq \mathcal{I}(0) \implies \frac{d\mathcal{I}}{d\varepsilon}(0) = 0.$$

Eq.(4.15),(4.16),(4.4.1.1) and condition $\frac{d\mathcal{I}}{d\varepsilon}(0) = 0$ lead to

$$\frac{1.6}{\ln 2} \cdot \frac{\min\{\vec{\gamma}\}}{1.6 \cdot \min\{\vec{\gamma}\} S - \bar{S} \ln(5\theta)} + \lambda_0 = 0,$$

$\forall \sigma$, and for all $\vec{\gamma}$ such that $p^*(\vec{\gamma}) \neq 0$.

Hence the theoretical optimal power scheme, noted as $S_{opt}(\vec{\gamma})$, is

$$S_{opt}(\vec{\gamma}) = \frac{c \bar{S}}{\min\{\vec{\gamma}\}} - \frac{1}{\lambda_0 \ln 2} \quad (4.17)$$

where $c = \ln 5\theta/1.6$.

For an practical instantaneous BER limit (usually $10^{-3} \sim 10^{-6}$), there must be $\theta < 0.2 \rightarrow c < 0$, hence S_{opt} is a monotonically increasing function of

$\{\min\{\vec{\gamma}\}, \bar{\gamma}\}$. Since γ_i are i.i.d. we can assume Ω has the form $[\gamma_0, +\infty)^N$, where γ_0 is the threshold for transmission turn-on/turn-off.

Then it should be possible to find the region Ω in $(R_0^+)^N$, in which $\min\{\vec{\gamma}\} \geq \gamma_0$, and substitute $S(\vec{\gamma})$ in Eq.(4.10) with Eq.(4.17) and take the upper-limit of the power, we get

$$\int_{\Omega} \left[\frac{c \bar{S}}{\min\{\vec{\gamma}\}} - \frac{1}{\lambda_0 \ln 2} \right] p^*(\vec{\gamma}) d\vec{\gamma} = \bar{S} \quad (4.18)$$

Let

$$\Delta := \int_{\Omega} \frac{p^*(\vec{\gamma})}{\min\{\vec{\gamma}\}} d\vec{\gamma} \quad (4.19)$$

$$\alpha := \int_{\Omega} p^*(\vec{\gamma}) d\vec{\gamma} \quad (4.20)$$

$$\rightarrow \lambda_0 = \frac{\alpha}{\bar{S} \ln 2 \cdot [c\Delta - 1]}$$

which leads to

$$\frac{S}{\bar{S}} = \begin{cases} \frac{c}{\min\{\vec{\gamma}\}} + \frac{1-c\Delta}{\alpha}, & \min\{\vec{\gamma}\} \geq \gamma_0 \\ 0, & \text{otherwise.} \end{cases} \quad (4.21)$$

And use (4.21) in (4.14)

$$k = \begin{cases} \log_2 \left(\frac{c\Delta - 1}{\alpha c} \min\{\vec{\gamma}\} \right), & \min\{\vec{\gamma}\} \geq \gamma_0 \\ 0, & \text{otherwise.} \end{cases} \quad (4.22)$$

The optimal spectrum efficiency can be computed by

$$\frac{R}{B} = \int_{\Omega} \log_2 \left(\frac{c\Delta - 1}{\alpha c} \min\{\vec{\gamma}\} \right) p^*(\vec{\gamma}) d\vec{\gamma} \quad (4.23)$$

So far we derived the general form of the optimal S and k allocation schemes, and the problem remains how to find the value of α and Δ , which depend on the region Ω . As we have assumed Ω has the form $[\gamma_0, +\infty)^N$, searching for the proper Ω

reduce to searching for a single threshold γ_0 (we name it as Cut-Off SNR). The detailed searching criteria for γ_0 is described in Sec.4.4.2.2.

4.4.1.2 Constant Power and Optimal Rate (CRSc)

The previous optimal solution exploits the degrees of freedom in both power and rate dimensions. In practise, sub-optimal solutions with implementation simplicity may be preferred. In this section we develop the suboptimal solution with only optimal rate adaptation and constant power. Consider power is assigned in region Ω and zero elsewhere, Eq.(4.10) with constant power S_c becomes

$$\begin{aligned} \int_{\Omega} S_c \cdot p^*(\vec{\gamma}) d\vec{\gamma} &= \bar{S}, \\ \Rightarrow \frac{S_c}{\bar{S}} &= \frac{1}{\alpha} \end{aligned} \quad (4.24)$$

The corresponding k from (4.22) is

$$k = \begin{cases} \log_2 \left(1 - \frac{\min\{\vec{\gamma}\}}{\alpha c} \right), & \min\{\vec{\gamma}\} \geq \gamma_0 \\ 0, & \text{otherwise.} \end{cases} \quad (4.25)$$

The sub-optimal spectrum efficiency is

$$\frac{R}{B} = \int_{\Omega} \log_2 \left(1 - \frac{\min\{\vec{\gamma}\}}{\alpha c} \right) p^*(\vec{\gamma}) d\vec{\gamma} \quad (4.26)$$

4.4.1.3 Linear Power and Optimal Rate

To reveal whether other power algorithms can achieve comparable performance as the derived optimal solution, the third scheme is developed. Intuitively, the power and rate should increase as the normalized SNR increases to exploit more

spectrum efficiency. Hence we assume power scheme S_L :

$$\frac{S_L}{S} = \beta \min\{\vec{\gamma}\} + \varphi \quad (4.27)$$

where β and φ are parameters to be found to maximize spectrum efficiency.

This function subject to average power constraint

$$\begin{aligned} \int_{\Omega} \frac{S_L}{S} \cdot p^*(\vec{\gamma}) d\vec{\gamma} &= 1 \\ \rightarrow \beta \int_{\Omega} \min\{\vec{\gamma}\} p^*(\vec{\gamma}) d\vec{\gamma} + \varphi \alpha &= 1 \end{aligned} \quad (4.28)$$

This power scheme was investigated together with rate scheme E.q (4.14) as the third adaptation scheme in this work.

4.4.2 Numerical Result of Case Studies

We computed the numerical results for the optimal and sub-optimal forms of S , k and R/B with $N = 2$, and the Normalized SNRs following Rayleigh distribution, such as

$$p(\gamma_i) = \frac{\gamma_i \exp\left(-\frac{\gamma_i^2}{2\sigma^2}\right)}{\sigma^2}. \quad (4.29)$$

where $\theta = 10^{-3}$. So far there is not a single distribution model that can describe the overall SNR results caused by pathloss, shadowing and multi-path. Rayleigh distribution is frequently used in link adaptation study ([1],[4]), because multipath is the most challenging part to be coped with link adaptations.

Use Eq.4.29 in Eq.4.20 and Eq.4.19, then

$$\alpha = \left[\exp\left(-\frac{\gamma_0^2}{2\sigma^2}\right) \right]^2$$

$$\Delta = \int_{\gamma_0}^{\infty} \int_{\gamma_0}^{\infty} \frac{\gamma_1 \gamma_2 \exp\left(-\frac{\gamma_1^2 + \gamma_2^2}{2\sigma^2}\right)}{\sigma^4 \cdot \min(\gamma_1, \gamma_2)} d\gamma_1 d\gamma_2$$

Here, Δ can only be computed with numerical methods. Then we numerically search for γ_0 which maximizes

$$\frac{R}{B} = \int_{\gamma_0}^{\infty} \int_{\gamma_0}^{\infty} \log_2 \left(\frac{c\Delta - 1}{\alpha c} \min(\gamma_1, \gamma_2) \right) \cdot \frac{\gamma_1 \gamma_2 \exp\left(-\frac{\gamma_1^2 + \gamma_2^2}{2\sigma^2}\right)}{\sigma^4} d\gamma_1 d\gamma_2$$

The resulted S_{opt} versus $\min(\gamma_1, \gamma_2)$ (dB) is plotted in Fig. 4.1, where $\sigma = 10$ corresponds to the average Normalized SNR $\bar{\gamma} \approx 11dB$. The optimal rate adaptation

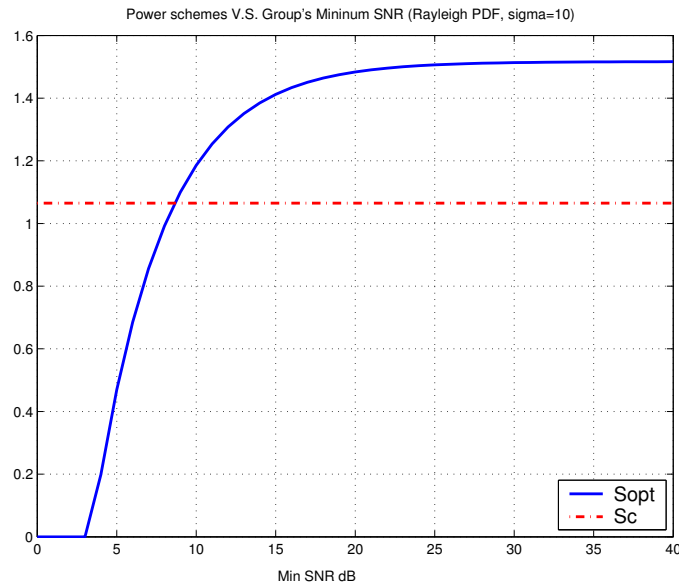


Figure 4.1: S/\bar{S} versus $\min\{\bar{\gamma}\}$

scheme k versus $\min(\gamma_1, \gamma_2)$ under the same $\bar{\gamma}$ is depicted in Fig. 4.2, and the optimal rate scheme with constant power ($\gamma_0 = 0dB$) is plotted as well.

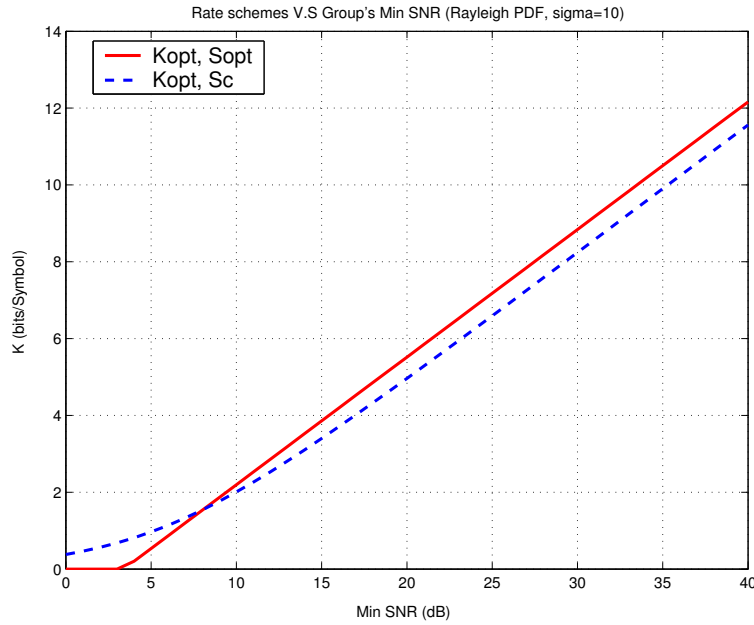


Figure 4.2: k versus $\min\{\bar{\gamma}\}$

4.4.2.1 Spectrum Efficiency

Numerical searching has been done to derive the optimal γ_0 which maximizes spectrum efficiencies under different $\bar{\gamma}$ values, since γ_0 cannot be solved with close-form expression. The derived maximum spectral efficiency are illustrated in Fig. 4.3 for k with optimal S (the red curve) and k with constant S (the blue dotted curve) under Rayleigh channel with $N = 2$. Interestingly, the spectrum efficiency loss due to fixed power is less than 3% compared to the one with joint k and S adaptation in the numerical results.

If we rewrite Eq.4.14 for a single user case with the SNR expression in Eq.4.6,

$$k = \log_2 \left(1 + \frac{SNR}{\frac{\ln(5\theta)}{1.6}} \right).$$

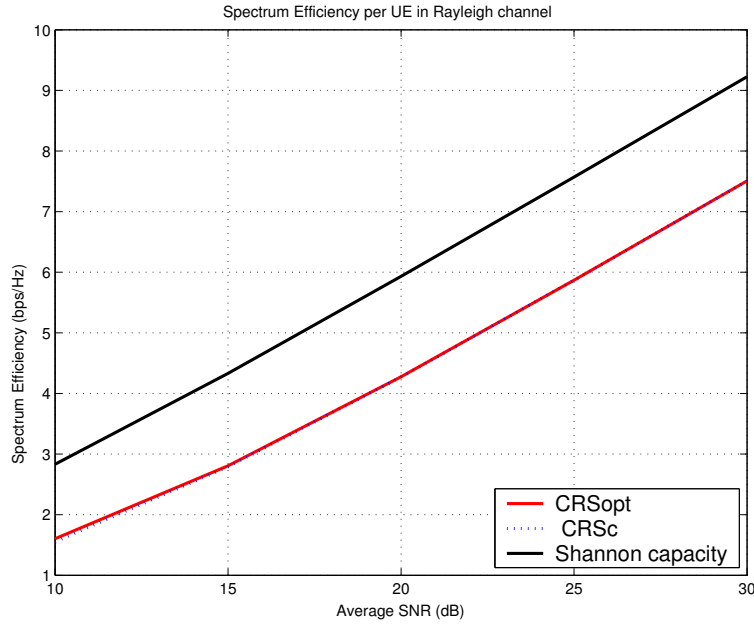


Figure 4.3: Spectrum Efficiency per User in Rayleigh Channel

Comparing with Eq.4.2, it is obvious that we can assume

$$\Upsilon = \frac{-\ln(5\theta)}{1.6} \quad (4.30)$$

Hence the capacity gap Υ depends on the modulation scheme and the target BER, i.e, $\Upsilon = 3.314$ at $\theta = 10^{-3}$ for MQAM.

To compare the performance upper bound that can be derived from Shannon capacity and the one from our approach, we rewrite Eq.4.15 as

$$\begin{aligned} \left(\frac{\mathbb{R}}{\mathbb{B}}\right)_{Shannon} &= \int_{(\mathbb{R}_0^+)^N} k(\vec{\gamma}) p^*(\vec{\gamma}) d\vec{\gamma} \\ &= \int_{(\mathbb{R}_0^+)^N} \log_2 \left[1 - \min\{\vec{\gamma}\} \frac{S(\vec{\gamma})}{\bar{S}} \right] p^*(\vec{\gamma}), \end{aligned}$$

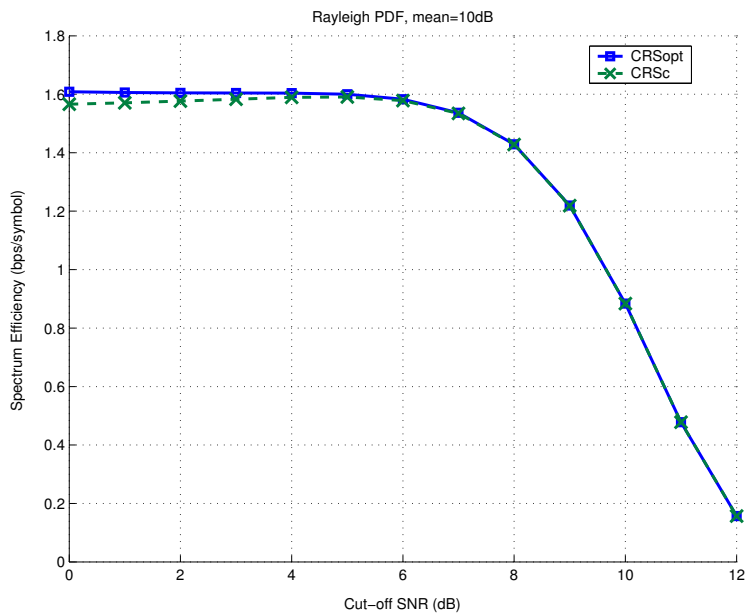
and apply the same Lagrange method as in the CRSopt scheme. The results are depicted as the black curve in Fig. 4.3, which reveals that the spectral efficiency

upper bound derived from Shannon capacity is much higher than the upper bound MQAM signal can achieve. For example, the Shannon upper bound is higher than our upper bound (both with CRSopt scheme) by 1.23bit/s/Hz at 10dB, and 1.72bit/s/Hz at 20dB (43.4% and 18.6% more than CRSopt). This means, the optimal spectral efficiency analysis with our method is much more accurate than that based on Shannon capacity.

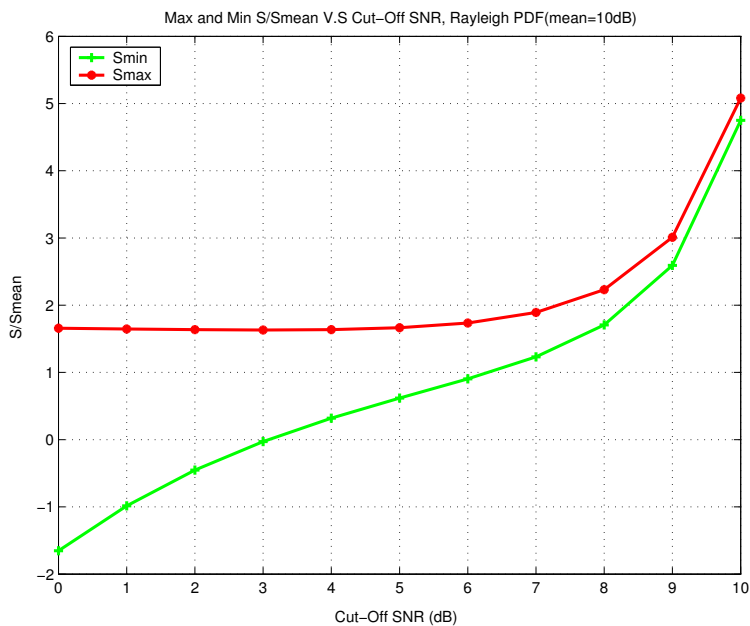
4.4.2.2 Selection of Cut-Off SNR Value

In this subsection we describe how to select the optimal Cut-Off SNR value. The Cut-Off SNR should both maximize the spectrum efficiency for the given adaptation scheme and be physically meaningful, such that $S(\gamma_0) \geq 0$, and $S(\gamma_0) \geq 0 \Rightarrow k(\gamma_0) \geq 0$. The relation between spectrum efficiency and the Cut-Off SNR values in $CR - S_{opt}$ solution is illustrated by the blue curve in Fig. 4.4(a), and the maximum and minimum values of power in CRS_{opt} scheme derived from different Cut-Off SNRs are plotted in Fig. 4.4(b). In Fig. 4.4(a), the spectrum efficiency (SE) keeps decreasing as Cut-Off SNR increases (as in 4.4(a)), but the loss of efficiency is negligible when $\gamma_0 \leq 6$ dB. On the other hand, the minimum power values in Fig. 4.4(b) are negative when $\gamma_0 < 3$ dB. Therefore the optimal valid Cut-Off SNR should be about 3dB. Such study has been done for SNR_{mean} between 10dB and 25dB, and the results suggest the optimal valid Cut-Off SNR should be between 3dB and 6dB for this SNR_{mean} range.

For $CRSc$ solution (the green curve in Fig. 4.4(a)), the allocated power value is positive and constant, and the Cut-Off SNRs which leads to the maximum spectral efficiency is between 4 and 6dB.



(a) Impact on per User Spectrum Efficiency



(b) Impact on Min and Max Power for CRSopt

Figure 4.4: Impact of Cut-Off SNR (Rayleigh PDF, Mean=10dB)

4.4.2.3 Linear Power and Optimal Rate

Different β and φ were tested to maximize the spectrum efficiency of the $\{k_{opt}, S_L\}$. Due to the constraint (4.28), once β , Mean SNR and Cut-Off SNR are selected, φ is decided. The value of β is also limited by $S(\gamma_0) \geq 0$. In Fig. 4.5, differ-

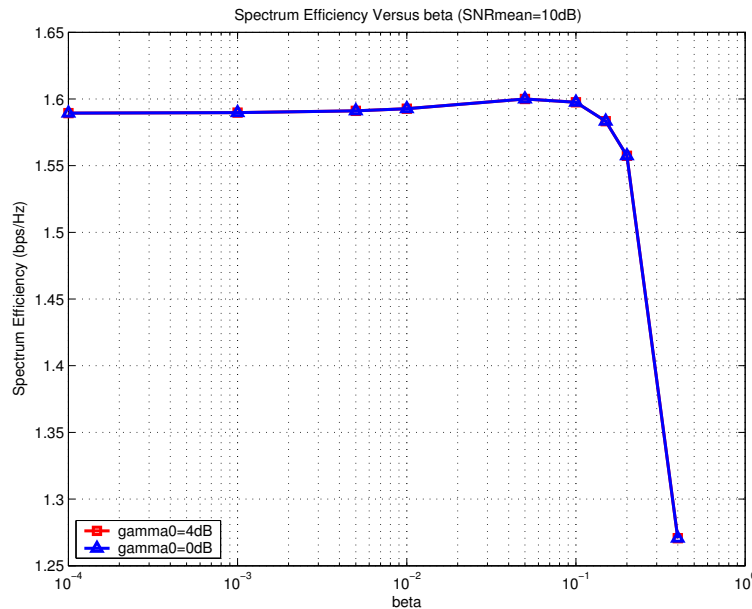


Figure 4.5: Linear Power Adaptation, Impact of Slope β on Spectrum Efficiency

ent Cut-Off values did not make much difference since the curve with Cut-Off at 0dB and 4dB are overlapping with each other. The maximum spectrum efficiency in Fig. 4.5 are only 1% less than that of $\{k_{opt}, S_{opt}\}$ while $\beta \leq 0.05$. This result shows that other options of power schemes can also achieve nearly optimal performance, if applied together with Eq.4.14 and carefully designed parameters.

Actually in such optimum scenario of β the curve of 4.27 would be very close to the curve of Eq.(4.24). For simplicity reason, the constant power and optimal rate adaptation scheme would still be the best adaptation scheme.

4.5 Solutions with Discrete Rate Adaptation

In this section, Lagrange method is applied with discrete transmission data rate, where k can only be chosen from a set of integer numbers $\{k_m\}_{m=0}^{M-1}$. A sub-optimal solution with constant power is also derived.

4.5.1 Discrete Rate and Optimal Power (DRSopt)

4.5.1.1 Unicast Case

For a point-to-point channel, the rate k_m can be assigned when the γ falls into a region $[\Gamma_m, \Gamma_{m+1})$ ($m = 0..M - 1$ and $\Gamma_M = \infty$). No data is transmitted if $\gamma < \Gamma_0$. For such a fixed set of rate values, the optimal rate adaptation becomes to find the optimal rate region boundaries Γ_m . The Lagrangian for this problem can be set as:

$$\begin{aligned} \mathcal{J}(S(\gamma), \Gamma_0, \Gamma_1, \dots, \Gamma_M) \\ := \sum_{m=0}^{M-1} k_m \int_{\Gamma_m}^{\Gamma_{m+1}} p(\gamma) d\gamma + \lambda \left[\int_{\Omega} S(\gamma) p(\gamma) d\gamma - \bar{S} \right] \end{aligned} \quad (4.31)$$

From Eq.4.12 we can derive

$$\frac{S(\gamma)}{\bar{S}} = \frac{F(k_m)}{\gamma} \quad (4.32)$$

where

$$F(k_m) = c_1 \cdot (2^{k_m} - 1)$$

and $c_1 = \frac{\ln(5\theta)}{-1.6}$.

Hence the Lagrange function can be rewritten as:

$$\begin{aligned} \mathcal{J}(\Gamma_0, \Gamma_1, \dots, \Gamma_M) := & \sum_{m=0}^{M-1} k_m \int_{\Gamma_m}^{\Gamma_{m+1}} p(\gamma) d\gamma \\ & + \lambda \left[\sum_{m=0}^{M-1} \int_{\Gamma_m}^{\Gamma_{m+1}} \frac{F(k_m)}{\gamma} p(\gamma) d\gamma - 1 \right] \end{aligned} \quad (4.33)$$

By solving the following equations for Γ_m

$$\frac{\partial \mathcal{J}}{\partial \Gamma_m} = 0, \quad 0 \leq m \leq M-1 \quad (4.34)$$

we can obtain the optimal boundaries with the forms:

$$\Gamma_0 = -\lambda \cdot \frac{F(k_0)}{k_0} \quad (4.35)$$

$$\Gamma_m = -\lambda \cdot \frac{F(k_m) - F(k_{m-1})}{k_m - k_{m-1}} \quad 1 \leq m \leq M-1, \quad (4.36)$$

and the value of λ can be derived from the power constraint:

$$\sum_{m=0}^{M-1} \int_{\Gamma_m}^{\Gamma_{m+1}} \frac{F(k_m)}{\gamma} p(\gamma) d\gamma - 1 = 0 \quad (4.37)$$

For a Rayleigh fading channel, Eq.4.37 can be calculated as

$$\sum_{m=0}^{M-1} F(k_m) \int_{\Gamma_m}^{\Gamma_{m+1}} \frac{1}{\gamma} \cdot \frac{\gamma}{\sigma^2} \exp\left(-\frac{\gamma^2}{2\sigma^2}\right) d\gamma = 1 \quad (4.38)$$

$$\Rightarrow \frac{1}{\sigma} \sqrt{\frac{\pi}{2}} \cdot \sum_{m=0}^{M-1} F(k_m) \left[\operatorname{erf}\left(\frac{\Gamma_{m+1}}{\sigma\sqrt{2}}\right) - \operatorname{erf}\left(\frac{\Gamma_m}{\sigma\sqrt{2}}\right) \right] = 1 \quad (4.39)$$

Assume $k_m = 2, 4, 6, 8$ ($m = 0, 1, 2, 3$) for 4QAM, 16QAM, 64QAM and 256QAM under Rayleigh fading channel, and let $\Gamma_4 = \inf$. We can solve Eq. 4.39 to get

λ , Γ_m and calculate corresponding spectral efficiency, as plotted in Fig. 4.8. The curves shows for unicast case the DRSopt only causes a negligible spectral efficiency loss comparing to CRSopt.

4.5.1.2 Multicast Case ($N = 2$)

When we try to apply the same approach for $N = 2$, we adopt a similar form of the Lagrangian function:

$$\begin{aligned} \mathcal{J}(S(\gamma), \Gamma_0, \Gamma_1, \dots, \Gamma_M) \\ := \sum_{m=0}^{M-1} k_m \int_{\Omega_{\Gamma_m}} p(\vec{\gamma}) d\vec{\gamma} + \lambda \left[\int_{\Omega} S(\gamma) p(\vec{\gamma}) d\vec{\gamma} - \bar{S} \right] \end{aligned} \quad (4.40)$$

where Ω_{Γ_m} is the two dimensional rate region of modulation mode m (as depicted in Fig. 4.6), where $\min\{\vec{\gamma}\} \in [\Gamma_m, \Gamma_{m+1})$, and

$$\frac{S(\gamma)}{\bar{S}} = \frac{F(k_m)}{\min\{\vec{\gamma}\}}. \quad (4.41)$$

Hence

$$\begin{aligned} \mathcal{J}(S(\gamma), \Gamma_0, \Gamma_1, \dots, \Gamma_M) \\ := \sum_{m=0}^{M-1} k_m \int_{\Omega_{\Gamma_m}} p(\vec{\gamma}) d\vec{\gamma} + \lambda \left[\sum_{m=0}^{M-1} \int_{\Omega_{\Gamma_m}} \frac{F(k_m)}{\min\{\vec{\gamma}\}} p(\vec{\gamma}) d\vec{\gamma} - 1 \right] \end{aligned} \quad (4.42)$$

In similar way we can get Eq.4.35 and 4.36 from Eq.4.34 for the two user case. The value of Γ_m depends on k_m and λ . When k_m is fixed, λ can be derived from the average power constraint:

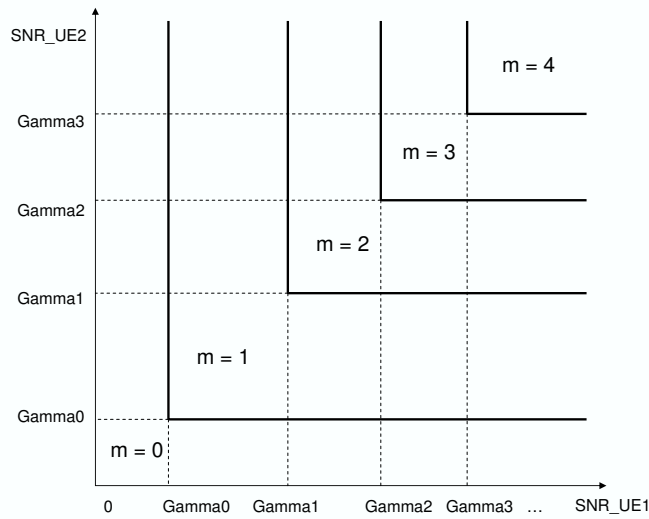


Figure 4.6: Integration Region of 2 UE, D-Rate

$$\sum_{m=0}^{M-1} \int_{\Omega_{\Gamma_m}} \frac{F(k_m)}{\min\{\vec{\gamma}\}} p(\gamma) d\gamma - 1 = 0, \quad (4.43)$$

which is solved by numerical search since there is no close-form for the integral in this equation. The derived optimal spectral efficiency is also depicted in Fig. 4.8, and the power schemes of DRSopt corresponding to average SNR at 10dB and 30dB are depicted in Fig. 4.7(a) and Fig. 4.7(b).

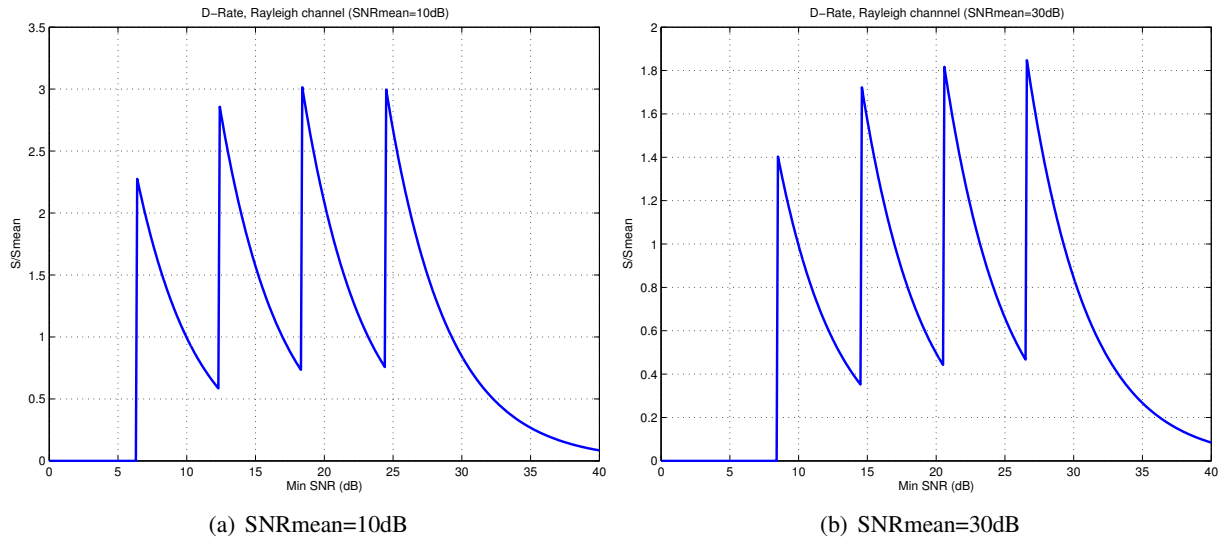


Figure 4.7: Optimal Power Schemes with Discrete Modulation Rate

4.5.2 Discrete Rate and Constant Power (DRSc)

In this case the allocated power level also follows 4.4.1.2 and the spectral efficiency follows

$$\frac{R}{B} := \sum_{m=0}^{M-1} k_m \int_{\Omega_{\Gamma_m}} p(\vec{\gamma}) d\vec{\gamma} \quad (4.44)$$

with the constraints on the threshold of each modulation scheme

$$BER_m = 0.2 \exp\left(\frac{-1.6\Gamma_m \frac{S_c}{S}}{2^{k_m} - 1}\right) = 0.2 \exp\left(\frac{-1.6\frac{\Gamma_m}{\alpha}}{2^{k_m} - 1}\right) \leq \theta \quad (4.45)$$

and

$$\Gamma_m = c_1 \alpha (2^{k_m} - 1) \quad (4.46)$$

For a known SNR PDF, α can be derived by jointly solve

$$\Gamma_0 = c_1 \alpha (2^{k_0} - 1) \quad (4.47)$$

$$\alpha = \int_{\Gamma_0}^{\infty} p^*(\vec{\gamma}) d\vec{\gamma} \quad (4.48)$$

The spectral efficiency results for Rayleigh PDF, D-Rate and Constant power scheme in unicast and multicast ($N = 2$) cases are illustrated in Fig. 4.8.

4.5.3 Numerical Results of Case Studies

The spectral efficiency curves of all Lagrange-based solutions are presented in Fig. 4.8 for comparison and analysis.

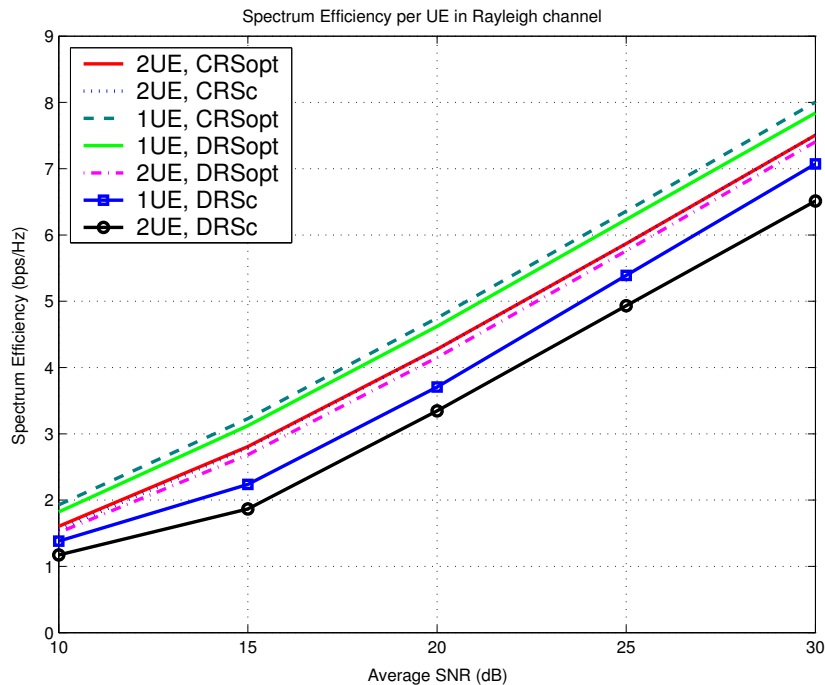


Figure 4.8: Per User Spectral Efficiency of All Adaptation Schemes

4.5.3.1 Spectral Efficiency Loss due to Discrete Rate Adaptation

In Fig. 4.8, the performance of DRSopt is only slightly lower than that of CRSopt. This means the optimal solution with discrete data rate and continuous power can achieve the spectral efficiency which is very close to the upper bound provided by the optimal one with continuous rate and power. Because continuous rate adaptation cannot really be implemented with practical modulation constellations, but

the exact spectral efficiency of discrete rate adaptations may change according to the available modulation modes, the optimal spectral efficiency of CRSopt can be considered as a general upper bound, and a very accurate estimation (comparing to Shannon-capacity-based upper bound) for the optimal rate and power adaptation schemes in practice.

4.5.3.2 Spectral Efficiency Loss due to Fixed Power

Unlike the continuous rate scenario, significant performance losses can be observed for the DRSc scheme comparing to the DRSopt scheme in both unicast and multicast (2 UEs). E.g, the per user spectral efficiency loss increases from about 0.33 bps/Hz up to about 0.89 bps/Hz for the multicast group of 2 UEs as the average SNR increases from 10dB to 30dB. This fact suggests that discrete rate adaptation should always be applied jointly with power adaptation to maximize the spectral efficiency.

4.5.3.3 Spectral Efficiency Loss and Gain due to Multicasting

If we compare the per user performance of the same adaptation schemes (CRSopt, DRSopt, DRSc) under unicast and multicast as depicted in Fig. 4.8, a gap can be observed between each pair of them . The multicast spectral efficiencies are around 0.32 to 0.50bps/Hz less than the unicast values for the same adaptation scheme. This performance loss is due to the fact that the instantaneous rate assigned to the channel is limited by the worst fading state among users in a multicast group. And such loss is expected to increase as group size increases. However, such spectrum efficiency has been achieved by two receivers each in multicast,

so the total spectrum efficiency of the multicast channel has been nearly doubled comparing to the unicast channel. This fact implies that even though the multicast adaptation is limited by the instantaneous worst channel during each transmission burst, it is still much more efficient to serve two users with a multicast channel than with two unicast channels.

4.6 Conclusion and Future Work

In this work we analytically derived the spectral efficiency upper-bound of a multicast channel and the optimal joint power and rate adaptation scheme. With an ideal assumption that the data rate can be allocated continuously, nearly optimal spectrum efficiency can also be achieved with constant power and optimal rate allocation. However, under a more practical setting with discrete data rate and limited modulation modes options, joint power and rate adaptation significantly outperforms constant power scheme. Last but not the least, the maximum average spectrum efficiency per user of a multicast group is close enough to the unicast case, such that the system spectrum efficiency gain can be improved dramatically. Therefore it is always more efficient to switch to multicast mode from unicast mode.

So far all the studies in this thesis only optimize link adaptation schemes on bit level. However, in practice bit streams are transmitted in packets/frames, and the performance on packet level may influence on the user perceived QoS more significantly. That is, we extend our study to packet level adaptations, i.e., on the data link layer, in the next chapter.

Note: The works presented in this chapter have been published in [5], and will also appear in [6].

Bibliography

- [1] Q. Du and X. Zhang, "Joint Power and Constellation Size Adaptation for Mobile Multicast Employing MQAM Over Wireless Fading Channels," in *Proc. IEEE Int. Conf. on Communications 2007 (ICC 2007)*, Glasgow, UK, Jun. 2007.
- [2] W. Ge, J. Zhang, and S. Shen, "A Cross-Layer Design Approach to Multicast in Wireless Networks," in *Proc. IEEE Trans. Wireless Commun.*, vol. 6, np. 3, Mar. 2007.
- [3] H. Wang, H. P. Schwefel and T. S. Toftegaard, "History-based Adaptive Modulation for a Downlink Multicast Channel in OFDMA systems," in *Proc. IEEE Wireless and Networking Conference (WCNC'08)*, Las Vegas, USA, Mar. 2008.
- [4] S. T. Chung, A. J. Goldsmith, "Degrees of Freedom in Adaptive Modulation: A Unified View," in *IEEE Trans. Commun.*, vol. 49, no. 9, pp. 1561-1571, Sept. 2001.
- [5] H. Wang, H. P. Schwefel and T. S. Toftegaard, "The Optimal Joint Power

and Rate Adaptation for Mobile Multicast: A Theoretical Approach,” in *Proc. IEEE Sarnoff Symposium*, Princeton, USA, Mar. 2008.

- [6] H. Wang, H. P. Schwefel and T. S. Toftegaard, “Mobile Multicast: the Optimal Power and Rate Adaptations in a Unified View,” in preparation.

Chapter 5

Cross Layer Design for Multicast

In this chapter, the reliability constraint is re-considered to include the influence of multiple layers. We extend the cross-layer model proposed in [3] from unicast to multicast scenario, and develop packet-combine-based multicast ARQ schemes and related AMC schemes within this cross-layer context. The performances of several multicast ARQ and AMC combinations, with or without cross-layer design, are analyzed with numerical results.

5.1 Motivation

In the previous chapters we have only included the reliability constraint in error probability (i.e., BER) for wireless video applications, but have not considered the impact of error patterns toward the quality of video transmissions. Such impact involves both the error pattern due to wireless channel, and the process in which the video stream is encoded on the application layer, and encapsulated into the transmission data units on the network layer, the link layer and the physical layer. Let us first briefly review a video-streaming transmission process.

In a video streaming transmission over wireless networks, application level

video frames (a *video frame* in this chapter refers to a coded single still image) are generated from the original video streams by a video encoder, with contemporary video compression and transmission standards (e.g., Moving Picture Experts Group (MPEG) -2, MPEG-4 and H.264). In these standards, some frames are reused for motion-compensated prediction [1] so that many repeated parts among consecutive images need not to be transmitted in each coded frame, which efficiently compress the data volume of the generated frames. As a consequence, the coded video contents are correlated on frame level. Then the coded video frames are passed through the network layer, i.e, encapsulated in IP packets. On the link layer, the video in IP packets need to be segmented into Packet Data Unit (PDU) to be delivered to the physical layer,. The segmentation is necessary since Layer 2 (L2) PDU is usually smaller than the IP packets, for the ease of correct transmission in wireless mobile channels (In the rest of this chapter, the term *packet* will refer to a L2 PDU only, since the network layer study is out of our scope.). In the physical layer transmissions, the wireless channels may introduce burst of errors so that a whole L2 packet is dropped. Unlike distributed bit errors, such burst errors are hard to be recovered by error correction codes no matter with physical layer FEC or with application layer FEC. On the application layer, these errors will propagate to following video frames and seriously degrade the video quality. Hence we consider that the instantaneous L2 Packet Error Ratio (PER) is crucial for the user perceived QoS, and start improving spectral efficiency on the data link layer with this PER constraint.

As the previous chapters revealed, when the error constraint (i.e, BER) is instantaneous, the transmitter has to adapt to the worst link receiver in the group.

If this instantaneous constraint can be relaxed, more spectral efficiency may be exploited in the efficiency-reliability tradeoff. From a cross-layer perspective, in a system with L2 ARQ, the instantaneous PER constraint can be seen as the residual PER after retransmission, and the PER limit for the first transmission may be relaxed if the physical layer and data link layer can be jointly designed.

The main problem when applying ARQ to Multicast is scalability [2]. Assume the channel fading of all users are i.i.d, and the average packet loss ratio is P . If in a unicast link the probability that a packet is lost and requires retransmissions is P , in a multicast link with N users, the probability to request retransmission for a multicast packet is $1 - (1 - P)^N$, since any of N users lost this packet would trigger a retransmission. When N is large, retransmission will be requested frequently, which will cost lots of transmission capacity and reduce the overall spectral efficiency. However, if several retransmission packets can be combined, such scalability problem may be solved.

Motivated by these considerations, we adopt the cross-layer design framework from [3], and jointly optimize the AMC schemes and ARQ scheme for wireless multicast. Multiple cross-layer designed AMC-ARQ strategies are proposed and compared with other strategies, e.g., AMC without ARQ strategies and AMC-ARQ strategies without cross-layer design. We also develop a packet-combine-based ARQ to solve the scalability problem.

5.2 Related Work

ARQ with packet combining has been proposed by some researchers. The authors of [4] had proposed to use *XOR* operation among retransmitted packets for

multiple unicast links. In their solution, each receiver has to overhear the packets transmitted to other users and store them. The transmitter will put multiple lost packets of different receivers into one Combined Packet (CP) with 'XOR' operation, and resend such a CP. Then each receiver expecting its retransmission can extract its own retransmitted packet utilizing its stored correct packets of other receivers. However, the price of this scheme in multi-user unicast case is that each receiver consumes N times the power as if it had only received its own packet. When there are N unicast receivers in a cell, the power consumption of each one will be N times larger than without this packet XOR.

This drawback does not exist in multicast case. E.g, if there is a $1/N$ outage ratio within N receivers for a given transmission rate according to their mean SNR, and let $D(k)$ represent the k th multicast data packet. During N transmission bursts each receiver got $N - 1$ packets correctly, and failed to receive one out of N packets. They send their requests via an error-free feedback channel, and the transmitter resends the $D(N+1) = D(1) \oplus D(2) \oplus \dots \oplus D(N)$ afterward. Each receiver will be able to extract its intended packet from $D(N + 1)$ and all its previously received and stored $N - 1$ packets.

More systematical packet combining methods are the packet level Reed-Solomon coding. A group of K consecutive packets are feed into a packet-based encoder to generate $L - K$ parity packets, and the L output packets, including K original packets and $L - K$ redundant packets, are sent along on the channel as a *Transmission Group (TG)*. Three HARQ schemes based on packet level Reed-Solomon codes were designed in [5] for UMTS downlink multicast channel, and the authors conclude that which design is better rather depends on the

multicast channel error process in reality (e.g, independent error model or burst error model). The authors of [6] further proposed two more HARQ schemes as the extensions of scheme A2 and A3 in [5] and achieve a certain improvement in throughput and mean Service Data Unit delay, especially when the multicast group size is large.

A cross-layer design was proposed in [3] for unicast links, which combined AMC and HARQ. In the spectral efficiency results of this work, the cross-layer scheme with one retransmission outperforms AMC without ARQ scheme by about 0.25 bits/symbol. However, further increase of maximum allowed retransmissions only results in diminishing gain. This work implies that one retransmission should be sufficient in joint AMC and ARQ design if the optimization target is to improve spectral efficiency while a residual packet loss ratio is allowed. This work inspired our proposals in its cross-layer framework.

5.3 Cross-Layer System Model

A wireless transmitter in contemporary systems (e.g, UMTS HSDPA, IEEE 802.11 a, b and g) usually has both Adaptive Modulation and Coding (AMC) and ARQ functionalities. Hence we assume the transmitter includes both functions, which are aware of each other. We also assume constant power transmission to reduce the design complexity in the cross-layer framework. Assume a base station multicasting to a group of N mobile receivers, where the Layer-1 (L1) feedback channels can provide instantaneous and perfect CSIs from the receivers to the BS transmitter, and the packet level, Layer-2 (L2) feedbacks will be also errorfree. The cross-layer system model between the transmitter and one of the receiver is illustrated in Fig. 5.1. The channels are assumed as frequency-flat block fading channels, hence the SINR, noted as $\gamma_i (i = 1..N)$, will not change during the transmission time of a PDU. The PDFs of γ_i follow Independent Identical Distributions (i.i.d), noted as $p(\gamma_i)$. The random vector $\vec{\gamma} := (\gamma_1, \gamma_2, \dots, \gamma_N)$ represents a fading state of the Multicast group, with probability density function $p^*(\vec{\gamma}) = \prod_{i=1}^N p(\gamma_i)$. The transmitted data block includes both error detection (ED) coding CRC and forward error correction (FEC) coding.

At the physical layer, we assume the available modulation and FEC code combinations (referred as AMC modes) are as in HIPERLAN/2. Based on the CSI reported from all multicast receivers and the link adaptation strategy, the AMC selector at the transmitter determines the AMC mode. At the data link layer, different ARQ protocols are implemented. A packet from the input buffer is sent to the physical layer and a copy of it is also stored in the ARQ buffer as shown in Fig. 5.1. If an error is detected in a packet, a retransmission request is sent

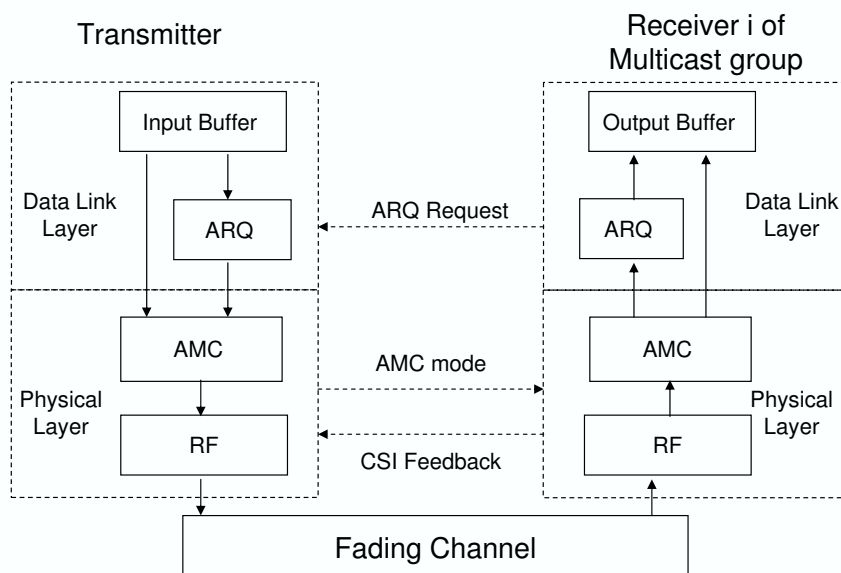


Figure 5.1: Multicast System Model with Cross-Layer Design

to the ARQ controller at the transmitter via a feedback channel; otherwise, no retransmission request is sent. The ARQ controller at the transmitter arranges retransmission of the requested packet that is stored in the buffer. If a certain packet is not requested to be resent for any of the receivers, it will be removed from the retransmission buffer; if it is requested by all the receivers, it will be pushed down from the ARQ buffer to the physical layer for retransmission immediately; if it is requested by some of the receivers, the operation will depend on the investigated ARQ schemes.

The optimization target is to maximize packet level spectral efficiency given the following constraints:

1. Constraint 1: Maximum allowed number of retransmissions T_r^{max} . T_r^{max} is set to 1, since the results in [3] shows that the spectral efficiency gain from cross-layer designed ARQ diminishes as retransmission time increases.

2. Constraint 2: The residual packet loss ratio bound after T_r^{max} retransmissions,

$$P_{loss} = 10^{-2}.$$

On packet level, exact close-form PERs of coded modulation versus γ are not available, but an approximation is provided in [3] as

$$PER_m(\gamma) \approx \begin{cases} a_m \exp(-g_m \gamma), & \text{if } \gamma \geq \Gamma_m \\ 1, & \text{if } 0 \leq \gamma < \Gamma_m \end{cases} \quad (5.1)$$

where m refer to AMC mode index, γ is the SINR of a receiver, a_m , g_m are parameters depend on AMC mode, which are presented in Table. 5.1. Γ_m is the threshold of AMC mode m . I.e., in a point-to-point link, mode m is chosen when $\gamma \in [\Gamma_m, \Gamma_{m+1})$. The value of Γ_m can be varied according to the target packet loss ratio, and the channel SINR distributions. If we only consider point-to-point

	Mode 1	Mode 2	Mode 3	Mode 4	Mode 5	Mode 6
Modulation	BPSK	QPSK	QPSK	16-QAM	16-QAM	64-QAM
Coding Rate	1/2	1/2	3/4	9/16	3/4	3/4
Rate (bits/symbol)	0.5	1.0	1.5	2.25	3.0	4.5
a_m	274.7229	90.2514	67.6181	50.1222	53.3987	35.3508
g_m	7.9932	3.4998	1.6883	0.6644	0.3756	0.0900

Table 5.1: Transmission AMC Modes with Convolutional-Coded Modulation

transmission without ARQ, the AMC threshold can be derived from 5.1 as

$$\Gamma_m = \frac{1}{g_m} \ln \left(\frac{a_m}{P_{loss}} \right) \quad (5.2)$$

where P_{loss} is the PER constraint. Given ARQ exist, if the expected average packet loss ratio per transmission is P_0 , and let $PER_{T_r^{max}+1}$ represent the residual PER after $T_r^{max} + 1$ transmissions for a specific packet (one original transmission and

T_r^{max} retransmissions), there must be

$$PER_{T_r^{max}+1} = P_0^{T_r^{max}+1} \leq P_{loss}. \quad (5.3)$$

In this case the thresholds can be rewritten as

$$\Gamma'_m = \frac{1}{g_m} \ln \left(\frac{a_m}{P_0} \right) \quad (5.4)$$

Since $0 < P_0 < 1$, $0 < P_{loss} < 1$ and $P_0 > P_{loss} \Rightarrow \Gamma'_m < \Gamma_m$, higher data rates can be allocated under thresholds Γ'_m than under Γ_m . However, the retransmission will also reduce the spectral efficiency due to the parity packet transmission. Whether such SINR threshold relaxation leads to higher spectral efficiency in total will depend on the comparison of

$$Se(1) = \sum_{m=1}^M R_m P_r(m) \quad (5.5)$$

and

$$Se(T_r^{max} + 1) = \frac{1}{\bar{T}} \sum_{m=1}^M R_m P'_r(m). \quad (5.6)$$

where $Se(1)$ is the spectral efficiency without retransmission, $Se(T_r^{max} + 1)$ is the one with at most T_r^{max} retransmission. R_m is the bit per symbol in each AMC mode, $P_r(m)$ and $P'_r(m)$ are the cumulated probability of SINR staying in rate region m , and they are different due to the different rate region thresholds as in 5.2 and 5.4. \bar{T} is the expected transmissions per packet,

$$\bar{T} = 1 + P_0 + P_0^2 + \dots + P_0^{T_r^{max}} = \frac{1 - P_0^{T_r^{max}+1}}{1 - P_0} \quad (5.7)$$

If, for a given SINR distribution, $Se(T_r^{max} + 1) > Se(1)$, then we gain spectral

efficiency with cross layer AMC at the price of packet delay.

5.4 Multicast ARQ with Packet-Combining

We analyze our multicast ARQ design in a two phase setting, the original data transmission phase and the retransmission phase, namely the first phase and the second phase. These two phases are considered separately for the ease of analysis, even though they will be fulfilled alternatively and partially overlap each other in practice. In the first phase, a large number of data packets are transmitted, such that the packets number is enough for probabilistic analysis. The packet loss of each user in the first phase will be reported to the transmitter. In the second phase, the transmitter will select the most efficient way to combine the lost packets with *XOR* operation in the ARQ buffer and resend them. Under design constraint 1, each data packet lost in the first phase will only be retransmitted once in the second phase, thus constraint 2 and Eq.5.3 lead to

$$P_0 = \sqrt{P_{loss}} = 0.1 \quad (5.8)$$

in which P_{loss} is the target residual PER and P_0 is the instantaneous PER constraint.

In the rest of this section two cases of packet combining are discussed, a simple case with only two users in a group, and the general case for a group with N users ($N \geq 2$).

5.4.1 Two Users Group

In a group with only two receivers, a packet loss pattern in the first phase is illustrated in Fig. 5.2. For data packets D_2, D_4, D_5, D_{10} which are only lost by one user each, the BS can combine the retransmission, e.g. $CP_1 = D_2 \oplus D_4$ (CP stands for Combined Packet), $CP_2 = D_5 \oplus D_{10}$, and both users can decode them using its previously correctly received packet (e.g, UE1 use $D_2 \oplus CP_1 = D_4$ and UE2 use $D_4 \oplus CP_1 = D_2$). In this case, we call the packets which can be combined into one CP as *match packet* to each other, e.g, D_2 and D_4 , D_5 and D_{10} . For

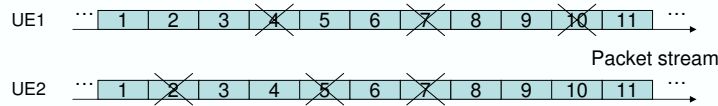


Figure 5.2: Multicast Packet Loss Pattern for 2 UEs

D_7 , both users lost it and it cannot be combined with other lost data packets in the retransmission, otherwise there will be at least one user who cannot decode it.

For any arbitrary packet , define L as the number of users who lost it. To calculate the transmission per packet T when packet combination is adopted, define

$$\eta = 1/(\text{Number of data packets included in 1 CP})$$

and $T = 1 + \eta$. E.g. $\eta(D_2) = \eta(D_4) = \eta(D_5) = \eta(D_{10}) = 1/2$ for packets D_2, D_4, D_5, D_{10} and $T = 1 + \frac{1}{2}$ for each of them. Hence it has to be retransmitted by itself and $\eta(D_7) = 1$.

From the example in Fig. 5.2, we can derive the expected number of retransmissions and probabilities. That is, there are three cases for a multicast group with $N = 2$:

- If no user lost this packet, no retransmission is necessary:

$$Pr(L = 0) = (1 - P)^2,$$

$$\eta(L = 0) = 0;$$

- If one user lost this packet, packet combination with a packet lost by the other user can be performed:

$$Pr(L = 1) = \binom{2}{1} P(1 - P),$$

$$\eta(L = 1) = \frac{1}{2};$$

- If both users lost this packet, no packet combination is possible:

$$Pr(L = 2) = P^2,$$

$$\eta(L = 2) = 1.$$

And the expectation of the effective transmission time for any arbitrary packet is

$$\begin{aligned} E[T] &= 1 + \sum_{i=0}^2 \eta(L = i) Pr(L = i) \\ &= 1 + P \end{aligned} \quad (5.9)$$

5.4.2 N Users Group

Now we generalize such analysis to the N user case ($N \geq 2$). There are two lemmas for the general case:

- *Lemma 1:* For any arbitrary packet D_j (j is the packet index), its match packet(s) exist iff $1 \leq L(D_j) \leq N - 1$, and its match packet(s) are not unique.
- *Lemma 2:* A CP can be made up of a subset of lost packets $D_{j_1}, \dots, D_{j_k}, \dots,$ ($1 \leq L(D_{j_k}) \leq N - 1$)

iff $L(D_{j_1}) + \dots + L(D_{j_k}) + \dots \leq N$ and there are no overlapping users among the loss patterns of each lost packet in this subset. (Put it another way, each user can have at most one lost packet in the subset of packets retransmitted in one CP.)

Refer to the system model in Fig. 5.1, our proposed ARQ function can work in this way: the transmitter sends data packets from its input buffer to the physical layer, and keep copies of these packets in the ARQ buffer; if one packet is reported as correct by all users ($L = 0$), it is removed from the ARQ buffer; if one packet is lost by all users ($L = N$), it will be retransmitted immediately and removed from the ARQ buffer; otherwise one packet is lost by i users ($L = i, 1 \leq i \leq N - 1$), it will be kept in the ARQ buffer and wait to be combined with other loss packets. As the number of packets in the ARQ buffer increases, the ARQ function will first find the match packets for the first packet in the queue, and combine them and send the CP, then remove these sent packets. According to the three packet lost cases described above, the corresponding probabilities and the expected number of retransmissions of any arbitrary packet are:

- $Pr(L = 0) = (1 - P)^N, \eta(L = 0) = 0;$
- $Pr(L = N) = P^N, \eta(L = N) = 1,$
- If $L = i, 1 \leq i \leq N, Pr(L = i) = \binom{N}{i} P^i (1 - P)^{N-i}.$

There are many ways to find match packets for this packet as indicated in Lemma 1, but the most efficient one is to find $N - i$ loss packets in the rest of the queue, and each of them is lost only by one user and there is no overlapping of users among them. This is called an optimal combination set

where $\eta(L = i) = \frac{1}{N-i+1}$, and

$$\begin{aligned} E[T]_{opt} &= 1 + \sum_{i=0}^N \eta(L = i) Pr(L = i) \\ &= 1 + \sum_{i=1}^N \frac{1}{N-i+1} \binom{N}{i} P^i (1-P)^{N-i} \end{aligned} \quad (5.10)$$

However, it may take very long time to cumulate all $N - i + 1$ match packets for the optimal combination. Hence we also propose a suboptimal combination scheme, such that the current packet with $L = i$ only need to be combined with another packet with $L = j$, $i + j \leq N$ and there is no overlapping users between the two packets, and $\eta(L = i) = \eta(L = j) = \frac{1}{2}$,

$$E[T]_{SubOpt} = 1 + P^N + \frac{1}{2} \sum_{i=1}^{N-1} \binom{N}{i} P^i (1-P)^{N-i} \quad (5.11)$$

Note: when $N = 2$, the optimal and sub-optimal combination become the same.

5.5 AMC Strategies

When ARQ is not adopted in the system, the rate adaptation is limited by the minimum received SINR among all multicast receivers, namely the Minimum-SINR AMC strategy. With the help of ARQ, the instantaneous PER constraint of the worst-channel receiver can be temporarily violated such that AMC strategies other than the Minimum-SINR strategy can also be adopted. And the lost packets of the worst-channel receiver can be retransmitted such that its residual PER may still be within P_{loss} . The AMC strategies we investigate jointly with ARQ are:

1. Minimum SINR AMC

In this strategy the data rate has to satisfy the instantaneous PER constraint of the worst SINR receiver, such as

$$\text{AMC mode } m \text{ is chosen if } \min\{\vec{\gamma}\} \in [\Gamma_m, \Gamma_{m+1})$$

2. Second Minimum SINR AMC

In this strategy the data rate has to satisfy the instantaneous PER constraint of the second least SINR receiver, noted as γ_{Min2} , i.e.,

$$\text{AMC mode } m \text{ is chosen if } \gamma_{Min2} \in [\Gamma_m, \Gamma_{m+1})$$

3. Average PER-based AMC

In this strategy the data rate is chosen such that the corresponding average instantaneous PER among group members is the closest to the PER constraint of all rate options. Before each transmission burst is sent,

For AMC mode $m = 1..M$,

$$\overline{PER}_m = \sum_{i=1}^N PER_m(\gamma_i)$$

$$m_{opt} = \arg \min |\overline{PER}_m - P_0|$$

Assign m_{opt} .

Since strategy 2 and 3 do not guarantee the instantaneous PER of each receiver during the first transmission, the residual PER of a packet has to be guaranteed by the ARQ schemes.

5.6 Evaluation Methods

In total, there are three adaptation strategies to be compared in this chapter.

- The proposed cross layer approach, where the instantaneous PER relaxation due to ARQ is adopted, so

$$P_0 = \sqrt{P_{loss}} = 0.1$$

- Layered multicast AMC and ARQ. In this case multicast AMC and ARQ functions both exist in the system, but they are not jointly designed. I.e, the AMC thresholds are derived from

$$P_0 = P_{loss} = 0.01;$$

- AMC alone.

The AMC strategy 1 can be applied with or without ARQ, with or without cross-layer design, since it uses an absolute instantaneous PER constraint in AMC mode selection for the first transmission. E.g., the target residual PER is 0.01, hence the PER constraint without ARQ is 0.01; it is also 0.01 with ARQ but no X-layer design, since then AMC part is not aware the exist of ARQ; it is relaxed to 0.1 with ARQ and cross-layer awareness. But AMC strategy 2 and 3 must be applied with ARQ, as explained in Sec. 5.5.

On the other hand, three different ARQ schemes are to be compared:

- Optimal packet combining
- Sub-optimal packet combining

- Plain ARQ, no packet combining

5.7 Case Study I: $N = 2$

In this case study, a group of 2 users under i.i.d Rayleigh fading channels is considered. The attempt is to derive the close-form solution of the spectral efficiencies for two AMC strategies, strategy 1 and 2, with or without cross-layer design. Strategy 3 is not studied since it is difficult to build a close-form model for its algorithm. So there are four AMC-ARQ strategies to be evaluated:

- Strategy S1: Minimum SINR AMC, with the packet-combining ARQ and cross-layer design.
- Strategy S2: Maximum SINR AMC, with the packet-combining ARQ and cross-layer design. In a two users group, the strategy 2 of Sec. 5.5 reduces to this Maximum SINR AMC. Also, this scheme cannot be adopted without ARQ.
- Strategy S3: Minimum SINR AMC, without ARQ.
- Strategy S4: Minimum SINR AMC, with ARQ but not cross-layer design.

As explained in Sec. 5.4.2, the optimal and sub-optimal packet-combining ARQ are the same at $N = 2$.

5.7.1 Performance Analysis in Close-Form Expression

According to Eq.5.5, the per user spectral efficiency from the first transmission is

$$Se(1) = \sum_{m=1}^M R_m \int \int_{\Omega_m} p(\gamma_1, \gamma_2) d\gamma_1 \quad (5.12)$$

where the rate region Ω_m corresponding to rate R_m is a two-dimensional area depending on the rate adaptation strategy, and p is the joint PDF of γ_1 and γ_2 .

Assume only one combined retransmission is allowed for any loss packet, hence the per user spectral efficiency after the retransmission is

$$Se(T_r^{max} + 1) = \frac{Se(1)}{\bar{T}}. \quad (5.13)$$

For the ease of presenting different AMC strategies in the integrals, let γ_d represent the dominant SINR for rate selection, hence

- Min-SINR AMC, $\gamma_d = \gamma_{min} := \min\{\gamma_1, \gamma_2\}$;
- Max-SINR AMC, $\gamma_d = \gamma_{max} := \max\{\gamma_1, \gamma_2\}$.

On average, the expected transmission time per packet with loss probability P among users are $\bar{T} = 1 + P$, where

$$\begin{aligned} P &= \overline{PER_1} = \overline{PER_2} \\ &= \frac{\sum_{m=1}^M R_m \int \int_{\Omega_m} PER_m(\gamma_1) p(\gamma_1, \gamma_2) d\gamma_1 d\gamma_2}{Se(1)}, \end{aligned} \quad (5.14)$$

in which $PER_m(\gamma_1)$ can also be $PER_m(\gamma_2)$ given the users' SINR PDFs are i.i.d. According to Eq. 5.9, Eq.5.13 and 5.14, the expected per user spectral efficiency is

$$Se(T_r^{max} + 1) = \frac{Se(1)}{1 + \frac{1}{Se(1)} \sum_{m=1}^M R_m \int \int_{\Omega_m} PER_m(\gamma_1) p(\gamma_1, \gamma_2) d\gamma_1 d\gamma_2} \quad (5.15)$$

To observe the system performance, it is necessary to derive $Se(1)$, P and $Se(T_r^{max} + 1)$. Hence we have to solve the integral of PER_m and the integral of $p(\gamma_1, \gamma_2)$ in rate region Ω_m , and the shape of Ω_m depends on the AMC strategy.

5.7.1.1 Close-Form Solution for Min-SINR AMC

Starting with AMC strategy 1, the rate regions will have the shapes as in Fig. 5.3, and the integration of PER_m in such rate regions can be calculated as

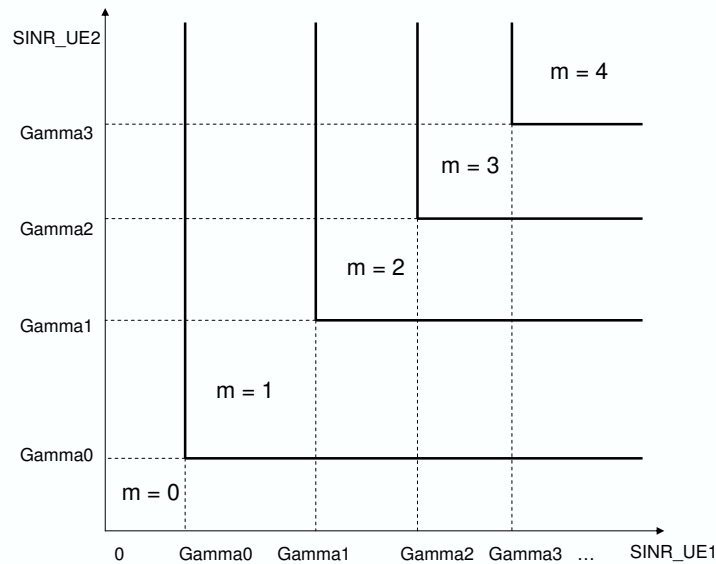


Figure 5.3: Integration Region of 2 UEs, D-Rate

1. $m < M$,

$$\begin{aligned}
& \int \int_{\Omega_m} PER_m(\gamma_1) p(\gamma_1, \gamma_2) d\gamma_1 d\gamma_2 \\
&= \int_{\Gamma_{m+1}}^{\infty} \int_{\Gamma_m}^{\Gamma_{m+1}} a_m \exp(-g_m \gamma_1) p(\gamma_1) p(\gamma_2) d\gamma_1 d\gamma_2 \\
&+ \int_{\Gamma_m}^{\Gamma_{m+1}} \int_{\Gamma_m}^{\infty} a_m \exp(-g_m \gamma_1) p(\gamma_1) p(\gamma_2) d\gamma_1 d\gamma_2 \\
&= Q(m+1) \int_{\Gamma_m}^{\Gamma_{m+1}} \frac{a_m \gamma_1}{\sigma^2} \exp(-g_m \gamma_1 - \frac{\gamma_1^2}{2\sigma^2}) d\gamma_1 \\
&\quad + (Q(m) - Q(m+1)) \int_{\Gamma_m}^{\infty} \frac{a_m \gamma_1}{\sigma^2} \exp(-g_m \gamma_1 - \frac{\gamma_1^2}{2\sigma^2}) d\gamma_1
\end{aligned} \tag{5.16}$$

where $Q(m) = \exp(-\Gamma_m^2/2\sigma^2)$.

2. $m = M$

$$\begin{aligned}
& \int \int_{\Omega_M} PER_M(\gamma_1) p(\gamma_1, \gamma_2) d\gamma_1 d\gamma_2 \\
&= \int_{\Gamma_m}^{\infty} \int_{\Gamma_m}^{\infty} a_M \exp(-g_M \gamma_1) p(\gamma_1) p(\gamma_2) d\gamma_1 d\gamma_2 \\
&= Q(M) \int_{\Gamma_m}^{\infty} \frac{a_M \gamma_1}{\sigma^2} \exp(-g_M \gamma_1 - \frac{\gamma_1^2}{2\sigma^2}) d\gamma_1
\end{aligned} \tag{5.17}$$

5.7.1.2 Close-Form Solution for Max-SINR AMC (Second-Min-SINR AMC @ N=2)

For AMC strategy 2, rate region Ω_m is represented in Fig. 5.4. The integration of

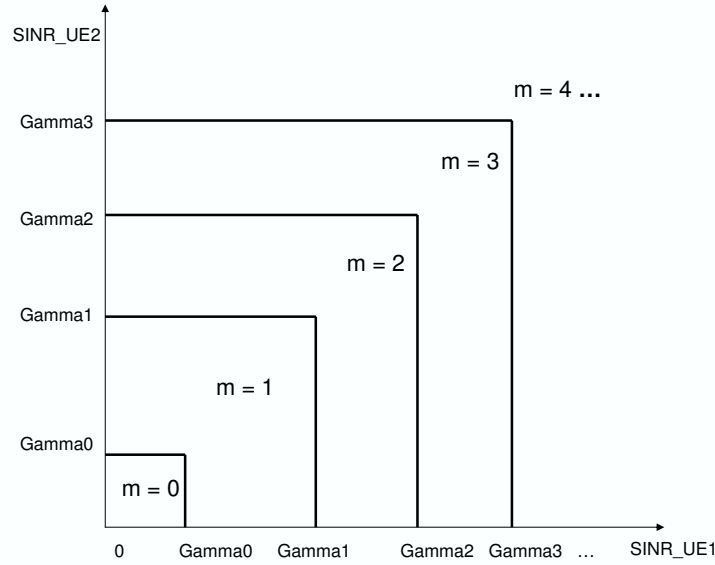


Figure 5.4: Rate Regions of Max-SINR Strategy

PER_m in such rate regions can be calculated as

1. $m < M$,

$$\begin{aligned}
 & \int \int_{\Omega_m} PER_m(\gamma_1) p(\gamma_1, \gamma_2) d\gamma_1 d\gamma_2 \\
 &= \int_0^{\Gamma_{m+1}} \int_{\Gamma_m}^{\Gamma_{m+1}} a_m \exp(-g_m \gamma_1) p(\gamma_1) p(\gamma_2) d\gamma_1 d\gamma_2 \\
 & \quad + \int_{\Gamma_m}^{\Gamma_{m+1}} \int_0^{\Gamma_m} 1 \cdot p(\gamma_1) p(\gamma_2) d\gamma_1 d\gamma_2 \\
 &= (1 - Q(m+1)) \int_{\Gamma_m}^{\Gamma_{m+1}} \frac{a_m \gamma_1}{\sigma^2} \exp(-g_m \gamma_1 - \frac{\gamma_1^2}{2\sigma^2}) d\gamma_1 \\
 & \quad + (Q(m) - Q(m+1))(1 - Q(m)) \tag{5.18}
 \end{aligned}$$

where $Q(m) = \exp(-\Gamma_m^2/2\sigma^2)$.

2. $m = M$

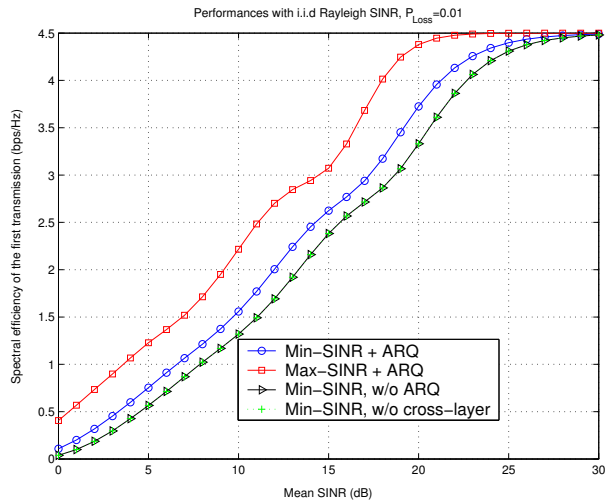
$$\begin{aligned}
& \int \int_{\Omega_M} PER_M(\gamma_1) p(\gamma_1, \gamma_2) d\gamma_1 d\gamma_2 \\
&= \int_0^\infty \int_{\Gamma_M}^\infty a_M \exp(-g_M \gamma_1) p(\gamma_1) p(\gamma_2) d\gamma_1 d\gamma_2 \\
&+ \int_{\Gamma_M}^\infty \int_0^{\Gamma_M} 1 \cdot p(\gamma_1) p(\gamma_2) d\gamma_1 d\gamma_2 \\
&= \int_{\Gamma_M}^\infty \frac{a_M \gamma_1}{\sigma^2} \exp(-g_M \gamma_1 - \frac{\gamma_1^2}{2\sigma^2}) d\gamma_1 + Q(M)(1 - Q(M)) \quad (5.19)
\end{aligned}$$

So far, the integrals of PER_m s can be calculated, and the calculation of $\sum_{m=1}^M R_m \int \int_{\Omega_m} p(\gamma_1, \gamma_2) d\gamma_1 d\gamma_2$ can be done in the similar way. That is, the values of P in Eq.5.14 and $Se(T_r^{max} + 1)$ in Eq.5.15 can be derived accordingly.

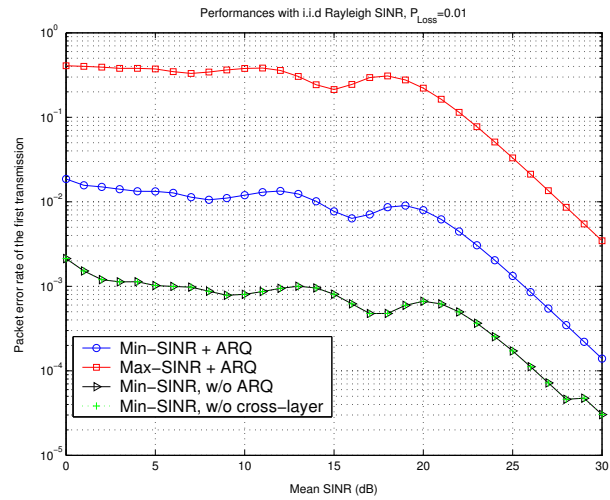
5.7.2 Numerical Results

The resulted performances and behaviors of all four strategies are plotted in Fig. 5.5. From Fig. 5.5(a) it can be observed that the Max-SINR strategy(strategy S2) has the highest spectral efficiency for the first transmission with significant gain over the other three strategies. Strategy S1 outperforms strategy S3 and S4, and the curves of S3 and S4 are overlapping with each other. This is because S3 and S4 follow the most strict instantaneous PER constraints, while S2 allocates data rate more aggressively than S1. On the other hand, such aggressive adaptation of Max-SINR resulted in a very high PER even when the average SINR is good, while the PERs of the other two decreased fast as average SINR increase, as shown in Fig. 5.5(b). The overall spectral efficiency results in Fig. 5.5(c) are:

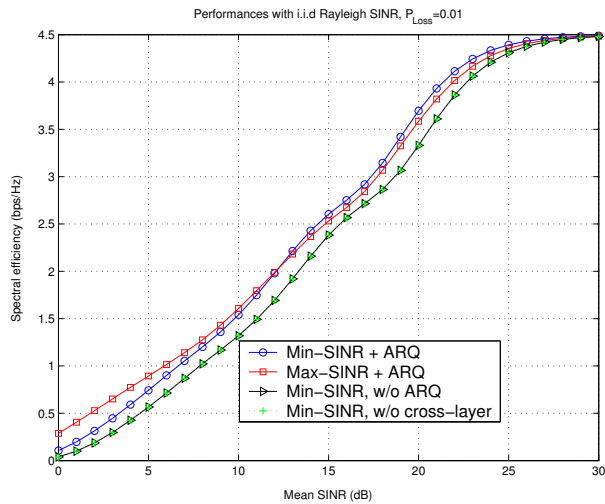
when the average SINR is less than 12dB, strategy S2 performs the best, since the rate allocation gain overcomes the efficiency loss of retransmission. The



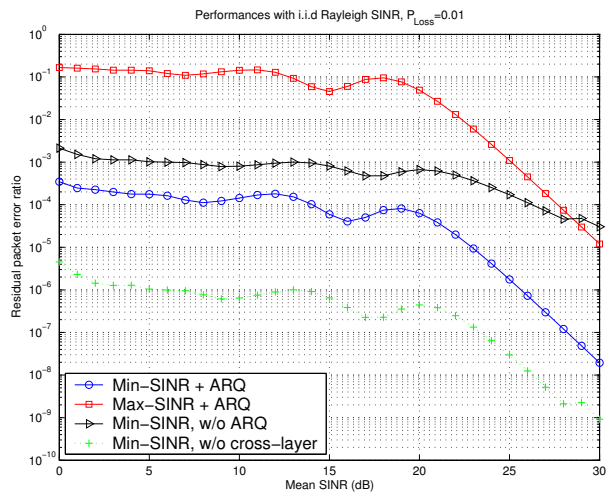
(a) Spectral Efficiency of the First Transmission



(b) Packet Error Ratio



(c) Overall Spectral Efficiency



(d) Residual Packet Error Ratio

Figure 5.5: Performances of Different Adaptation Strategies, $N = 2$

spectral efficiency gain of strategy S2 can achieve at most 0.4bit/s/Hz in this region. As average SINR gets higher than 12dB, the performance of S1 exceeds S2, but the difference is quite small. As the average SINR approaches 30dB, the three curves converge. This is due to the finite modulation and coding schemes available (i.e, the adopted 6 modulation and coding combinations). When the SINR is so high, the packet loss is small enough such that the spectral efficiency is only limited by the highest modulation and coding rate.

However, the residual PER curves in Fig. 5.5(d) shows that strategy S2 fails to keep the PER constraint ($P_{loss} = 10^{-2}$) when the average SINR is less than 23dB. That is, strategy S1 is the best one for the two user group case.

5.8 Case Study II: $N \geq 2$

In this section, Monte-Carlo method is adopted in numerical integrations to derive the performances for different AMC-ARQ strategies when the multicast group size $N \geq 2$. This choice is due to two reasons: first, it is difficult to express more complex AMC strategies such as the strategy 3 in Sec. 5.5 in close-form; second, when $N > 2$, it is difficult to solve the integral along rate region Ω_m in close-form, since the shape of Ω_m becomes complex as N is large. When the complexity of deriving close-form solution is avoid, it is possible to investigate the behavior of more AMC and ARQ combinations, as the group size increases.

Here we compared the performance of 5 different schemes in total:

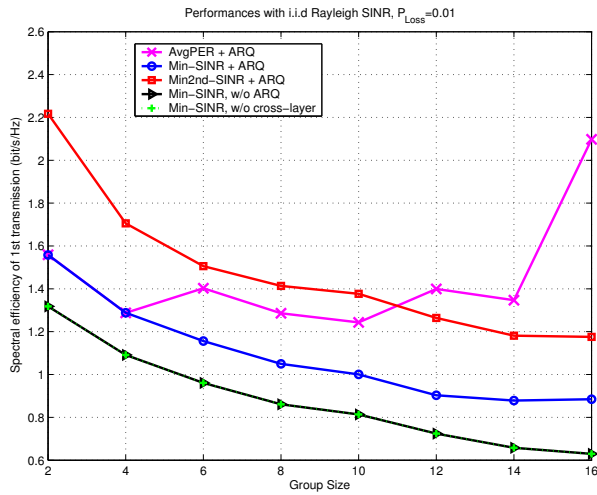
- Strategy S1: Average PER AMC as the AMC strategy 3 in Sec. 5.5, with ARQ and cross-layer design, $P_0 = \sqrt{P_{loss}} = 0.1$.

- Strategy S2: Minimum SINR AMC as the AMC strategy 1 in Sec. 5.5, with ARQ and cross-layer design, $P_0 = \sqrt{P_{loss}} = 0.1$.
- Strategy S3: Second minimum SINR AMC as the AMC strategy 2 in Sec. 5.5, with ARQ and cross-layer design, $P_0 = \sqrt{P_{loss}} = 0.1$.
- Strategy S4: Minimum SINR AMC, without ARQ, $P_0 = P_{loss} = 0.01$.
- Strategy S5: Minimum SINR AMC, with ARQ but not cross-layer design, $P_0 = P_{loss} = 0.01$.

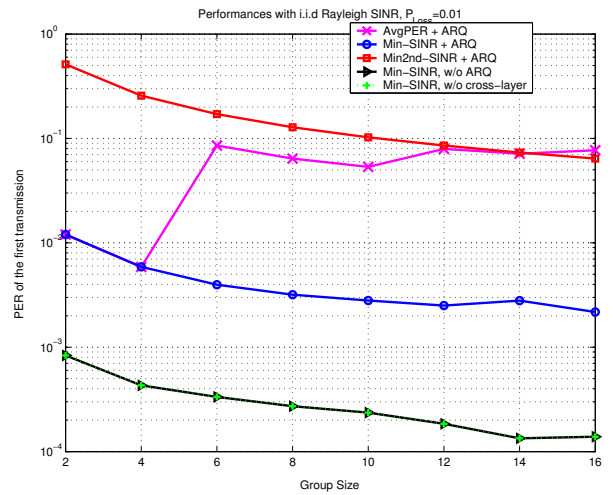
In this section, the performances of strategy S1, S2, S3 and S5 are analyzed with the optimal packet-combining ARQ, the sub-optimal packet-combining ARQ and the plain ARQ (no packet-combining).

5.8.1 Numerical Results

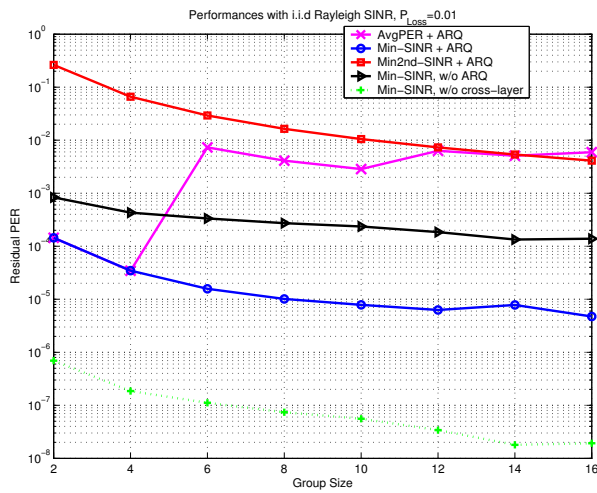
The numerical result of all investigated adaptation schemes are presented in Fig. 5.6 for the average SINR at 10dB. In these results, the spectral efficiencies of the first transmission stage are depicted in Fig. 5.6(a), and the PERs of the first transmission are presented in Fig. 5.6(b). After the retransmissions, the residual PERs are shown in Fig. 5.6(c), Fig. 5.6(d), Fig. 5.6(e) and Fig. 5.6(f) illustrate the overall spectral efficiencies after the retransmissions with the optimal packet-combining ARQ, the sub-optimal packet-combining ARQ and the plain ARQ, respectively.



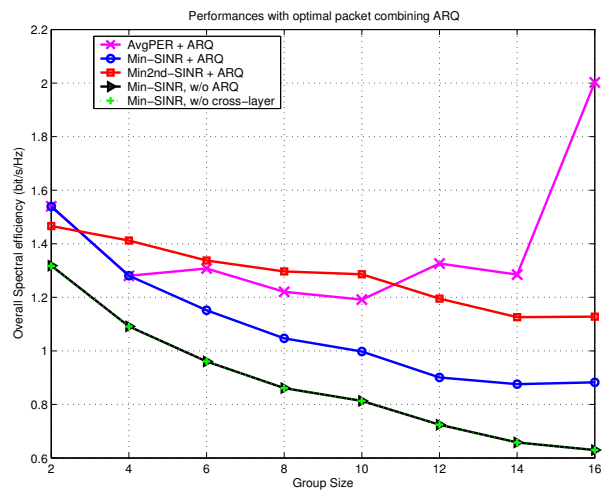
(a) Spectral Efficiency of the First Transmission



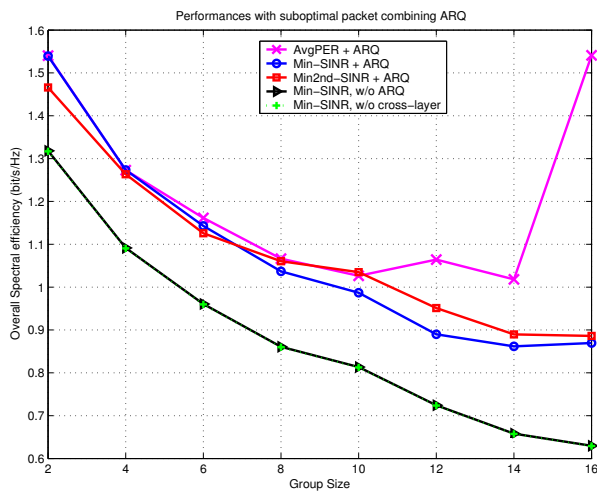
(b) Packet Error Ratio



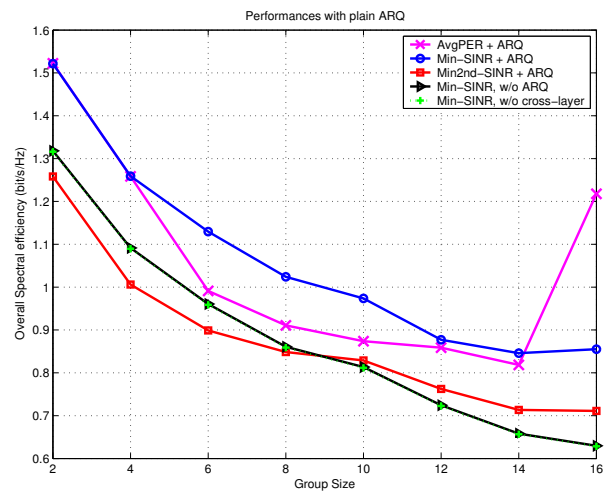
(c) Residual Packet Error Ratio



(d) Spectral Efficiency after Optimal Packet-Combining



(e) Spectral Efficiency after Sub-Optimal Packet-Combining



(f) Spectral Efficiency after Plain ARQ

Figure 5.6: Performances of AMC-ARQ Strategies VS Group Size, $\overline{SINR} = 10\text{dB}$

Fig. 5.6(a) reflects the performances of all strategies before ARQ, hence the performance differences are due to different AMC schemes and different P_0 s. It can be observed that S1 (the red curve) and S3 (the purple curve) achieved the best spectral efficiency in the first transmission stage. But S3 fails to keep the residual PER bound when the group size is less than 10 (Fig. 5.6(b)), hence it should be out of consideration. The spectral efficiency of S2 is less than S1 and S3, but better than S4 and S5. S1 outperforms S2 when $N > 4$ and the performance gain keeps increasing as the group size is getting larger, from about 0.2bit/s/Hz when $N = 6$ to 1.4bits/s/Hz when $N = 16$. This is because S1 exploits the efficiency-reliability tradeoff more extensively, as shown in Fig. 5.6(b), where the PER of S1 is only slightly less than 0.1 when $N > 4$. In S1, there is higher possibility that the worst PER can be averaged out by the PERs of other group members as the group size increases, so that the average PER of the group allows higher rate assignment. It is also clear in Fig. 5.6(b) that such benefit does not exist when $N \leq 4$, where the spectral efficiency of S1 before ARQ is almost the same as S2 (in Fig. 5.6(a)). That is because the group size is too small and the worst PER due to the least SINR dominates the rate assignment. Besides, the PER of S1 is still within $P_0 = 10^{-1}$ boundary (as in Fig. 5.6(b)), and the residual PER is within $P_{loss} = 10^{-2}$ (as in Fig. 5.6(c)). Comparing S1 and S2 in Fig. 5.6(a), we can conclude that: S1 exploits the user diversity in their SINRs and corresponding PERs, so its spectral efficiency is not decreasing monotonically as group size increases; while the rate assignment of S2 is limited by the worst SINR, and its spectral efficiency keeps decreasing as the group size/diversity increases. Comparing S2, S4 and S5, it can be seen that the gain of cross-layer design (relaxing P_0 from 0.01 (S4 and S5) to

0.1 (S2)) is between 0.2 and 0.3 bit/s/Hz. The curves of S4 and S5 are overlapping each other since they share the same AMC scheme and the same P_0 , hence they perform the same during the first transmission stage.

Then let us look at the overall spectral efficiencies after the retransmissions presented in Fig. 5.6(d), Fig. 5.6(e) and Fig. 5.6(f). If the optimal packet combining is adopted (Fig. 5.6(d)), S1 is still the best strategy, but its performance gain over S2 is slightly less than the gain before retransmission, from 0.16 bit/s/Hz ($N = 6$) up to about 1.1bit/s/Hz ($N = 16$). This gain reduction is due to the more retransmissions required in S1, since its PER is much higher than that of S2 (shown in Fig. 5.6(b)). If the sub-optimal packet combined ARQ is adopted

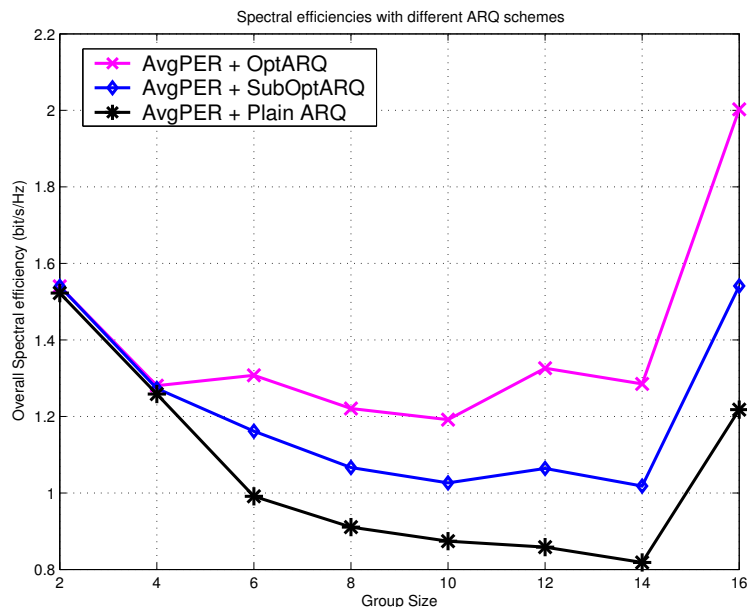


Figure 5.7: Spectral Efficiencies of S1 with Different ARQs, $\overline{SINR} = 10\text{dB}$

(Fig. 5.6(e)), S1 still outperforms S2, but the gain of S1 over S2 is not significant until $N \geq 12$. In the plain ARQ case (Fig. 5.6(f)), the spectral efficiency of S1 is even less than or equal to that of S2 unless $N = 16$. That is, without the packet-combining ARQs, the spectral efficiency gain of S1 over S2 would have

been cancelled by its frequent retransmissions. The spectral efficiencies of S1 with all three ARQs are also compared in Fig. 5.7, where the gain of the optimal ARQ over the sub-optimal ARQ can be up to 0.44bit/s/Hz ($N = 16$), and the gain of the sub-optimal ARQ over the plain ARQ can be up to 0.32bit/s/Hz ($N = 16$).

Last but not the least, the gain of cross-layer design itself is stable with all three ARQ schemes. S2, S4 and S5 adopt the same rate adaptation strategy, and S2 outperforms the other two strategies by 0.2 to 0.24 bit/s/Hz in its overall spectral efficiencies with any of the three ARQ schemes (Fig. 5.6(d), Fig. 5.6(e) and Fig. 5.6(f)). The spectral efficiency curves of S4 and S5 after retransmissions are also overlapping each other, since their performance are the same in Fig. 5.6(a), and the PERs are so small (less than 10^{-3}) that the spectral efficiency loss introduced by the very few retransmissions in S5 comparing to S4 (no retransmission) is trivial.

The performance results for the average SINR at 5dB and 15dB have also been derived, and are presented in the appendix.

5.9 Conclusion and Future Work

In this section we propose a innovative multicast ARQ scheme in its optimal and suboptimal forms. This scheme utilize the packet level 'XOR' operation to reduce the number of retransmissions, in order to solve the scalability problem of multi-cast ARQs. We adopt this packet-combining ARQ scheme in a cross-layer design framework, which allows the instantaneous PER constraint to be relaxed and the data rate to increase. An average-PER-based (average over instantaneous group PERs) rate adaptation algorithm has also been developed within this cross-layer

framework.

The performance analysis has been fulfilled in two case studies: the first analysis is for the group with only two multicast receivers, and the close-form solutions for both spectral efficiencies and residual PERs are derived; the second analysis is for the group with N receivers ($N \geq 2$) based on the Monte-Carlo integration method, and in this way more combinations of AMC and ARQ strategies have been studied. Both case studies are based on the assumptions that the SINRs of the receivers are i.i.d and Rayleigh distributed. Since the second case study covers more general scenarios and more adaptation strategies than the first one does, the conclusions of this chapter are mainly drawn from the second case study.

The numerical results shows that our jointly designed average PER adaptation and optimal packet-combining ARQ achieve the best spectral efficiency among all AMC-ARQ strategies, and successfully keep the residual PER constraint at the same time. The second-minimum SINR-based AMC is also efficient in spectral efficiency, but fail to keep the residual PER constraint even with ARQ. The results also reveal that the gain of cross-layer design over non-cross-layer design with the same rate adaptation strategy is stable under different ARQ schemes.

The work in this chapter is based on the following assumptions:

Perfect and instantaneous CSI feedbacks for the AMC function in the BS. In reality the CSI feedbacks must be delayed and may include errors, and there could also be a scalability problem for the CSI feedbacks while the group size is large. To include these issues, more detailed analysis and simulations need to be done in our future work. However, though the spectral efficiencies

of the evaluated solutions in this chapter are expected to decrease with imperfect CSIs comparing to the current results with perfect CSIs, the optimal solution S1 should still outperform the others.

Correct PDU-level feedbacks for the ARQ function in the BS. Since the feedbacks for the ARQ function is simply ACK/NACK messages, which requires rather low data rate and can be transmitted with the most robust AMC mode, this assumption should hold unless some feedback channels are in deep fading.

Rayleigh distributions and i.i.d for the SINRs of all receivers. Strictly speaking the i.i.d Rayleigh assumption can only describe the SINRs of the receivers if they are at the same distance to the BS and with the same Shadowing level. This assumption is adopted since multi-path fading is the main challenge for the link adaptation approaches to cope with in this PhD thesis. The analytical model based on this assumption in this chapter can be seen as the first step toward building a more sophisticated cross-layer model for joint AMC-ARQ optimizations. In our future work, the proposed AMC-ARQ strategies can be analyzed with the general Nakagami-m model [7], or with detailed simulations which are able to evaluate these strategies under non-i.i.d SINRs.

Due to the time limitation, the delay caused by the packet-combining ARQ could not have been discussed quantitatively. In general, the delay introduced by the optimal packet-combining scheme might be too long to be implemented in practical systems, and the sub-optimal packet-combining scheme is more implementable. The reason has been explained in Sec. 5.4.2. The spectral efficiency advantage of the sub-optimal packet-combining ARQ over plain ARQ is less than that of the

optimal packet-combining ARQ, but still significant (Fig. 5.7). In our future work, a detailed delay analysis for the proposed ARQ schemes should be fulfilled.

Note: The works presented in this chapter will be published in [8].

Bibliography

- [1] O. Harmanci and A. M. Tekalp, "A Stochastic Framework for Rate-Distortion Optimized Video Coding Over Error-Prone Networks," in *IEEE Trans. Image Processing*, vol. 16, no. 3, pp. 684-697, Mar. 2007.
- [2] S. Sesia, G. Caire, and G. Vivier, "On the Scalability of H-ARQ Systems in Wireless Multicast," in *Proc. IEEE ISIT'04*, pp. 321-321, 2004.
- [3] Q. Liu, S. Zhou, and G. B. Giannakis, "Cross-Layer combining of adaptive Modulation and coding with truncated ARQ over wireless links," *IEEE Trans. Wireless Commun.*, vol. 3, no. 5, pp. 1746-1755, Sept. 2004.
- [4] P. Larsson and N. Johansson, "Multi-User ARQ," in *IEEE Vehicular Technology Conference 2006 (VTC'06-Spring)*, Melbourne, Australia, May 2006.
- [5] F. Fitzek, M. Rossi, and M. Zorzi, "Error Control Techniques for Efficient Multicast Streaming in UMTS Networks," in *Proc. SCI 2003*, 2003.
- [6] G. D. Papadopoulos, G. Koltsidas, and F. N. Pavlidou, "Two Hybrid ARQ Algorithms for Reliable Multicast Communications in UMTS Networks," *IEEE Commun. Letters*, vol. 10, no. 4, pp. 260-262, Apr. 2006.

-
- [7] G. L. Stüber, *Principles of Mobile Communication*, 2nd ed., Kluwer Academic Publishers, 2001.
- [8] H. Wang, H. P. Schwefel and T. S. Toftegaard, “A Cross-layer Design for Mobile Multicast with Packet-Combining ARQ,” in preparation.

Chapter 6

Conclusion

6.1 Summary

This PhD dissertation has focused on the wireless multicast link adaptation problem, and has explored the spectral efficiency and reliability tradeoff of a wireless multicast channel with both simulation-based and analytical-model-based approaches. In order to optimize the average spectral efficiency per multicast user with QoS constraints, multicast-specific rate adaptation, power adaptation, joint power and rate adaptation, cross-layer design combining AMC and ARQ have been investigated, and new algorithms are proposed and evaluated. Numerical results also reveals the necessary user number switching from unicast mode to multicast mode.

Our optimization methods and their corresponding constraints can be summarized as follow:

- Optimization I
 - Reliability Constraint: Average BER per multicast receiver.
 - Adaptation approaches: discrete rate adaptations.

- Optimal solution in the evaluated schemes: History-based rate adaptation (Sec. 3.5).
- Optimization II
 - Reliability Constraint: Instantaneous BER per multicast receiver.
 - Adaptation approaches: continuous or discrete rate adaptations, continuous power adaptations.
 - Optimal solution in the evaluated schemes: the optimal joint rate and power adaptation functions for both continuous and discrete rate cases (Sec. 4.4 and Sec. 4.5).
- Optimization III
 - Reliability Constraint: Instantaneous PER per multicast receiver.
 - Adaptation approaches: discrete rate adaptations and ARQs within cross-layer design framework.
 - Optimal solution in the evaluated schemes: the average PER-based rate adaptation and packet-combining ARQ (Sec. 5.8).

The recommendations will depend on the QoS constraints mapping from the applications to the link layer and the physical layer, which are decided by the media type, the way in which the media is coded and compressed, its corresponding QoS requirements on network layer, link layer, and physical layer, and so on. For the concerned real-time video service to be multi-casted via a shared downlink wireless channel,

- if it is sensitive to both the instantaneous BER and the link level delay (such

that layer 2 ARQ is not allowed), then the average spectral efficiency of receiver have to be limited by the receiver in the worst channel condition and the proposed joint power and rate adaptation solution in the optimization II is recommended.

- if it is not sensitive to the instantaneous BER but sensitive to the link level delay, then the history-based rate adaptation algorithm in optimization I is recommended;
- if it is sensitive to the instantaneous BER or PER (due to the correlation among different video frames on the application layer) but not too sensitive to the link layer delay (so that the PDUs are allowed to be buffered within a certain time constraint and ARQ is feasible), the joint design of AMC-ARQ strategy of optimization III is recommended.

All the optimal solutions and the corresponding performances have been based on one common assumption that the CSI feedbacks are delay-free and error-free. In reality these feedbacks are with delays and may include errors, either due to the error introduced by wireless transmissions, or due to that the channel condition has varied from the moment those CSIs were created to when they were utilized at the BS. We expect the spectral efficiencies of the optimal solution in each of the evaluation scenario in case of imperfect CSIs will be less than the ones derived with perfect CSIs, but still better than other solutions in each of the evaluation scenario.

6.2 Outlook

Based on the analysis and discussions in this dissertation, it is understandable that the link level adaptations for multicast receivers and for multimedia services are highly complex. The basic dilemma is that the radio resource is shared among mobile receivers and the applied QoS constraints are the same, while the received channel conditions of different users are highly diversified. We have proposed several solutions to improve the user perceived QoS by maximizing the average spectral efficiency per user, and keeping the reliability constraints inviolated.

Based on the analysis and discussions in this dissertation, further research effort can be done in the following directions:

Link adaptation for diversified channel conditions The study scenarios in this project cover either the heuristic varying of group channel conditions with homogeneous mobilities (in Chapter 3) or Ergodic i.i.d link conditions (in Chapter 4 and 5). Future work can evaluate and extend the algorithms in this thesis in group members with heterogeneous mobilities, or non-i.i.d link conditions, which may be even more precise to the multicast scenario in reality.

Feedback reduction As the multicast group size increase, the quantity of CSI feedback messages required by link adaptation and the ACK/NAK required by multicast ARQ functions will grow rapidly. It may cost too much uplink transmission capacity and take longer for the transmitter to collect and process all this feedbacks. Hence it would be preferred if new link adaptation and ARQ algorithms can be designed to work with reduced feedbacks.

Optimization in multi-cell setting In the multi-cell setting, there are more de-

degrees of freedom to explore for multicast. E.g., if a cluster of cells are multi-casting the same service on the same multicast channel, the receivers in bad channel condition can combine the signals received from multiple base stations to improve their overall signal quality.

In a broader view, the approaches from even more dimensions and layers can be considered in the future work. E.g., cooperative transmissions/retransmissions can be performed among different receivers to help receivers in bad channel conditions. On the other hand, new application level achievements may allow the instantaneous constraints on link level to be relaxed, which will allow more multicast adaptation approaches to be adopted or less design complexity with existing approaches. I.e., new video coding methods may be optimized for the mobile transmission environment to reduce the sensitivity of video frames to the instantaneous BER or PER.

Appendix A

Additional Results of the Cross-Layer Strategies

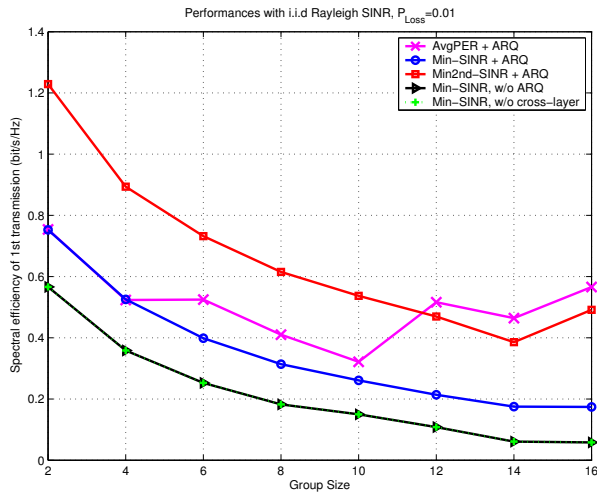
This section presents the additional results from the analysis in Sec.5.8, which are derived for the scenarios of $\overline{SINR} = 5\text{dB}$ (in Fig. A.1) and $\overline{SINR} = 15\text{dB}$ (in Fig. A.2), respectively.

In general, similar behaviors of each AMC-ARQ strategies as the ones at $\overline{SINR} = 10\text{dB}$ can be observed also in these two scenarios. In Fig. A.1(a) and Fig. A.2(a), the spectral efficiency advantages of S1 over S2 are less than those at $\overline{SINR} = 10\text{dB}$. Also the gain due to cross-layer design of S2 over S4 and S5 ($0.1 \sim 0.2$ bit/s/Hz) are less than those at $\overline{SINR} = 10\text{dB}$ ($0.2 \sim 0.3$ bit/s/Hz). The PER and residual PER results in Fig. A.1(b) and Fig. A.2(b) looks almost the same as the counterparts at $\overline{SINR} = 10\text{dB}$.

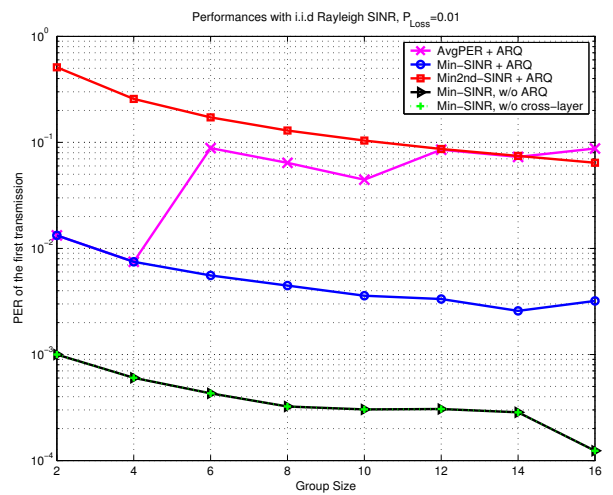
Concerning the performances after ARQs at $\overline{SINR} = 5\text{dB}$, the spectral efficiency trends of S1 versus S2 are similar to the counterpart at $\overline{SINR} = 10\text{dB}$ in Fig. A.1(d) and Fig. A.1(e).

For the $\overline{SINR} = 15\text{dB}$ case, the spectral efficiency curves of S1 (in Fig. A.2(a),

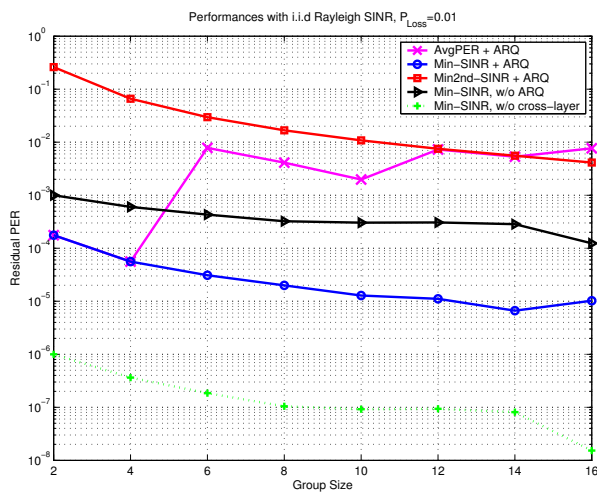
Fig. A.2(d)) is different from its counterparts at 5dB and 10dB cases, because it does not increase when N increase from 14 to 16. From the existing results we expect that the spectral curves of S1 (in the first transmission and after the optimal packet-combining ARQ) in all the SINR scenarios will not keep increasing when $N > 16$, but keep fluctuating. This assumption need to be examined with the results for more group sizes.



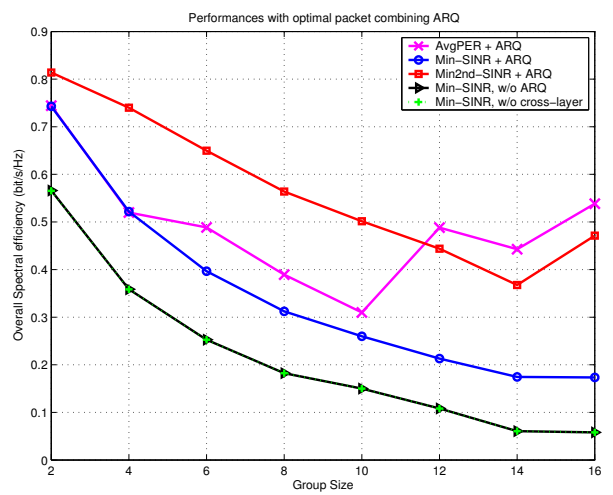
(a) Spectral Efficiency of the First Transmission



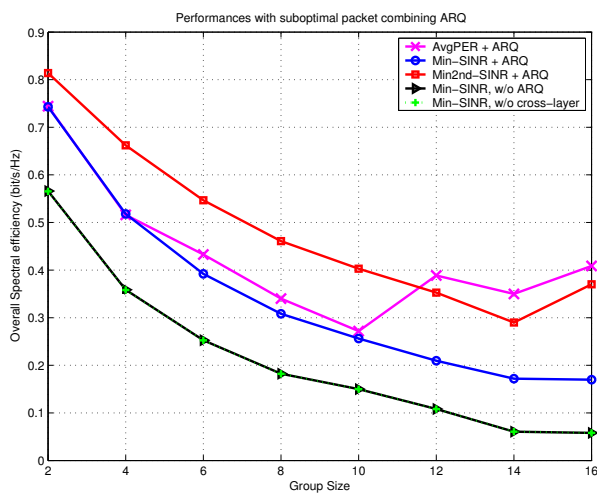
(b) Packet Error Ratio



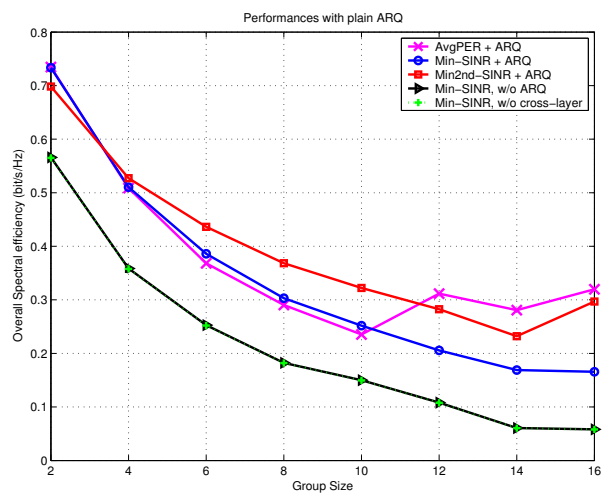
(c) Residual Packet Error Ratio



(d) Spectral Efficiency after Optimal Packet-Combining

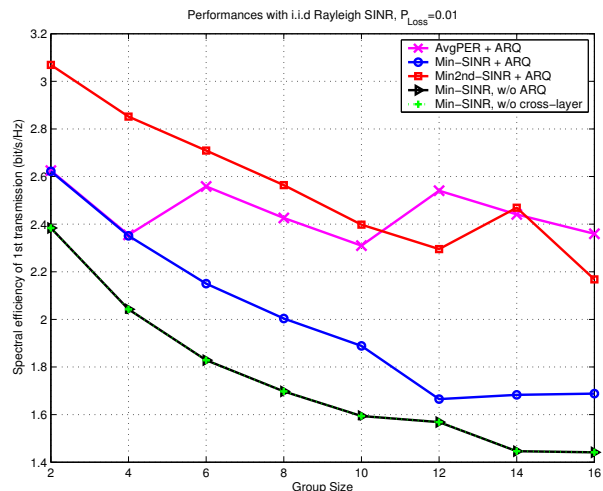


(e) Spectral Efficiency after Sub-Optimal Packet-Combining

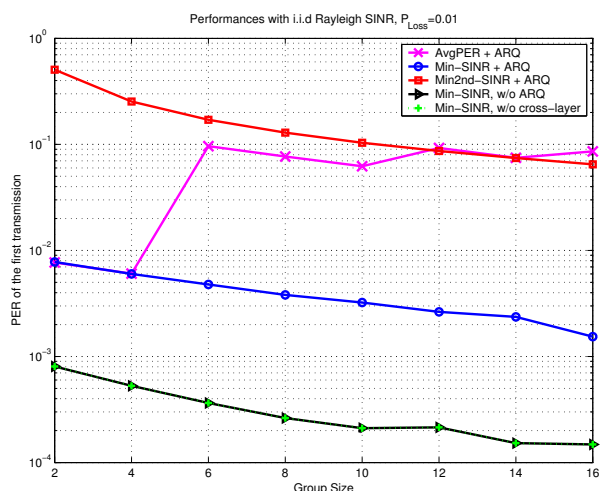


(f) Spectral Efficiency after Plain ARQ

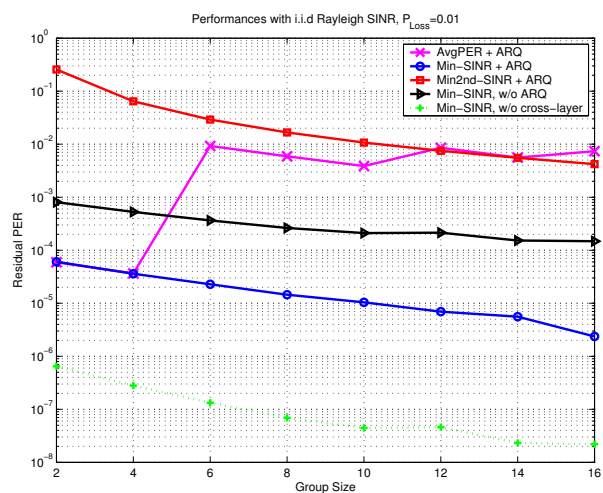
Figure A.1: Performances of AMC-ARQ Strategies VS Group Size, $\overline{SNR} = 5\text{dB}$



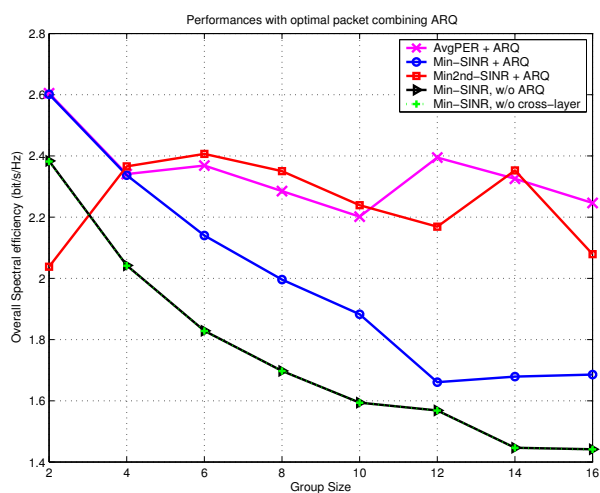
(a) Spectral Efficiency of the First Transmission



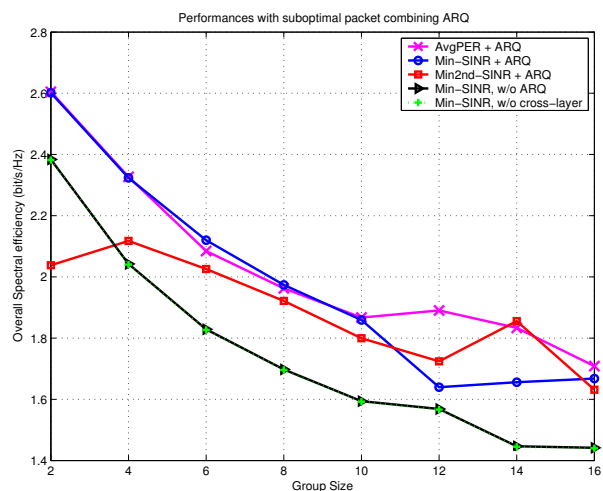
(b) Packet Error Ratio



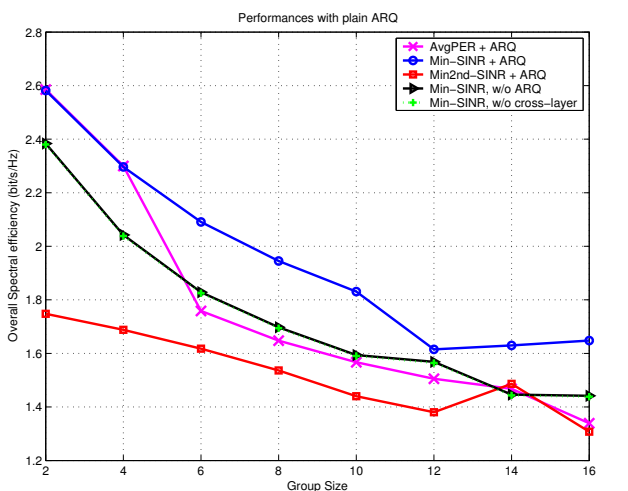
(c) Residual Packet Error Ratio



(d) Spectral Efficiency after Optimal Packet-Combining



(e) Spectral Efficiency after Sub-Optimal Packet-Combining



(f) Spectral Efficiency after Plain ARQ

Figure A.2: Performances of AMC-ARQ Strategies VS Group Size, $\overline{SINR} = 15\text{dB}$

Appendix B

List of Abbreviations

3GPP Third Generation Partnership Project

ACK Acknowledgement

ADC Analog-to-Digital Converter

ADSL Asymmetric Digital Subscriber Line

AM Adaptive Modulation

AMC Adaptive Modulation and Coding

ARQ Automatic Repeat reQuest

AWGN Additive White Gaussian Noise (AWGN)

BER Bit Error Ratio

BPSK Binary Phase Shift Keying

BS Base Station

CATV Cable Television

CDF Cumulative Distribution Function

CDMA Code Division Multiple Access

CP Combined Packet

CSI Channel State Information

DAB Digital Audio Broadcasting

DAC Digital to Analogue Converter

DVB-T Digital Video Broadcasting - Terrestrial

ED Error Detection

FDMA Frequency Division Multiple Access

FEC Forward Error Correction

FFT Fast Fourier Transform

GBN Go-Back-N

GSM Global System for Mobile Communications

HARQ Hybrid Automatic Repeat reQuest

HSDPA High-Speed Downlink Packet Access

HSUPA High-Speed Uplink Packet Access

IETF International Engineering Task Force

IFFT Inverse Fast Fourier Transform

i.i.d Independent Identical Distributions

ISI Inter-Symbol interference

LA Link Adaptation

LOS Line-Of-Sight

LTE Long Term Evolution

MBMS Multimedia Broadcast and Multicast Service

MCM Multiple Carrier Modulation

MIMO Multiple Input Multiple Output

MT Mobile Terminal

OFDM Orthogonal Frequency Division Multiplexing

OFDMA Orthogonal Frequency Division Multiple Access

PER Packet Error Ratio

PDF Probability Density Function

PDU Packet Data Unit

PTM Point to Multi-point

PTP Point to Point

QAM Quadrature Amplitude Modulation

QoS Quality of Service

QPSK Quadrature Phase-Shift Keying

RF Radio Frequency

RFC Request for Comments

RRM Radio Resource Management

RUNE Rudimentary Network Emulator

SAW Stop-And-Wait

SCM Single Carrier Modulation

SINR Signal-to-Interference-and-Noise-Ratio

SNR Signal-to-Noise-Ratio

SR Selective Retransmission

TS Time-Slots

TTI Transmission Time Interval

UE User Equipment

UMTS Universal Mobile Telecommunications Systems

UTRAN Universal Terrestrial Radio Access Network

WCDMA Wide-band Code Division Multiple Access

WiMAX Worldwide Inter-operability for Microwave Access

WLAN Wireless Local Area Networks

Appendix C

List of Math Notations and Symbols

Chapter 2

L : the path-loss in decibels (dB);

n : the path-loss exponent, no unit;

d : the distance between the transmitter and the receiver in meters;

C : a constant which depends on the carrier frequency, environment type (e.g., rural, urban, suburban, indoor), and other system loss factors, in decibels;

T_d : delay spread, is defined as the time difference between the first and the last received impulses, measured in s, ms or ns;

t : time;

$\tau_i(t), \tau_j(t)$: the arrival time of two impulses from the same transmitted signal due to multipath;

B_c : coherence bandwidth in Hz;

B_s : bandwidth of a baseband symbol in Hz;

f : frequency in Hz;

$S(f)$: power function along frequency domain, usually in watt;

$G(f)$: channel gain function along frequency domain in linear unit.

Chapter 3

i : the index of multicast receivers;

j : the index of OFDM subcarriers within a multicast subchannel;

$SNR(i, j)$: signal-to-noise-ratio of multicast receiver i over subcarrier j ;

M : the modulation mode, e.g., BPSK, 4QAM, 16QAM, 64QAM, 256QAM, or turn-off;

K_M : the number of bits per symbol on a subcarrier corresponding to a modulation mode;

v_d : the sampled complex delay profile, no unit;

D_{rms} : the rms delay in sample unit;

D_{max} : the maximum delay spread in sample unit;

w_d : a complex Normal random process;

V : the normalization factor, no unit;

N : the number of mobile receivers in the investigated multicast group;

S : the user satisfaction rate, not unit;

T : the Normalized Average user Goodput per session, no unit;

$Goodput_i$: the correctly received bits by receiver i during one service session;

$R(T, S)$: Reward function made up of S and T , no unit;

\overline{BER}_i : the average BER of receiver i during the whole multicast service session;

θ : the average BER constraint, no unit, $\theta = 10^{-3}$;

$W1, W2$: the relative weights of T and S used in Reward function definition in Sec. 3.4;

$BER(M, SNR_{i,j})$: the instantaneous BER of receiver i on subcarrier j ;

$S'(M, j)$: the instantaneous satisfaction rate of mode M on subcarrier j ;

$T'(M, j)$: the instantaneous goodput of mode M on subcarrier j ;

$R'(M, j)$: the local Reward of mode M on subcarrier j ;

$w1', w2'$: the local/instantaneous relative weights of $T'(M, j)$ and $S'(M, j)$ used in the instantaneous Reward function definition in Sec. 3.4;

$M_{opt}(j)$: the optimal modulation mode on subcarrier j ;

Γ_M : the SNR thresholds of each modulation mode;

BER_c : the cumulated BER at receiver i since the multicast transmission start until the current time;

θ_1 : the arbitrary low boundary of the optimal BER interval in Sec. 3.5;

$\theta_t(i)$: the instantaneous BER Threshold for the next transmission for UE_i in Sec. 3.5;

θ_{max} : the arbitrary upper boundary of $\theta_t(i)$ in Sec. 3.5;

δ : the multiplicative factor to increase $\theta_t(i)$ in Sec. 3.5.

Chapter 4

N : the number of receivers in a multicast group;

C : Shannon capacity of a channel, in bit/s;

B : channel bandwidth, in Hz;

\mathcal{R} : achievable data rate of practical system, bit/s;

Υ : the gap between Shannon capacity and the achievable capacity/capacity of real systems, no unit;

x : the transmitted multicast signal amplitude in volt;

g_i : the channel gain of receiver i ;

σ_i : the noise amplitude at receiver i in volt;

y_i : the received signal amplitude at receiver i , in volt;

γ_i : the instantaneous Normalized SNR measured under average transmitted power level, in linear unit in all math expressions, but presented in decibels in all figures;

SNR_i : the received SNR of receiver i after power adaptation, in linear unit in math expressions, but in decibels in all figures;

$\vec{\gamma}$: a random fading state vector, made up of all the instantaneous γ_i of the multicast group receivers;

$p^*(\vec{\gamma})$: the probability density function of $\vec{\gamma}$;

k : transmitted data rate as a function of $\vec{\gamma}$ in this chapter, bits per symbol;

T_s : duration of a baseband symbol;

S : power in watt, a function of $\vec{\gamma}$ in this chapter;

θ : BER constraint, $\theta = 10^{-3}$ in this chapter;

$(\mathcal{R}/\mathcal{B})_T$: transmitted spectral efficiency in bits/s/Hz;

$(\frac{\mathcal{R}}{\mathcal{B}})_i$: received spectral efficiency by receiver i , in bits/s/Hz;

$\overline{(\frac{\mathcal{R}}{\mathcal{B}})}$: average spectral efficiency among all multicast receivers;

$\mathbb{E}\{.\}$: the mathematical expectation of a random variable;

\overline{S} : the average power constraint, in watt;

Ω : a region of $\vec{\gamma}$ in the non-negative N-dimensional space;

$(\mathbb{R}_0^+)^N$: a space of N-dimensional space with non-negative real values on each dimension;

$\mathcal{J}(\cdot)$: the Lagrange function;

λ_0 : the Lagrange multiplier for the power constraint;

σ : an arbitrary function;

ε : a sufficient small number;

c : a constant, no unit;

S_{opt} : the optimal power adaptation function;

γ_0 : a threshold of the normalized SNR to turn-on the transmission on the multi-cast channel;

Δ, α : two arbitrary values derived from the multi-dimensional integrations.

S_c : the constant transmission power level average power constraint, in watt;

S_L : a linear power function, in watt;

β, φ : parameters of the linear power function, no unit;

$\left(\frac{\mathbb{R}}{\mathbb{B}}\right)_{Shannon}$: Shannon capacity of a multicast channel under the worst-link-dominant limit.

Chapter 5

N : the total number of receivers in a multicast group;

m : index of AMC mode;

P : average packet loss ratio;

K : number of original data packets to be coded;

L : (in page 81) number of output packets after the packet encoder;

T_r^{max} : maximum allowed number of retransmissions;

P_{loss} : residual packet loss/error ratio after retransmissions;

P_0 : the expectation of the instantaneous packet error ratio of a transmission;

$PER_m(\cdot)$: packet error ratio estimation function of transmission mode m (a AMC mode);

a_m, g_m : parameters depend on AMC mode, no unit;

Γ_m : AMC threshold of mode m corresponding to P_{loss} ;

Γ'_m : AMC threshold of mode m corresponding to P_0 ;

Se : spectral efficiency in bits/s/Hz;

R_m : bits per symbol of AMC mode m ;

T : the overall expected number of transmissions to correctly deliver an original packet;

η : packet combining efficiency, 1 divided by the number of data packets included in 1 combined packet;

L : (since page 86) the number of receivers which lost a same packet;

j : packet index;

k : index of receivers;

D : an original data packet, to be distinguished with the retransmitted combined packet;

\overline{PER}_m : instantaneous average PER of AMC mode m among the group;

m_{opt} : the optimal instantaneous AMC mode;

i : index of the receiver which lost a packet.